

Mechanisms of transmitter release and synaptic plasticity at excitatory synapses in the hippocampus

A thesis submitted for the degree of Doctor of Philosophy

at

The Australian National University

July 1998

Christopher Alan Reid

BPharm (University of Tasmania)

BSc (Hons) (Australian National University)

Division of Neuroscience

The John Curtin School of Medical Research

Australian National University

Canberra

Statement

All the work in this thesis is original. All experimental work was carried out by myself, except where specifically acknowledged, under the supervision of Dr John Bekkers and Dr John Clements.

During this time a number of presentations of this work were made at scientific meetings. The following abstracts were published in conjunction with these presentations.

Reid, C. A., Bekkers, J. M. & Clements, J. D. (1998) LTP in the dentate: An increase in the mean quantal amplitude. *Proc Aust Neurosci Soc* 9: 65.

Reid, C. A., Clements, J. D. & Bekkers, J. M. (1997) Presynaptic Ca²⁺ channel subtypes and Ca²⁺ cooperativity for transmitter release in hippocampal cultures. *Soc Neurosci Abstr* 23: 1182.

Reid, C. A., Clements, J. D. & Bekkers, J. M. (1997) Quantitative analysis of the nonuniform distribution of Ca²⁺ channel subtypes on presynaptic terminals. *Proc Aust Neurosci Soc* 8: 70.

Reid, C. A., Clements, J. D. & Bekkers, J. M. (1996) Nonhomogenous distribution of different calcium channel subtypes on presynaptic terminals in the hippocampus. *Soc Neurosci Abstr* 22: 6.

Reid, C. A., Clements, J. D. & Bekkers, J. M. (1996) Nonuniform probability of glutamate release associated with different subtypes of presynaptic calcium channels at hippocampal synapses. *Proc Aust Neurosci Soc* 7: 151.

The following published papers describe some of the work presented in this thesis:

Reid, C. A., Bekkers, J. M. & Clements, J. D. (1998) N-type and P/Q-type Ca^{2+} channels mediate transmitter release with a similar cooperativity at rat hippocampal autapses. *J Neurosci* 18: 2849-2855.

Reid, C. A., Clements, J. D. & Bekkers, J. M. (1997) Nonuniform distribution of Ca^{2+} channel subtypes on presynaptic terminals of excitatory synapses in hippocampal cultures. *J Neurosci* 17: 2738-2745.

A handwritten signature in black ink, appearing to read 'C. A. Reid'. The signature is written in a cursive, flowing style.

Christopher Alan Reid

Acknowledgments

I would like to express my gratitude to both my supervisors, Dr John Bekkers and Dr John Clements, for their guidance, encouragement and friendship throughout the last three years. I also thank Dr Greg Stuart for helpful discussion along the way and Garry Rodda for his technical assistance.

Many people from the John Curtin School of Medical Research gave me encouragement and friendship over the years: Amanda, Cath, Caryl, Dave, Garry, Greg, Jackie, Kim, Luc, Rebecca, Sharon, Shaun and Sven.

I would like to thank my parents for encouraging me to pursue my goals. Rod and Liz were generous in their continued help and support. I thank my Grandmother for motivating me in her unique way. I would like to acknowledge Andrew and Ivan for their friendship. I would also like to thank the rest of my family for their continued interest and support.

Finally, a special thanks to Isobel, without whose support and encouragement none of this would have been possible. Her patience, understanding and care never wavered.

Abstract

The work presented in this thesis addresses two distinct questions: What is the distribution and role of presynaptic calcium channels involved in the release of glutamate at excitatory synapses in hippocampal cultures? What is the locus of expression of long-term potentiation at the perforant path-granule cell synapse in slices of the dentate gyrus?

A number of different subtypes of Ca^{2+} channels are known to support the release of glutamate at excitatory synapses. The pattern of co-localisation of these subtypes on presynaptic terminals in hippocampal cultures was investigated. N-type (ω -conotoxin GVIA-sensitive, ω -CTx) or P/Q-type (ω -agatoxin IVA-sensitive, ω -Aga) Ca^{2+} channels were selectively blocked and the reduction in transmitter release probability (P_T) was measured using MK-801. The toxins completely blocked release at some terminals, reduced P_T at others, and failed to affect the remainder. In contrast, nonselective reduction of presynaptic Ca^{2+} influx by adding Cd^{2+} or lowering external Ca^{2+} reduced P_T uniformly at all terminals. It was concluded from these results that the mixture of N-type and P/Q-type channels varies markedly between terminals on the same afferent. A model was developed incorporating a non-uniform distribution of Ca^{2+} channel subtypes across presynaptic terminals. The model suggests that about 10% of terminals have only N-type channels, about 45% of terminals have only P/Q-type channels, and the remaining 45% have a mixture of subtypes. This non-uniform distribution may enable terminal-specific modulation of synaptic function by neuromodulators that differentially affect a particular Ca^{2+} channel subtype.

The relationship between extracellular Ca^{2+} concentration and EPSC amplitude was investigated at excitatory autapses on cultured hippocampal neurons. This relationship was steeply non-linear, implicating the cooperative involvement of several Ca^{2+} ions in the release of each vesicle of transmitter. The cooperativity was estimated to be 3.1 using a power function fit, and 3.3 using a Hill equation fit. However, simulations

suggest that these values underestimate the true cooperativity. The role of different Ca^{2+} channel subtypes in shaping the Ca^{2+} dose-response relationship was studied using the selective Ca^{2+} channel blockers ω -Aga (P/Q-type channels) and ω -CTx (N-type channels). Both toxins broadened the dose-response relationship, and the Hill coefficient was reduced to 2.5 by ω -Aga and to 2.6 by ω -CTx. This broadening is consistent with a non-uniform distribution of Ca^{2+} channel subtypes across presynaptic terminals. The similar Hill coefficients in ω -Aga or ω -CTx suggest that there was no difference in the degree of cooperativity for transmitter release mediated via N-type or P/Q-type Ca^{2+} channels. A model of calcium's role in transmitter release was developed. It is based on a modified Dodge-Rahamimoff equation that includes a non-linear relationship between extra- and intracellular Ca^{2+} concentration, has a cooperativity of 4, and incorporates a non-uniform distribution of Ca^{2+} channel subtypes across presynaptic terminals. The model predictions are consistent with all of the results reported in this study.

Long-term potentiation (LTP) of synaptic transmission is the putative mechanism underlying certain forms of learning and memory. Despite intensive study, it remains controversial whether LTP is expressed at a pre- or postsynaptic locus. A novel approach was used to investigate this question at excitatory synapses onto granule cells in acute slices of the dentate gyrus. The variance of the evoked synaptic amplitude was plotted against mean synaptic amplitude at several different Cd^{2+} concentrations. The slope of the variance-mean plot estimates the average amplitude of the response following the release of a single vesicle of transmitter (Q_{av}). The variance-mean technique was tested by applying the analysis before and after three different synaptic modulations: (i) a reduction in Q_{av} by the addition of the glutamate receptor antagonist, CNQX, (ii) a reduction in the average probability of transmitter release (P_{T}) by the addition of baclofen, and (iii) an increase in the number of active synaptic terminals (N) by increasing the stimulus strength. CNQX reduced the average synaptic amplitude and Q_{av} to the same extent, consistent with a postsynaptic action. In contrast, neither a change in N or P_{T} altered Q_{av} . This confirmed that the variance-

mean technique can distinguish between a pre- and a postsynaptic site of modulation. The induction of LTP increased the synaptic amplitude and Q_{av} to the same extent, strongly supporting a postsynaptic locus of LTP expression in the dentate gyrus. A postsynaptic increase in synaptic efficacy could be due to the insertion of additional AMPA receptors into the postsynaptic membrane, the unmasking of AMPA receptors already present in the membrane or a change in the single channel conductance of the AMPA receptor.

Table of contents

Statement

Acknowledgments

Abstract

Table of Contents

Abbreviations

Chapter 1	1
Introduction	1
Part I: Ca²⁺ channel subtypes and neurotransmitter release	1
Pharmacological and biophysical identification of Ca ²⁺ channel subtypes	2
Molecular biology of neuronal Ca ²⁺ channels	3
Matching cloned Ca ²⁺ channels to their physiological subtypes	3
Ca ²⁺ channel subtypes which support fast transmitter release at central synapses	4
Is transmitter release at hippocampal synapses supported by only N- and P/Q-type Ca ²⁺ channels?	5
Specificity of ω -CTx and ω -Aga	6
How are N- and P/Q-type Ca ²⁺ channels distributed on excitatory presynaptic terminals?	6
The relationship between Ca ²⁺ influx and transmitter release	8
Differences in the Ca ²⁺ cooperativity for influx through different Ca ²⁺ channel subtypes	10
Ca ²⁺ microdomains.....	10
Summary	12
Part II: Long term potentiation	13
Historical perspective	13
Different forms of LTP	13
Different stages of synaptic potentiation	14
Associativity, cooperativity and input specificity of LTP	15
The NMDA receptor: a molecular coincidence detector	15

Ca ²⁺ involvement in LTP induction	16
Does LTP occur at a pre or postsynaptic locus?	17
Quantal analysis	17
Miniature analysis	21
Paired pulse facilitation as an index of P _r	21
Progressive block in MK-801 as a measure of P _r	23
Scaling NMDA and AMPA receptor components of the EPSC as an index of P _r	23
Miscellaneous techniques	24
Silent synapse theory of LTP	25
Extrasynaptic glutamate spill-over	26
Retrograde messengers	27
Summary	27
Chapter 2	29
General Methods	29
I. Hippocampal Culture Experiments	29
Culture preparation	29
Dissociation procedure	29
Maintenance of hippocampal neurons.	30
Solutions used in the culture preparation.....	31
Electrophysiology	32
Data acquisition and analysis.....	34
Solution exchange.....	34
Characterisation of autaptic synaptic currents	34
II. Hippocampal Slice Experiments	35
Electrophysiology	35
Data acquisition and analysis.....	36
Appendix	37
Chapter 3	38
A Non-uniform Distribution of Ca²⁺ Channel Subtypes on Presynaptic Terminals	38
Introduction	38
Methods	39

Results	41
Progressive block of NMDA EPSCs by MK-801 yields P_r	41
ω -CTx and ω -Aga affect P_r non-uniformly	44
Paired-pulse depression gives an average measure of P_r	46
High- P_r and low- P_r terminals do not correlate with Ca^{2+} channel subtypes.....	47
Discussion	47
Modelling the effect of toxins on P_r	47
Exploring the model	49
Developmental change in Ca^{2+} channel subtype supporting transmitter release	50
Other evidence for a non-uniform distribution of Ca^{2+} channels	51
Functional implications of a non-uniform distribution of Ca^{2+} channels	53
Differential modulation of Ca^{2+} channel subtypes.....	53
What determines P_r at a given synaptic terminal?	55
Conclusion	56
Appendix	58
Chapter 4	62
Ca^{2+} Cooperativity of Release and Ca^{2+} Channel Subtypes	62
Introduction	62
Methods	63
Approaches used to estimate Ca^{2+} cooperativity	64
Results	66
Ca^{2+} dose-response curve for autaptic EPSCs	66
Estimating Ca^{2+} cooperativity	66
Ca^{2+} cooperativity in the presence of Cd^{2+}	68
Ca^{2+} cooperativity in the presence of ω -CTx and ω -Aga	68
Non-uniform distribution of Ca^{2+} channel subtypes	69
Experimental sources of non-linearity	70
The modified Dodge-Rahamimoff equation.....	70
A model synapse	72
Discussion	73
Dose-response analysis in the presence of Ca^{2+} channel non-linearity	73
The modified Dodge-Rahamimoff equation.....	74
No difference between cooperativities for N- and P/Q-type channels	75
The non-uniform distribution of Ca^{2+} channel subtypes.....	77
The overlap of Ca^{2+} microdomains	79
Conclusions	81

Chapter 5.....	82
Long Term Potentiation in the Dentate Gyrus	82
Introduction	82
Methods	83
Variance-mean analysis	84
Results	85
Computer simulation testing of the variance-mean technique	85
Variance-mean analysis measures mean quantal amplitude	86
Variance-mean technique reliably identifies site of synaptic modulation	87
A postsynaptic mechanism for LTP	88
Discussion	88
Other evidence concerning the site of LTP expression in the dentate.....	88
Variance-mean technique vs $1/CV^2$ technique	90
Variance-mean technique vs other methods	91
Presynaptic mechanisms which could increase Q_{av}	92
Signal transduction mechanisms.....	94
CaM Kinase II and LTP	94
Conclusion	96
Appendix	97
Chapter 6.....	100
General Discussion	100
Future studies	103
References	106

Abbreviations

ACSF	artificial cerebrospinal fluid
ω -Aga	ω -agatoxin IVA
AMPA	α -amino-3-hydroxy-5-methylisoxazole-4-propionic acid
4-AP	4-aminopyridine
APV	D-2-amino-5-phosphonovaleric acid
araC	cytosine β -D-arabinofuranoside
$[\text{Ca}^{2+}]_{\text{it}}$	intra-terminal Ca^{2+} concentration
$[\text{Ca}^{2+}]_{\text{o}}$	extracellular Ca^{2+} concentration
CNQX	6-cyano-7-nitroquinoxaline-2,3-dione
CNS	central nervous system
CV	coefficient of variation
ω -CTx	ω -conotoxin GVIA
DHP	dihydropyridine
EDTA	ethylenediaminetetraacetic acid
EGTA	ethylene glycol-bis (β -aminoethyl ether)
EPSC	excitatory postsynaptic current
EPSP	excitatory postsynaptic potential
HVA	high voltage-activated
LPP	lateral perforant path
LTP	long term potentiation
LVA	low voltage-activated
MEM	Minimum Essential Medium
mEPSC	miniature excitatory postsynaptic current
MPP	medial perforant path
NMDA	N-methyl-D-aspartic acid
NMJ	neuromuscular junction
N	number of active synapses contributing to a synaptic response
q	quantal amplitude

Q_{av}	average quantal amplitude
PKA	protein kinase A
PPF	paired pulse facilitation
P_o	open probability
P_r	probability of transmitter release
R_s	series resistance
SD	standard deviation
STP	short term potentiation
μ	mean EPSC amplitude
σ^2	variance
σ_n	recording noise

Chapter 1

Introduction

Communication between neurons involves the release of neurotransmitter from synaptic terminals. A major challenge in neuroscience is to understand the mechanisms of synaptic transmission and its modulation. This thesis examines questions relating to synaptic function and modulation at excitatory hippocampal synapses. Chapters 3 and 4 explore the relationship between presynaptic voltage activated Ca^{2+} channels and the transmitter release mechanism. Chapter 5 investigates the mechanism underlying long lasting plasticity. The Introduction is presented in two parts: Part I introduces Ca^{2+} channel physiology and relates to Chapters 3 and 4; Part II introduces long term potentiation (LTP) and relates to Chapter 5.

Part I: Ca^{2+} channel subtypes and neurotransmitter release

The release of neurotransmitter from a presynaptic terminal involves multiple steps. A key step in this process is the entry of Ca^{2+} into the presynaptic terminal via voltage activated Ca^{2+} channels (Katz and Miledi, 1968; Llinas *et al.*, 1981; Augustine and Charlton, 1986; Borst and Sakmann, 1996). It is well established that a wide diversity of Ca^{2+} channel subtypes exist. Electrophysiological studies have indicated that there are at least six discernible Ca^{2+} channel types: L-, N-, P-, Q-, R- and T-type (Tsien *et al.*, 1995). The N-, P-, Q- and R-type Ca^{2+} channels have all been implicated in the action potential-dependent release of neurotransmitter at central synapses (Luebke *et al.*, 1993; Regehr and Mintz, 1994; Wheeler *et al.*, 1994; Wu and Saggau, 1994b; Mintz *et al.*, 1995; Wu *et al.*, 1998). Numerous unresolved questions remain about how different presynaptic Ca^{2+} channel subtypes interact with the transmitter release mechanism. This thesis addresses two such questions at excitatory synapses in the hippocampus. First, Chapter 3 investigates how the different Ca^{2+} channel subtypes are distributed across different presynaptic terminals. Second, Chapter 4 examines if

the Ca²⁺ sensitivity of the transmitter release mechanism differs for Ca²⁺ influx through different channel subtypes.

Pharmacological and biophysical identification of Ca²⁺ channel subtypes

Voltage activated Ca²⁺ channels can be divided into high voltage-activated (HVA) or low voltage-activated (LVA) classes based on the membrane potential range over which the channel is activated. LVA Ca²⁺ channels will activate at membrane potentials as low as -70mV while HVA Ca²⁺ channels require depolarisation to at least -20mV to be activated (Tsien *et al.*, 1988). The only identified member of the LVA group has been termed the T-type Ca²⁺ channel. The T-type channel can also be defined by its high sensitivity to Ni²⁺ and insensitivity to low Cd²⁺ concentrations (< 10µM) (Fox *et al.*, 1987). The different subtypes of HVA Ca²⁺ channels are primarily distinguished pharmacologically (see Table 1.1). The L-type channel is blocked by a group of drugs known as the dihydropyridines (DHP, eg. nifedipine, nimodipine) and are facilitated by BAY K 8644 (Nowycky *et al.*, 1985). The N-type channel is blocked by ω-conotoxin GVIA (ω-CTx) (Nowycky *et al.*, 1985; Olivera *et al.*, 1985; Fox *et al.*, 1987; Williams *et al.*, 1992a; Fujita *et al.*, 1993). Both the P- and the Q-type channels are sensitive to ω-agatoxin IVA (ω-Aga) with the P-type channel having a 100 fold greater affinity than the Q-type channel for the toxin (Mintz *et al.*, 1992a; Mintz *et al.*, 1992b; Wheeler *et al.*, 1994; Randall and Tsien, 1995; Scholz and Miller, 1995). A defining biophysical characteristic of the P-type channel is that it exhibits little or no inactivation during a depolarisation of up to 1 second while the Q-type channel inactivates at a similar rate to the N-type channel (~35% inactivation during a 0.1ms pulse, -80mV to 0mV) (Randall and Tsien, 1995). A further HVA Ca²⁺ channel, the R-type, has been identified in mammalian neurons. There are no known selective blockers of the R-type Ca²⁺ channel. Currents mediated by this channel are insensitive to ω-CTx, ω-Aga and the DHPs (Ellinor *et al.*, 1993; Zhang *et al.*, 1993; Randall and Tsien, 1995; Randall and Tsien, 1997). The R-type channel is known to be sensitive to low concentrations of Ni²⁺ (Wu *et al.*, 1998).

Table 1.1 Neuronal high voltage activated (HVA) Ca²⁺ channels. The different subtypes of HVA Ca²⁺ channels are primarily distinguished pharmacologically.

Channel types	Pore-forming $\alpha 1$ subunit	Pharmacology (blockers)
L	$\alpha 1C, \alpha 1D$	dihydropyridines
N	$\alpha 1B$	ω -conotoxin GVIA
P	$\alpha 1A(?)$	ω -agatoxin IVA (low concentrations)
Q	$\alpha 1A(?)$	ω -agatoxin IVA (high concentrations)
R	$\alpha 1E(?)$	Ni ²⁺ (low concentrations)

Molecular biology of neuronal Ca²⁺ channels

Early studies demonstrated that the Ca²⁺ channel was made up of several subunits (Catterall, 1991). Molecular cloning and expression studies have shown that the pore, voltage sensor and all pharmacological binding sites are encoded by the $\alpha 1$ subunit (Catterall, 1991; Catterall, 1995). Six $\alpha 1$ subunits have been cloned from the vertebrate central nervous system (CNS). The accepted nomenclature defines the $\alpha 1$ subunit as classes A through to E (Birnbaumer *et al.*, 1994) and the recently cloned subunit, $\alpha 1G$ (Perez-Reyes *et al.*, 1998). Three additional subunits are found to be associated with the $\alpha 1$ subunit: β , $\alpha 2$ and δ (Catterall, 1991). The $\alpha 2$ and δ subunits are often considered a single molecular entity since they are encoded by the same gene and are linked by disulphide bonds (Jay *et al.*, 1991). The $\alpha 2/\delta$ has little effect on channel kinetics or pharmacology but when co-expressed with the $\alpha 1$ subunit lead to an increase in whole-cell current amplitude (Williams *et al.*, 1992b; Gurnett *et al.*, 1996). In contrast the β subunit influences both the kinetic and pharmacological properties. The voltage activation range, the rate of inactivation and the pharmacology of an $\alpha 1$ subunit can be significantly altered by the co-expression of β subunits (Williams *et al.*, 1992a; Williams *et al.*, 1992b; Ellinor *et al.*, 1993; Stea *et al.*, 1993; Zhang *et al.*, 1993; Moreno *et al.*, 1997). The subunit composition of native Ca²⁺ channels remains unknown.

Matching cloned Ca²⁺ channels to their physiological subtypes

Parallels between the properties of expressed recombinant Ca²⁺ channels and Ca²⁺ channels found in neurons are slowly becoming established. The clearest example of such an association is the $\alpha 1B$ clone which has been shown to encode an ω -CTx-sensitive channel (Dubel *et al.*, 1992; Williams *et al.*, 1992a; Fujita *et al.*, 1993). A more controversial issue has been the assignment of the $\alpha 1A$ subunit. Preliminary data pointed to a match to the P-type Ca²⁺ channel (Mori *et al.*, 1991). However, expressed alone it demonstrated rapid inactivation and low sensitivity to ω -Aga which is more like the Q-type channel (Sather *et al.*, 1993; Stea *et al.*, 1994). More recent experiments in which the $\alpha 1A$ subunit is co-expressed with $\alpha 2/\delta$ and different β

subunits may provide the answer (Moreno *et al.*, 1997). The co-expression of $\alpha 1A$, $\alpha 2/\delta$ and $\beta 1b$ produced a robust inactivating current that was sensitive to low concentrations of ω -Aga, consistent with a P-type channel. These experiments also co-expressed different β subunits with the $\alpha 1A$ and $\alpha 2/\delta$ subunits and showed that the β subunit could greatly influence the specificity of the toxin block. Therefore, both the P- and the Q-type channel could be encoded by the $\alpha 1A$ subunit with their differing pharmacology and kinetics being explained by different β subunit composition.

The $\alpha 1E$ subunit expressed in oocytes exhibited a voltage activation range, rapid inactivation and sensitivity to Ni^{2+} consistent with a T-type Ca^{2+} channel. An opposing view is that the properties of the $\alpha 1E$ subunit are more closely related to the R-type channel (Randall and Tsien, 1997). This interpretation seems justified following the recent cloning of the $\alpha 1G$ subunit (Perez-Reyes *et al.*, 1998). When expressed in *Xenopus* oocytes the $\alpha 1G$ subunit exhibits low voltage dependence, slow deactivation kinetics and small single channel conductance, all characteristic of the T-type Ca^{2+} channel. L-type channels are encoded by two different clones $\alpha 1C$ and $\alpha 1D$ (Mikami *et al.*, 1989; Snutch *et al.*, 1991; Williams *et al.*, 1992b). $\alpha 1C$ encodes the classical cardiac L-type Ca^{2+} channel while $\alpha 1D$ encodes an L-type channel which is specific to brain and endocrine tissue.

Ca^{2+} channel subtypes which support fast transmitter release at central synapses

Multiple Ca^{2+} channels support the release of neurotransmitter at central synapses. ω -Aga-sensitive Ca^{2+} channels (P- or Q-type) seem to play the predominant role, although a significant component of release is also supported by ω -CTx-sensitive channels (N-type) at most central synapses (Luebke *et al.*, 1993; Regehr and Mintz, 1994; Wheeler *et al.*, 1994; Wu and Saggau, 1994b; Mintz *et al.*, 1995). The R-type Ca^{2+} channel, which is resistant to ω -CTx, ω -Aga and the DHPs, but sensitive to low concentrations of Cd^{2+} , has also been implicated in supporting transmitter release at many central synapses (Mintz *et al.*, 1995; Wu and Saggau, 1995a; Wu *et al.*, 1998).

There is a general consensus that the DHP-sensitive channel (L-type) does not play a role in action potential dependent release (Dunlap *et al.*, 1995).

Although ω -Aga-sensitive channels support release at most central synapses, the proportion of P-type and Q-type Ca^{2+} channels may differ for different terminals. For instance, transmitter release at the granule cell to Purkinje cell synapse in rat cerebellum is blocked by low concentrations of ω -Aga (~50nM) suggesting a predominance of the P-type Ca^{2+} channel (Mintz *et al.*, 1995). In contrast, experimental evidence in both hippocampal cultures and slices suggests that the Q-type Ca^{2+} channel predominates over the P-type (Wheeler *et al.*, 1994; Scholz and Miller, 1995). This conclusion is based primarily on the slow block of the evoked synaptic event by ω -Aga and the high concentration required (>200nM). This is consistent with the slow on-rate and low affinity of ω -Aga for the Q-type channel (Randall and Tsien, 1995). Additionally, ω -conotoxin MVIIC, a toxin known to have a high affinity for the Q-type channel, was shown to block the transmitter release resistant to ω -CTx and ω -Aga at low concentrations (Randall and Tsien, 1995). However, ω -conotoxin MVIIC will also block N- and P-type Ca^{2+} channels, complicating the interpretation of this finding (Sather *et al.*, 1993; Randall and Tsien, 1995). ω -Aga therefore cannot distinguish between P and Q-type Ca^{2+} channels unambiguously and ω -Aga-sensitive Ca^{2+} channels are often named the P/Q-type.

Is transmitter release at hippocampal synapses supported by only N- and P/Q-type Ca^{2+} channels?

As already noted many central synapses exhibit a component of release which is resistant to both ω -CTx and ω -Aga. Evoked release at hippocampal synapses is blocked by greater than 97% in both hippocampal slice and culture experiments by the co-application of ω -CTx and ω -Aga (Wheeler *et al.*, 1994; Wu and Saggau, 1994b; Scholz and Miller, 1995; Wheeler *et al.*, 1996). However, given the highly non-linear relationship between $[\text{Ca}^{2+}]$ and transmitter release (see below) it is possible that a significant proportion of presynaptic Ca^{2+} enters through a Ca^{2+} channel subtype

resistant to both toxins. The possibility that the resistant Ca^{2+} channel contributes significantly to release was addressed by maximising Ca^{2+} influx through Ca^{2+} channels (Wheeler *et al.*, 1996). This was achieved by prolonging the action potential using the K^+ channel blocker 4-aminopyridine (4-AP). The block of the evoked transmitter release by the co-application of toxins was not altered despite spike broadening. This limits the involvement of other possible Ca^{2+} channels such as the R-type but cannot rule them out entirely. The development of a specific R-type Ca^{2+} channel blocker is required to establish the role of this channel in transmitter release.

Specificity of ω -CTx and ω -Aga

The specificity of ω -CTx and ω -Aga in blocking independent classes of Ca^{2+} channels is critical for the interpretation of many experiments in this thesis. In recordings of somatic Ca^{2+} currents in dissociated neurons this assumption holds true (Dunlap *et al.*, 1995). However, the toxins might not be so selective on presynaptic Ca^{2+} channels involved in transmitter release. The best evidence for non-overlapping block of Ca^{2+} channels at presynaptic terminals has come from imaging studies. By measuring presynaptic Ca^{2+} transients using the Ca^{2+} sensitive dye fura-2 at the cerebellar synapse, Mintz *et al.* (1995) demonstrated the non-overlapping nature of the toxin block. The initial application of ω -Aga did not interfere with the measured reduction of the presynaptic Ca^{2+} transient on application of ω -CTx. Neither did the initial addition of ω -CTx interfere with the Ca^{2+} transient reduction on application of ω -Aga. Wu and Saggau (1994) did a similar experiment looking at CA3-CA1 synapses of the hippocampus. They found a similar reduction in presynaptic Ca^{2+} influx was caused by ω -Aga in the presence or absence of ω -CTx.

How are N- and P/Q-type Ca^{2+} channels distributed on excitatory presynaptic terminals?

Three experimental results are consistent with a scenario in which a mixed population of N- and P/Q-type Ca^{2+} channels co-exist at a single release site and contribute jointly to the local Ca^{2+} transient to trigger release at excitatory neurons. (i) The

percentage block of synaptic current by ω -CTx or ω -Aga adds to greater than 100% (Wheeler *et al.*, 1994; Wu and Saggau, 1994b; Mintz *et al.*, 1995; Wheeler *et al.*, 1996). For example, at hippocampal CA3-CA1 synapses ω -CTx blocks the excitatory postsynaptic current (EPSC) by 46% and ω -Aga by 85% (sum = 131%) (Wheeler *et al.*, 1994). Such supra-additivity can be explained if Ca^{2+} influx through N-type channels mixes with Ca^{2+} entering through P/Q-type channels at the release site. If N-type or P/Q-type Ca^{2+} channels were segregated (ie. found only on different presynaptic terminals) or their Ca^{2+} domains did not mix, then the sum of their block should be less than or equal to 100%. (ii) It is well established that a reduction in the probability of transmitter release (P_r) increases the degree of paired pulse facilitation (PPF) at central synapses (see below). Both ω -CTx and ω -Aga enhance PPF consistent with a reduction in P_r (Wheeler *et al.*, 1996). If N- and P/Q-type channels were segregated then a toxin would completely block release at those terminals containing only the subtype for which the toxin was specific and leave the other terminals untouched. The synaptic response would reduce but no change in PPF would be expected. (iii) Both ω -CTx block and ω -Aga block can be partially relieved by enhancing Ca^{2+} influx into the presynaptic terminal either by altering the action potential with the addition of 4-AP or increasing external $[\text{Ca}^{2+}]$ (Wheeler *et al.*, 1996). The increased influx of Ca^{2+} through the unblocked channel presumably partially substitutes for the loss of influx through the blocked channels. If the channel subtypes were segregated then no change in the percentage block of each toxin would be expected at elevated external $[\text{Ca}^{2+}]$ or in the presence of 4-AP (assuming these manipulations do not displace toxin block). These arguments have led to the proposal that the Ca^{2+} channel subtypes are uniformly distributed, with all excitatory presynaptic terminals containing both subtypes in the hippocampus and cerebellum. Although the experimental data strongly support a co-localisation of both channel subtypes at *some* presynaptic terminals, they do not demonstrate that *all* terminals contain both subtypes.

Few studies have attempted to set limits on the proportion of terminals that contain both Ca^{2+} channel subtypes. N-type Ca^{2+} channels were shown to be solely responsible for neurotransmitter release at ~45% of terminals in hippocampal culture (Reuter, 1995). This was illustrated by monitoring the depletion of the synaptic vesicle dye, FM1-43, at individual terminals. The rate of FM1-43 depletion gives a measure of P_r . A subset of terminals did not release transmitter in the presence of ω -CTx suggesting that release was supported by only N-type channels at these terminals. Using a different approach, Wheeler *et al.* (1996) suggested that a significant fraction of terminals cannot rely solely on N-type channels for neurotransmitter release. They concluded this by noting that under conditions of maximum Ca^{2+} entry into the presynaptic terminal (spike broadened with 4-AP) that ω -CTx block is significantly reduced from ~45% to ~9%. This suggests that P/Q-type channels can substitute for N-type channels and so largely restore synaptic transmission under conditions of increased Ca^{2+} influx.

In summary, there is conflicting evidence for the distribution of Ca^{2+} channel subtypes across different presynaptic terminals. Chapter 3 of this thesis addresses this issue by monitoring the probability of transmitter release in the presence of the selective Ca^{2+} channel blockers.

The relationship between Ca^{2+} influx and transmitter release

The non-linear relationship between extracellular Ca^{2+} concentration ($[\text{Ca}^{2+}]_o$) and transmitter release was first characterised at the frog neuromuscular junction (NMJ) by Dodge and Rahamimoff (1967). In this preparation the excitatory junction potential amplitude varies as the 4th power of $[\text{Ca}^{2+}]_o$ at low concentrations. This implicates the cooperative involvement of 4 Ca^{2+} ions in the release of each vesicle of transmitter (Dodge and Rahamimoff, 1967). A similar 4th power relationship was shown at the squid giant synapse (Augustine and Charlton, 1986; Stanley, 1986). The relationship between transmitter release and $[\text{Ca}^{2+}]_o$ is also steeply non-linear at central synapses. It is more difficult to measure the degree of cooperativity in CNS preparations due to

signal-to-noise limitations. Cooperativity estimates suggest that between 2 and 4 Ca^{2+} ions are involved in the release of each vesicle at CNS synapses (Wu and Saggau, 1994b; Mintz *et al.*, 1995; Borst and Sakmann, 1996; Takahashi *et al.*, 1996).

The Dodge-Rahamimoff equation was derived to explain the role of Ca^{2+} in triggering transmitter release at the frog NMJ (Dodge and Rahamimoff, 1967). The equation provides a useful physiological model of transmitter release and has been used to describe release at hippocampal synapses (Wheeler *et al.*, 1996). An assumption of this equation is that the relationship between $[\text{Ca}^{2+}]_o$ and intra-terminal Ca^{2+} concentration ($[\text{Ca}^{2+}]_{it}$) is linear. However, saturation of Ca^{2+} influx through Ca^{2+} channels has been demonstrated in many preparations (Augustine and Charlton, 1986; Hess *et al.*, 1986; Church and Stanley, 1996). Two recent studies have also demonstrated a non-linear relationship between $[\text{Ca}^{2+}]_o$ and $[\text{Ca}^{2+}]_{it}$ for Ca^{2+} influx through presynaptic Ca^{2+} channels at CNS synapses. (i) $[\text{Ca}^{2+}]_{it}$ was measured using the Ca^{2+} sensitive dye, fura-2, that was loaded into the presynaptic terminals of the parallel fibre onto purkinje cells in the cerebellum (Mintz *et al.*, 1995). The relationship between $[\text{Ca}^{2+}]_o$ and $[\text{Ca}^{2+}]_{it}$ was shown to be sublinear and this relationship was described by a bimolecular process. (ii) Borst and Sakmann (1996) show a similar relationship at the giant calyx-type synapse in the rat medial nucleus of the trapezoid body. This large synapse allows electrophysiological recordings to be made directly from the presynaptic terminal. A sublinear relationship between the measured Ca^{2+} current and $[\text{Ca}^{2+}]_o$ was observed but no mathematical relationship was described. Wheeler *et al.* (1996) noted that the Ca^{2+} dose-response curve deviates from the Dodge-Rahamimoff equation at higher $[\text{Ca}^{2+}]_o$, consistent with a sublinear relationship between $[\text{Ca}^{2+}]_o$ and $[\text{Ca}^{2+}]_{it}$. Chapter 4 of this thesis develops a model of the transmitter release process at excitatory hippocampal synapses. The model is based on the Dodge-Rahamimoff equation and incorporates a sublinear relationship between $[\text{Ca}^{2+}]_o$ and $[\text{Ca}^{2+}]_{it}$.

Differences in the Ca²⁺ cooperativity for influx through different Ca²⁺ channel subtypes

It has been suggested that different Ca²⁺ channel subtypes mediate transmitter release with different cooperativities (Mintz *et al.*, 1995) but this remains controversial (Wu and Saggau, 1994b). Mintz *et al.* (1995) find that release is more steeply dependent on [Ca²⁺]_{it} for P/Q- than for N-type Ca²⁺ channels at synapses in the cerebellum. Cooperativity was estimated at 4 for P/Q-type Ca²⁺ channels and 2.5 for N-type channels. This study used Ca²⁺ sensitive dyes to measure [Ca²⁺]_{it} before and after selective block of each Ca²⁺ channel subtype. Wu *et al.* (1994) using a similar technique in the hippocampus found no significant difference in the cooperativity associated with different Ca²⁺ channel subtypes (Wu and Saggau, 1994b). Chapter 4 examines this issue by comparing Ca²⁺ dose-response curves in the presence of ω-CTx with dose-response curves in the presence of ω-Aga.

Ca²⁺ microdomains

To achieve rapid exocytosis from a presynaptic terminal a high [Ca²⁺]_{it} is required. Photolysis of caged Ca²⁺ in the presynaptic terminal and the simultaneous recording of the postsynaptic response showed that [Ca²⁺]_{it} is required to be higher than 50 μM for release to be equal to action potential dependent release (Heidelberger *et al.*, 1994; Lando and Zucker, 1994). Concentrations as high as 50 μM are only likely to be achieved at the face of the plasma membrane which contains clusters of Ca²⁺ channels. The specialised region of the presynaptic plasma membrane involved in release is known as the active zone. This region is structurally distinct and is defined as the area of plasma membrane where synaptic vesicles are docked. Between the docked vesicles is a region of electron-dense material thought to be cytoskeletal elements and other structural proteins, including Ca²⁺ channels which have been shown to clustered at active zones (Neher, 1998). P/Q- and N-type Ca²⁺ channels are known to be associated with synaptic proteins and are thought to be part of a release complex at the active zone (Martin-Moutot *et al.* 1996; Sheng *et al.*, 1996). When the

Ca²⁺ channel opens, the influx of Ca²⁺ creates a local Ca²⁺ gradient. This local gradient has been termed the "Ca²⁺ microdomain".

The [Ca²⁺] achieved at the release site upon opening of Ca²⁺ channels will be determined by the interplay of many factors, most of which remain poorly understood. These include: (i) the distance between the release site and each Ca²⁺ channel; (ii) the number of Ca²⁺ channels near the active zone that open simultaneously; (iii) the local diffusion coefficient of Ca²⁺ at the active zone; and (iv) the presence of Ca²⁺ buffers at the active zone.

The above mentioned evidence for the clustering of Ca²⁺ channels at the active zone does not provide an estimate for the distance between Ca²⁺ channels and the release site. Some indirect evidence favours the close apposition of Ca²⁺ channels to the release mechanism, including the rapid triggering of release upon Ca²⁺ channel opening and the lack of effect of introduced Ca²⁺ buffers such as EGTA (Llinas *et al.*, 1981; Adler *et al.*, 1991; Sabatini and Regehr, 1996). However, at some central synapses EGTA has been shown to reduce transmitter release (Borst and Sakmann, 1996). This argues against a close apposition. Whether release is predominantly initiated by influx through an individual Ca²⁺ channel or whether it requires the opening of multiple channels also remains contentious (see Chapter 4, Discussion). The evidence suggesting a close apposition of Ca²⁺ channels to the release mechanism also argues for limited interaction between Ca²⁺ microdomains. Stanley (1993) provided further support for this by showing that the opening of a single Ca²⁺ channel was sufficient to evoke release. However, the supra-additivity of the selective Ca²⁺ channel toxins (Wheeler *et al.*, 1994; Wu and Saggau, 1994b; Mintz *et al.*, 1995; Wheeler *et al.*, 1996) argues strongly for a mixing of Ca²⁺ microdomains.

The complexity of the local diffusion and chelation of Ca²⁺ has been explored primarily with numerical models (Neher, 1998). However, little is understood about the properties of Ca²⁺ buffers at the active zone: Are the Ca²⁺ buffers mobile? Do

they saturate? What are their kinetic parameters? Given that transmitter release depends on a high power of $[Ca^{2+}]$ subtle changes in these parameters have profound effects on release. Models developed to explain the Ca^{2+} dynamics and transmitter release are therefore limited by these unknown parameters.

In short, we are a long way from understanding the intricacies of Ca^{2+} behaviour within the presynaptic terminal and the effect of this behaviour on transmitter release.

Summary

The entry of Ca^{2+} into the presynaptic terminal via voltage activated Ca^{2+} channels is a crucial step in the initiation and modulation of transmitter release. The physiological relevance for the diversity of Ca^{2+} channel subtypes remains largely unknown. The development of the selective toxins, ω -CTx and ω -Aga, has provided powerful tools with which to address such issues. Two series of experiments described in Chapters 3 and 4 use the selective toxins to examine how the N- and P/Q-type Ca^{2+} channels interact with the release mechanism at excitatory hippocampal synapses.

Part II : Long term potentiation

Historical perspective

An understanding of the physiological basis of learning and memory remains elusive. The most popular hypothesis, that memories might be stored by changing the strength of inter-neuronal connections, was proposed at the turn of the century by Ramon Cajal. This hypothesis was later formalised by Hebb (1949), who suggested that memories could be stored by forming associative connections between neurons. The increase of synaptic strength between neurons was proposed to be dependent on the simultaneous activation of both neurons. The discovery by Bliss and Lomo (1973) of a long lasting enhancement in synaptic efficacy in response to a train of electrical stimulation provided the first experimental model of synaptic plasticity. This phenomenon was termed long term potentiation (LTP) and has since been studied extensively as the proposed physiological mechanism underlying learning and memory. The finding was particularly exciting because: (i) it was demonstrated in the hippocampus, a structure that is known to be involved in spatial memory; (ii) the duration of the potentiation was long lasting (hours); and (iii) the LTP was induced by patterns of electrical stimulation that are similar to those demonstrated in living brains. Numerous physiological and behavioural studies have since established LTP as the primary candidate for the cellular process underlying memory. However, there is still considerable debate as to the mechanisms which produce the increase in synaptic efficacy.

Different forms of LTP

There are three major excitatory synaptic pathways in the hippocampus on which most LTP studies have focused: the perforant path onto granule cells in the dentate gyrus; the mossy fibre input to CA3 pyramidal neurons; and the Shaffer collateral/commissural pathway onto pyramidal cells in the CA1 region of the hippocampus. All three pathways use glutamate as their neurotransmitter which activates both α -amino-3-hydroxy-5-methylisoxazole-4-propionic acid (AMPA) and

N-methyl-D-aspartic acid (NMDA) postsynaptic receptors. However, it is well recognised that LTP induction differs between the mossy fibre pathway and the other two pathways (Nicoll and Malenka, 1995). Both CA1 and dentate gyrus LTP are dependent on the influx of Ca^{2+} through NMDA receptors (Bliss and Collingridge, 1993), while mossy fibre LTP occurs independently of the NMDA receptor (Zalutsky and Nicoll, 1990). It is also well established that the synaptic potentiation after LTP induction is a presynaptic phenomenon at mossy fibre synapses (Zalutsky and Nicoll, 1990; Nicoll and Malenka, 1995; Son and Carpenter, 1996). In contrast, the locus of expression of NMDA-dependent LTP remains controversial. This thesis examines LTP at synapses originating from the medial perforant path in the dentate gyrus, an NMDA receptor dependent form of LTP (Colino and Malenka, 1993).

Different stages of synaptic potentiation

High frequency stimulation induces two phases of decremental potentiation that are distinguished by their time course and D-2-amino-5-phosphonovaleric acid (APV) sensitivity. APV is a blocker of the NMDA receptor. The first phase, post-tetanic potentiation, has a very short duration (~1 - 4min), is insensitive to APV and is thought to be mediated by a simple presynaptic mechanism (Swandulla *et al.*, 1991). A second decremental phase, short term potentiation (STP), has a duration of ~10 -15min and is blocked by APV (Malenka, 1991). The following long-lasting, nondecremental component of potentiation is commonly considered to be LTP. The majority of studies comparing LTP and STP conclude that they are a similar form of potentiation. The induction of both are APV sensitive and require an increase in postsynaptic Ca^{2+} (Malenka, 1991). Additionally, STP has been shown to reversibly occlude LTP and *vice versa* (Huang *et al.*, 1992; but see Schulz and Fitzgibbons, 1997). Longer lasting LTP or late LTP (> 4 hours) can be distinguished from an earlier form of LTP by its dependence on protein synthesis (Nguyen *et al.*, 1994). Experiments presented in this thesis fit into the early phase LTP (> 20min but < 90min).

Associativity, cooperativity and input specificity of LTP

LTP has many of the characteristics expected from theories proposed for the formation of memory (Hebb, 1949) including three basic properties: associativity, cooperativity and input specificity (Bliss and Collingridge, 1993). Associativity describes how LTP induction at a given synapse can be influenced (or regulated) by other convergent synapses which terminate on a spatially distinct region of the postsynaptic cell. For instance, a weakly activated synapse which would not normally undergo LTP can increase synaptic strength if temporally associated with other, spatially distinct, synaptic inputs (McNaughton *et al.*, 1978; Levy and Steward, 1979). Cooperativity is a closely related concept which describes a stimulus intensity threshold for the induction of LTP. A weak stimulus activating relatively few afferent fibres does not trigger LTP while a larger stimulus intensity does. This is because a larger numbers of stimulated afferent fibres interact to produce mutual facilitation of LTP induction (McNaughton *et al.*, 1978). Input specificity refers to the finding that synaptic inputs that are not activated during the induction of LTP do not share the potentiation of the tetanised pathway in the same cell (Andersen *et al.*, 1977; Lynch *et al.*, 1977). All three of these properties are derived from an underlying requirement of LTP induction; that the postsynaptic cell needs to be strongly depolarised at the same time that the presynaptic terminals are releasing transmitter. These properties can all be explained by the unique properties of the NMDA receptor.

The NMDA receptor: a molecular coincidence detector

NMDA receptors play an instrumental role in LTP induction at certain synapses in the hippocampus. At low rates of synaptic activity NMDA receptors contribute very little to a synaptic response due to their Mg^{2+} block. The AMPA receptor plays the dominant role in fast communication between neurons. The size of the AMPA current is therefore the important parameter defining synaptic strength. However, NMDA receptors play an integral part in the LTP induction process. The NMDA receptor is highly permeable to Ca^{2+} . It is unusual in that it requires two events to occur simultaneously before it is capable of opening to allow the influx of Ca^{2+} . The

postsynaptic membrane must be sufficiently depolarised ($> -40\text{mV}$) to expel Mg^{2+} from the NMDA channel and at the same time glutamate needs to be released into the synaptic cleft promoting NMDA channel opening (Ascher and Nowak, 1988). It is the influx of Ca^{2+} into the postsynaptic cell through the NMDA receptor which is thought to initiate the cascade of events leading to an increase in synaptic efficacy.

Associativity, cooperativity and input specificity can all be explained by the unique properties of the NMDA receptor. The cooperativity threshold follows from the need to depolarise the cell to remove the Mg^{2+} block. Weak stimuli are unable to produce a depolarisation sufficient to unblock the NMDA receptor while stronger stimuli will depolarise the cell to greater than -40mV and remove the Mg^{2+} block. A similar explanation can be given for associativity, with sufficient depolarisation being provided by a different set of afferent fibres. Input specificity can be explained by the need for the presynaptic terminal to release glutamate at the same time as the cell is depolarised. It is important to note that NMDA receptor dependent LTP is not the only form; numerous other manipulations of Ca^{2+} entry into the postsynaptic neuron have also been shown to induce LTP (Bliss and Collingridge, 1993).

Ca^{2+} involvement in LTP induction

One of the few points of agreement in the LTP literature is that Ca^{2+} plays a central role in the induction of LTP. This was first illustrated by Lynch *et al.* (1983) who found that the induction of LTP could be blocked by the intracellular injection of the calcium chelator ethylene glycol-bis (β -aminoethyl ether) (EGTA) into the postsynaptic cell. Recent studies using other Ca^{2+} chelators confirm this result (Malenka *et al.*, 1988; Cowan *et al.*, 1998). Malenka *et al.* (1988) provided further evidence by injecting a Ca^{2+} caging compound into the postsynaptic cell. Flash photolysis of this compound releases Ca^{2+} and lead to an increase in synaptic strength similar to that observed in LTP. Also, the amount of LTP was shown to be progressively reduced at depolarised potentials (Malenka *et al.*, 1988; Perkel *et al.*, 1993). The positive potentials were postulated to reduce Ca^{2+} influx, thereby

suggesting an essential role for Ca^{2+} in LTP induction. The most likely candidate for the source of Ca^{2+} entry is through the NMDA receptor. Three other potential sources of Ca^{2+} include: (i) voltage activated Ca^{2+} channels, (ii) release from internal Ca^{2+} stores and (iii) influx of Ca^{2+} through certain AMPA channels. Debate exists as to the relative contribution of these different sources of Ca^{2+} to the induction of LTP and the relative contribution of each may vary between different synapses. The favoured hypothesis for NMDA-dependent LTP is that the Ca^{2+} influx through NMDA receptors elicits a cascade of events resulting in LTP induction (Bliss and Collingridge, 1993; Nicoll and Malenka, 1995).

Does LTP occur at a pre or postsynaptic locus?

One of the more enduring controversies in neuroscience has been the question of the pre- vs postsynaptic locus of LTP expression. The increase in synaptic efficacy after the induction of LTP could be accounted for by an increase of one or more of three synaptic parameters: (i) an increase in the probability of transmitter release (P_T); (ii) an increase in the postsynaptic amplitude in response to a vesicle of transmitter (quantal amplitude, q); or (iii) an increase in the number of active synapses contributing to a synaptic response (N). Numerous techniques have been developed to address whether LTP results from any one or a combination of these factors. This part of the introduction will outline several of these approaches.

Quantal analysis

Quantal analysis is the statistical analysis of synaptic transmission based on the assumption that it results from the probabilistic release of discrete vesicles of transmitter (the quantal model). The first use of quantal analysis examined transmitter release at the NMJ (Del Castillo and Katz, 1954). Quantal analysis has since been used to study synaptic transmission at both central and peripheral synapses (McLachlan, 1978; Redman, 1990). A number of techniques based on the basic assumptions of the quantal model have been developed: (i) $1/\text{CV}^2$ approach, (ii) the identification of peaks in amplitude histograms, (iii) detection of changes in the failure

rate and (iv) single release site analysis. Each has its advantages and inherent limitations which will be discussed.

1/CV² method

A frequently used method is based on changes in the coefficient of variation ($CV = \text{standard deviation}/\text{mean}$) of synaptic amplitude fluctuations after some modulation of synaptic strength. An advantage of the $1/CV^2$ method is that it does not require that individual quantal amplitudes be directly resolvable (McLachlan, 1978). The method assumes that a fixed population of individual release sites with identical quantal parameters (P_r and q). That is, the uniform binomial model is assumed to apply. A presynaptic change (P_r and/or N) predicts that $1/CV^2$ will change, while a postsynaptic site of expression (q) predicts that $1/CV^2$ will be unaltered following a modulation. If P_r is small, for a purely presynaptic modulation, the ratio of $1/CV^2$ before and following the modulation will equal the ratio of the EPSC amplitude before and after modulation. If both pre- and postsynaptic changes are involved the $1/CV^2$ ratio vs EPSC amplitude ratio will fall between the limits. Most studies that have used the $1/CV^2$ method in the CA1 region of the hippocampus have implicated an increase in the quantal content after LTP induction (Bekkers and Stevens, 1990; Malinow and Tsien, 1990; Manabe *et al.*, 1993; Kullmann *et al.*, 1996). Similarly, an increase in quantal content was observed in dentate (Wang *et al.*, 1996). However, this method assumes that transmitter release is described by a simple binomial process (Faber and Korn, 1991). Simulation experiments, in which EPSC amplitude fluctuations are generated from a number of synaptic terminals each with different quantal parameters, have shown that data typically interpreted as having both a pre- and postsynaptic locus may only be attributable to one or the other (Faber and Korn, 1991). Therefore, the use of the $1/CV^2$ method may be misleading given the possible variability in quantal parameters between release sites (eg. P_r (Rosenmund *et al.*, 1993)).

Quantal peaks method

The identification of peaks in amplitude histograms and determination of interpeak distance gives a measure of the quantal amplitude. Quantal analysis of amplitude histograms from the CA3 region of the hippocampus suggested a presynaptic mechanism for LTP. The amplitude histogram shifted to the right after LTP induction without any systematic changes in interpeak distances (Voronin, 1983). These studies were limited by the poor signal-to-noise ratio of conventional intracellular recordings. The application of the whole-cell voltage clamp technique allowed the study of synaptic transmission with much improved signal resolution. However, quantal analysis of amplitude histograms in the CA1 region of the hippocampus has produced varying results. A primarily presynaptic locus has been proposed in some studies (Malinow and Tsien, 1990) while other studies have proposed an increase in both quantal content (ie. the number of quanta per evoked EPSC) and quantal amplitude (Kullmann and Nicoll, 1992; Larkman *et al.*, 1992; Liao *et al.*, 1992; Stricker *et al.*, 1996a). Foster and McNaughton (1991) showed only a change in the quantal size. Quantal analysis of the lateral perforant path in the dentate region of the hippocampus suggests a presynaptic mechanism for LTP (Baskys *et al.*, 1991).

A strength of this approach is that the fitting of a theoretical function to peaks in the EPSC amplitude histogram may enable all synaptic parameters to be determined (Stricker *et al.*, 1996b). However, the identification of peaks in the amplitude histograms at central synapses is problematic. Reliable fitting of peaky histograms is dependent on a low quantal variance (ie. the variance of the amplitude in response to a single vesicle of transmitter) (Redman, 1990). There is considerable debate as to the true variance of the unitary synaptic amplitude with many reporting it to be high (Bekkers *et al.*, 1990; Liu and Tsien, 1995) while others suggesting it to be low (Jonas *et al.*, 1993; Stricker *et al.*, 1996b). Also, given the small number of EPSCs recorded in many of these studies, sampling error may be another potential concern for this form of analysis (Clements, 1991). Another problem is that the synaptic parameters of each activated release site may not be identical. The fitting of a theoretical function to

peaks in an amplitude histogram is dependent on underlying assumptions about the release mechanism. Simple binomial or Poisson distributions are often used but do not take into account variability between synaptic terminals. Finally, the identification of peaks in the histograms is based on the assumption that the response to an individual quanta can be identified over the background recording noise. The quantal amplitude is, however, close to the noise in many preparations. These limitations may explain the varying results obtained with this method.

Failures method

If the response to one quantum of transmitter can be detected reliably then the failure rate of synaptic transmission can be used as an indicator of P_T . This method has been frequently used in conjunction with either peak fitting or $1/CV^2$ methods. A reduction of synaptic failures has been observed in CA1 (Malinow and Tsien, 1990; Malinow, 1991; Kullmann and Nicoll, 1992; Stricker *et al.*, 1996a). This has been interpreted as meaning that there is a increase in P_T (Malinow and Tsien, 1990; Malinow, 1991; Kullmann and Nicoll, 1992; but see Stricker *et al.*, 1996a). This index of P_T will be compromised if there are difficulties with the detection of single quanta. For instance, if LTP increases q then, due to the improved detection of the larger quantal amplitude, there could be an apparent increase in P_T even in the absence of presynaptic change.

Single release site method

Quantal parameters can theoretically be estimated by stimulating a single release site. The failure rate gives a measure of P_T while the amplitude of successful EPSCs gives a measure of q . Three studies have now compared synaptic parameters before and following the induction of LTP at putative single release sites. A putative single release site is identified in these studies by strict criteria including uniform onset and waveform of consecutive EPSCs. LTP induction in the CA1 and CA3 regions reduced the failure rate at putative single release sites, consistent with a change in P_T , but little change in q (Stevens and Wang, 1994; Bolshakov and Siegelbaum, 1995). However, a more recent study using the same technique shows an increase in q after the induction

of LTP (Isaac *et al.*, 1996). Experimental limitations are a concern for this type of analysis because: (i) the intrinsic recording noise is close to the measured EPSC amplitudes and (ii) the relatively indirect assessment of the number of release sites. This apparently simple measure of the quantal parameters still gives conflicting results, raising doubts as to the technical feasibility of such studies.

Miniature analysis

The analysis of miniature excitatory postsynaptic currents (mEPSCs) is another technique that can distinguish between pre- and postsynaptic changes in synaptic efficacy. A mEPSC is thought to be generated by the spontaneous release of a single vesicle of transmitter and as such is a direct measure of q that is free of assumptions about the statistics of evoked transmitter release. Analysis of mEPSCs assumes that changes in mEPSC amplitude reflects a postsynaptic change while changes in the frequency reflects changes in P_r . In CA1 pyramidal cells the induction of LTP produced a large increase in the amplitude of mEPSCs consistent with a postsynaptic locus of expression (Manabe *et al.*, 1992). LTP induced by ionophoretically applied glutamate to the dendrites of CA1 pyramidal neurons also produced a marked increase in mEPSC amplitude (Cormier and Kelly, 1996). In contrast, glutamate induced LTP in cultured hippocampal neurons was shown to change the frequency of mEPSCs while their average amplitude was unaltered, implicating a presynaptic locus (Malgaroli and Tsien, 1992). The discrepancy may be explained by a difference in the experimental system (cultured *vs* CA1 slice). A methodological concern for mEPSC analysis is that it depends on the accurate detection of mEPSCs above normal recording noise (see Chapter 5, Discussion). Typically, detected mEPSCs exhibit a range of amplitudes that grade continuously into the noise suggesting that there may be a detection problem.

Paired pulse facilitation as an index of P_r

Paired pulse facilitation (PPF) refers to an increase in an evoked synaptic response to the second stimulus pulse of a paired pulse paradigm. The increased size of the second

response is presumably a result of an increase in P_T , due to residual Ca^{2+} in the presynaptic terminal (Zucker, 1989). Manipulations known to alter P_T also alter the degree of PPF. A reduction in PPF is observed when P_T is increased, conversely, an increase in PPF is observed if P_T is lowered. Thus PPF provides an index of P_T . Early studies looking at the perforant pathway to the dentate showed no change in PPF after the induction of LTP, indicating no change in P_T (McNaughton, 1982). A similar finding was observed more recently for the medial perforant path (MPP) in the dentate (Christie and Abraham, 1994). However, Christie and Abraham (1994) showed a reduction in PPF after LTP induction for the lateral perforant path (LPP) implicating a change in P_T . Paired pulse experiments in the CA1 region of the hippocampus have also shown no change in PPF following the induction of LTP (Muller and Lynch, 1989; Manabe *et al.*, 1993; Kuhnt and Voronin, 1994; Schulz *et al.*, 1995; Wang and Kelly, 1997). PPF was shown to be unaltered during associational-commissural LTP but was reduced during mossy fibre LTP in the CA3 region of the hippocampus, consistent with a presynaptic locus of expression for the latter (Zalutsky and Nicoll, 1990).

More recent papers have queried the validity of using PPF as an index of P_T . PPF was reduced in experiments in which AMPA receptor responsiveness was altered via a Ca^{2+} /calmodulin pathway (Wang and Kelly, 1996; Wang and Kelly, 1997). Therefore, the magnitude of PPF seemed to be regulated by a postsynaptic mechanism although no account of a retrograde messenger affecting presynaptic parameters was considered in their conclusion. Also, PPF might not change if LTP selectively enhanced release at synapses with very low P_T (Bliss and Collingridge, 1993; Kullmann and Siegelbaum, 1995). Normally a reduction in PPF after increasing P_T is thought to involve a saturation of the facilitatory mechanism. Following LTP induction, if the P_T is increased only at terminals with very low initial P_T , then the increase in P_T at these terminals may not saturate the facilitatory mechanism. Thus, no change in the observed PPF would be expected (Bliss and Collingridge, 1993; Kullmann and Siegelbaum, 1995). Conclusions drawn from changes in PPF

implicating either a presynaptic or postsynaptic loci of LTP expression therefore need to be made with caution.

Progressive block in MK-801 as a measure of P_r

P_r can also be estimated using the drug MK-801 (Hessler *et al.*, 1993; Rosenmund *et al.*, 1993). MK-801 is an open-channel blocker of NMDA channels that is effectively irreversible at hyperpolarised potentials (Huettner and Bean, 1988). The rate of progressive block of the NMDA EPSC amplitude on successive stimuli can be used to estimate P_r . When P_r is high for a given terminal it is more likely to release glutamate and open NMDA receptors, which will therefore be blocked more quickly. An increase in P_r after the induction of LTP would be expected to increase the rate of progressive block. After LTP induction in the CA1 region of the hippocampus there was no detectable change in the rate of progressive block arguing against any change in P_r (Manabe and Nicoll, 1994). In contrast Kullmann *et al.* (1996), also studying the CA1 region, showed an increase in the progressive block rate, albeit small, following LTP induction. LTP induction of the mossy fibre input to CA3 pyramidal neurons showed a more substantial increase in the progressive block rate, in keeping with the proposed presynaptic locus for this form of LTP (Weisskopf and Nicoll, 1995). Due to the irreversible nature of the MK-801 block these experiments compare control progressive block rate with post LTP progressive block rate from different cells or different inputs onto the same cell. There is a large variation in the rate of progressive block in slice experiments making subtle changes after modulation difficult to interpret. Additionally, if LTP induction alters the open probability or kinetic parameters of the NMDA receptor (Lu *et al.*, 1998), then the comparison of the rate of progressive block would no longer be valid.

Scaling NMDA and AMPA receptor components of the EPSC as an index of P_r

Given that both AMPA and NMDA receptors are co-localised on the postsynaptic density of excitatory synapses (Bekkers and Stevens, 1989) a change in P_r would be expected to alter both currents. Post-tetanic potentiation (a presynaptic form of

potentiation) resulted in an increase in both AMPA and NMDA receptor mediated currents as expected (Kauer *et al.*, 1988). The presynaptic modulator, baclofen (GABA_B agonist), also alters both components of synaptic response (Perkel and Nicoll, 1993). In contrast, the induction of LTP in the CA1 region was associated with a specific increase in the AMPA component of the synaptic response arguing for a purely postsynaptic locus (Kauer *et al.*, 1988; Muller *et al.*, 1988; Perkel and Nicoll, 1993). Similarly, LTP in the dentate exhibited a selective enhancement of the AMPA component of the EPSC (Wang *et al.*, 1996). More recent studies have shown that NMDA receptor mediated current can undergo LTP (Bashir *et al.*, 1991; Xie *et al.*, 1992; Kullmann *et al.*, 1996). However, the persistent increase in the NMDA mediated component is generally small in comparison with that of the AMPA component (Kullmann *et al.*, 1996). Whether the enhancement of the NMDA component is due to a persistent increase in glutamate release or some postsynaptic modification remains to be resolved.

Miscellaneous techniques

Numerous other methods have been used to address the LTP pre- vs postsynaptic question. Early studies measuring the overflow of radiolabeled or endogenous glutamate before and after LTP argue for an increase in transmitter release (Bliss and Collingridge, 1993). Similarly, LTP in the dentate gyrus was associated with an enhancement of synaptosomal glutamate release (Canevari *et al.*, 1994). An antibody specific for the intraluminal domain of the synaptic vesicle protein synaptotagmin was used to visualise an increase in vesicular cycling after induction of LTP in cultured hippocampal neurons supporting a presynaptic locus (Malgaroli *et al.*, 1995). A postsynaptic locus should produce a change in the sensitivity of a neuron to exogenously applied AMPA receptor agonist before and after LTP. An increase in sensitivity of AMPA receptors was noted after LTP in CA1 (Davies *et al.*, 1989). Also, an increase in AMPA receptor binding has been illustrated by using a quantitative autoradiography method (Maren *et al.*, 1993). Hjelmstad *et al.* (1997) developed a method of measuring P_r based on a synaptic refractory period at short

paired pulse intervals. They show no change in P_r following LTP, consistent with a postsynaptic locus of expression in CA1.

Silent synapse theory of LTP

If a proportion of excitatory synapses express NMDA receptors but do not express functional AMPA receptors a proportion of synapses will be silent at resting membrane potentials (Kullmann and Siegelbaum, 1995). The theory predicts that on induction of LTP these silent synapses are unmasked, by either the insertion or activation of AMPA receptors, with no change in transmitter release. Indirect evidence for the silent synapse theory came from studies which investigated the CVs of the AMPA receptor- and NMDA receptor-mediated EPSCs respectively (Kullmann, 1994). It was found that basal CV was larger for AMPA EPSCs than NMDA EPSCs, consistent with more synapses containing NMDA receptors than AMPA receptors. Following LTP induction, there was a significant change in the CV for the AMPA EPSC while no change was observed for the NMDA EPSC. Kullmann (1994) argues that the result supports the silent synapse theory. Other evidence for silent synapses and their implication for LTP has come from experiments using minimal stimulation protocols (Isaac *et al.*, 1995; Liao *et al.*, 1995). After initially stimulating an afferent to evoke a clear AMPA EPSC the stimulus level was reduced until only failures were recorded at negative membrane potentials. The depolarisation of the neuron revealed a response which was sensitive to APV, suggesting an NMDA receptor mediated current. This indicated that at these synapses only NMDA receptors were active. Following the induction of LTP a response was detected at hyperpolarised potentials and these currents were blocked by CNQX. This confirmed the unmasking of an AMPA receptor mediated current from previously silent synapses. This conclusion depends on the reliable detection of small EPSCs using minimal stimulation protocols. It may be that small AMPA EPSCs are not detectable prior to LTP induction. Still, this evidence supports a postsynaptic increase in the AMPA receptor mediated current, either from undetectably small or from zero amplitude.

More recent evidence challenges this view. Both AMPA and NMDA EPSCs are increased following LTP induction (Kullmann *et al.*, 1996). Also, an increase was seen in the rate of progressive block of the NMDA EPSC in MK-801 following LTP. In contrast with the silent synapse theory, these findings are consistent with an increase in P_r . Kullmann *et al.* (1996) argue for a presynaptic contribution to LTP and for extrasynaptic spill-over of glutamate onto NMDA receptors to explain the disparity in CV between the AMPA and NMDA EPSCs.

Extrasynaptic glutamate spill-over

The glutamate spill-over model suggests that glutamate, released into the cleft, reaches a high concentration, opening both the AMPA and NMDA receptors while glutamate which escapes the cleft only opens NMDA receptors on neighbouring postsynaptic densities (Kullmann and Asztely, 1998). NMDA receptors have a much higher affinity for glutamate than AMPA receptors ($\sim x100$) (Patneau and Mayer, 1990). It is therefore feasible that the low glutamate concentration experienced by the neighbouring postsynaptic densities will only open NMDA receptors. This model can therefore explain why the quantal content sensed by AMPA receptors is less than that sensed by the NMDA receptors. Kullmann and Asztely (1998) explains the observation of silent synapses (based on the minimal stimulation protocol) by suggesting that the majority of the NMDA receptor mediated component arises from glutamate spill-over. If P_r of the "observed" synapse(s) is very low (< 0.01) then no AMPA receptor mediated signal is seen because no glutamate is released. That is, they are presynaptically not postsynaptically silent. On induction of LTP the synapses undergo an increase in P_r and an AMPA EPSC is observed. The discrepancy between the increase in the NMDA receptor mediated compared with AMPA receptor mediated component of the EPSC is explained by proposing that the majority of the NMDA receptor mediated signal is generated by spill-over of glutamate from synapses which do not undergo LTP. The theory is complicated by the proposed temperature dependence of the glutamate spill-over. Also, supporting evidence for an increase in P_r is based on the NMDA receptor mediated component of the EPSC. Any

postsynaptic modification of the NMDA receptor following LTP induction (Lu *et al.*, 1998) would complicate interpretation of both the progressive block in MK-801 and increase in the NMDA receptor mediated component.

Retrograde messengers

Given that NMDA-dependent LTP induction relies on a postsynaptic influx of Ca^{2+} any presynaptic enhancement would require a subsequent signal from the postsynaptic cell, a retrograde messenger. Numerous potential retrograde messengers have been proposed including; nitric oxide, carbon monoxide, platelet activating factor and arachidonic acid (Bliss and Collingridge, 1993). Synapsin I, a predominantly presynaptic protein, has been shown to be phosphorylated after high frequency stimulation (Fukunaga *et al.*, 1995). This phosphorylation was blocked by NMDA antagonists and postsynaptic calmidazolol implicating a postsynaptic Ca^{2+} /calmodulin pathway. However, a direct effect of CaM kinase II on presynaptic function during LTP, via a retrograde messenger cascade, has yet to be shown. The involvement of other Ca^{2+} dependent enzymes in the induction of potential retrograde messengers has been well established but the role these play in LTP has been questioned (Medina and Izquierdo, 1995).

Summary

As demonstrated in this review of the LTP literature, there is an ongoing debate as to the true locus of LTP expression. The inherent limitations of the methods developed to date mean that other methods of determining synaptic parameters before and following LTP will need to be explored. Chapter 5 of this thesis describes a method based on the probabilistic nature of synaptic transmission, the variance-mean analysis, derived by Dr. J. D. Clements. The variance of the evoked synaptic amplitude is plotted against mean synaptic amplitude at several different Cd^{2+} or Ca^{2+} concentrations. The slope of the variance-mean plot estimates the average amplitude of the response following the release of a single vesicle of transmitter. The technique is free of many of the assumptions concerning the transmitter release mechanism

required for traditional quantal analysis. Also, because it can be applied to large compound EPSCs it is free of experimental limitations of having to resolve individual quantal amplitudes. This technique is used to investigate the locus of LTP expression in the dentate region of the hippocampus.

Chapter 2

General Methods

I. Hippocampal Culture Experiments

Culture preparation

The method of Furshpan and collaborators was used to grow single, isolated hippocampal neurons on "microdots" of growth substrate (Furshpan *et al.*, 1986).

Plate preparation

Except where specified, all of the following procedures were performed using sterile technique in a laminar flow hood. Clean coverslips were maintained under 95% ethanol and flamed dried before use to ensure sterility. The coverslips were placed in 24-well culture plates, thinly covered in 0.15% agarose (Sigma) solution in dH₂O and allowed to dry. A mixture of rat tail collagen (Sigma) at 0.25mg/ml and poly-D-lysine (Collaborative Research) at 0.4mg/ml was applied in a fine mist to the coverslips using a glass microatomizer (Fisher Scientific) and allowed to dry. This yielded randomly distributed spots of growth substrate on the coverslip (microdots). A small aliquot of culture medium (composition below) was placed into each well to wash the substrate and the plate was placed in a humidified 5% CO₂ incubator (Forma Scientific) overnight. This solution was removed just prior to use the following day.

Dissociation procedure

The enzyme solution (composition below) was prepared in 15ml Falcon tubes and placed in a 37°C water bath for 30 minutes prior to dissociation. The hippocampi of two new born Wistar rats were dissected out under Minimum Essential Medium (MEM, Gibco BRL) warmed to 37°C. The whole hippocampus was then cut into ~1mm cubes and placed into the enzyme solution in a sterile 15ml Falcon tube. The

tube was placed in a water bath at 37°C and gently agitated for 30-40 minutes. A lightly flame-polished Pasteur pipette was used to transfer the tissue from the enzyme solution into a new 15ml Falcon tube. In order to halt further enzymatic activity the tissue was rinsed four times with fresh culture medium (37°C), discarding the supernatant each time. After the final rinse 1-2ml of culture medium was added and the tissue was gently triturated using the flamed Pasteur pipette. The tissue was allowed to settle and the supernatant containing dissociated cells removed and placed in a fresh Falcon tube. This procedure was repeated 4-6 times triturating a little more vigorously each time. The concentration of cells was determined by counting them using a haemocytometer under a phase contrast microscope. The cell suspension was diluted with culture medium (37°C) to 4-6 x 10⁴ cells per ml and a 0.5ml aliquot was placed into each well of the prepared plate. The plated neurons were kept in a humidified 5% CO₂ incubator maintained at 37°C.

Maintenance of hippocampal neurons.

The cells were fed after 3-4 days or when the glia were 80% confluent. A 0.25ml aliquot of medium was removed and replaced with 0.25ml of fresh culture medium to which 10µM cytosine b-D-arabinofuranoside (araC, Sigma) had been added. The araC acts to suppress cell division, reducing the possibility of overgrowth by glia. The cells were fed again on day 7-8 using the same method but with fresh culture medium only. The neurons seemed to prefer self conditioned media and were not fed again. Neurons survived up to 28 days under these conditions. Usually 1-4 "microdots" per coverslip had a single neuron growing on them. As these isolated neurons develop in culture they form synapses onto their own dendrites (Fig. 2.1A, Fig. 2.2A, B). These synaptic connections have been termed "autapses" (Van der Loos and Glaser, 1972; Bekkers and Stevens, 1991).

Figure 2. 1

Figure 2. 1 Hippocampal neurons grown in isolation on a "microdot" form synapses onto their own dendrites (autapses).

A, Phase contrast micrograph of a neuron grown in culture for 9 days on a "microdot" of collagen/poly(d-lysine).

Bar = 50 μ m.

A

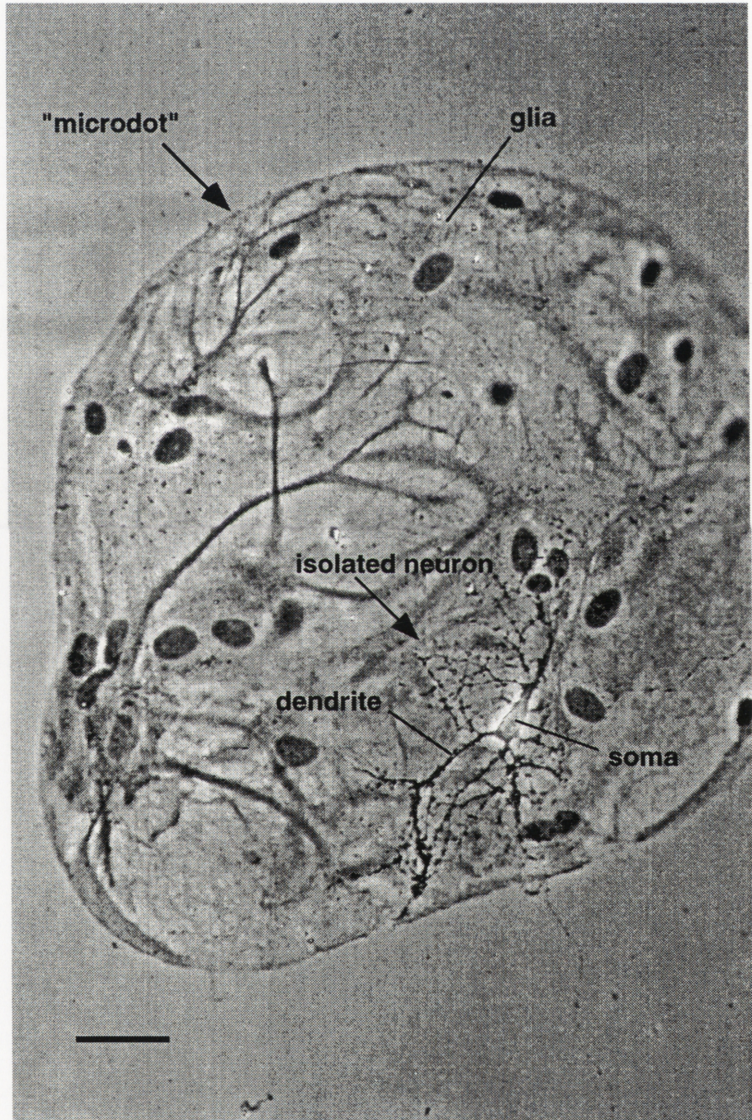
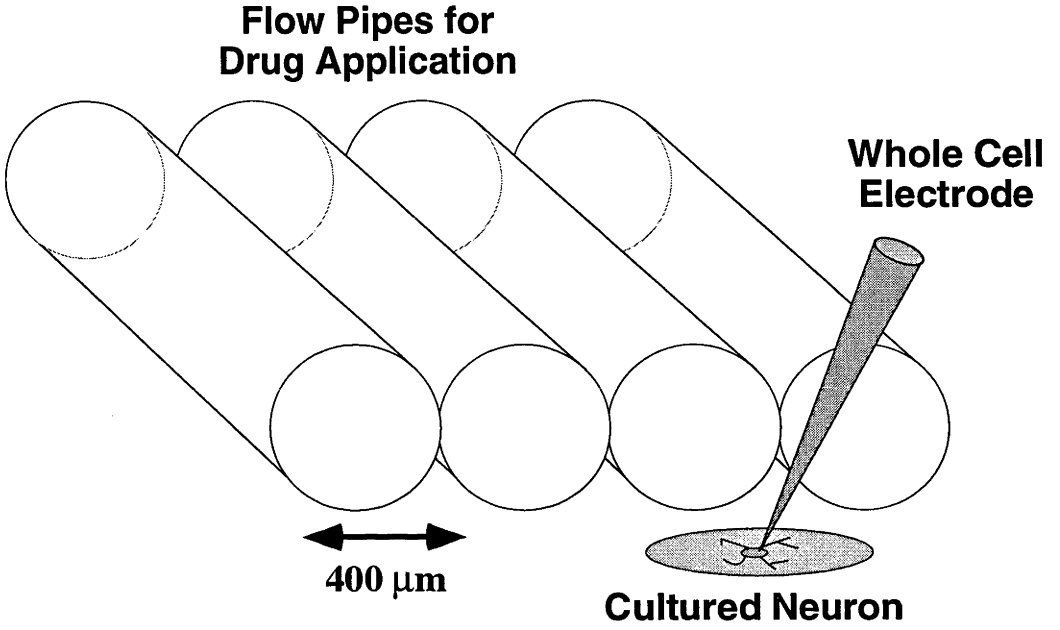


Figure 2. 2 A cartoon illustrating the autaptic culture system.

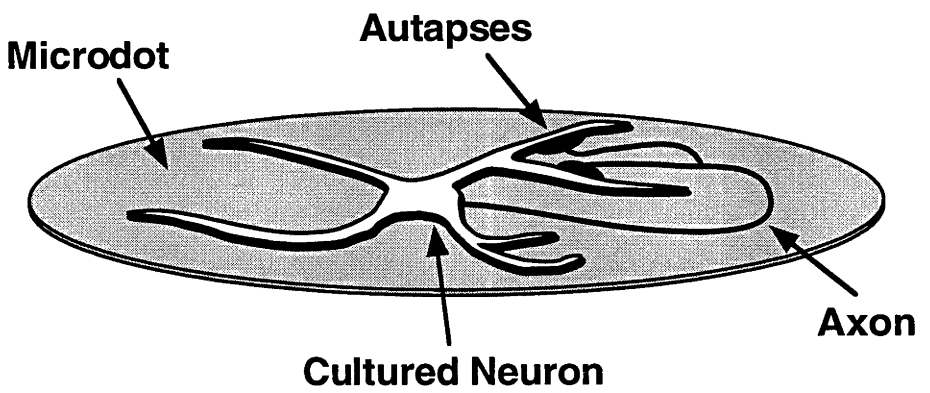
A, An illustration of the flow pipe set up used for drug application. The size of the pipes is greater than the "microdot" ensuring a uniform drug concentration at all terminals.

B, A cartoon illustration of an isolated neuron forming autaptic connections.

A



B



Solutions used in the culture preparation

Culture Medium:

To prepare 200ml of culture medium, the following were mixed in a sterile 200ml measuring cylinder:

- 4ml of 1M stock glucose in MEM
- 10ml of Fetal Bovine Serum (CSL)
- 2ml Penicillin/Streptomycin 5000 units/ml (CSL)
- 200µl Serum Extender (Collaborative Research)
- make to 200ml with Minimum Essential Medium (MEM, Gibco BRL)
(with Earle's salts
without L-glutamine
without phenol red)

The solution was filtered through a 0.22µm Millipore filter into sterile glass bottles for storage. The bottle in use was kept at 37°C in a humidified 5% CO₂ incubator, its lid slightly loosened to allow CO₂ equilibration.

Enzyme solutions:

Two alternative recipes were used depending on whether lyophilised papain or papain suspension was available.

(i) Lyophilised papain (to prepare 10ml):

- 2ml MEM
- 44µl of 50mM ethylenediaminetetraacetic acid (EDTA, pH adjusted to 7 with NaOH)
- 1.5-2mg cysteine (Sigma)
- 134µl of 1mM mercaptoethanol (Sigma)
- 200units lyophilised papain (Sigma)

The above reagents were added together in a 15ml Falcon tube and placed in a water bath at 37°C for 30min to activate the papain. The activated solution was then made up to 10ml with MEM and filtered through a 0.22µm Millipore filter.

(ii) Papain suspension (to prepare 10ml):

- 10ml MEM
- 100µl of 50mM EDTA (pH adjusted to 7 with NaOH)
- 150µl of 100mM CaCl₂
- 1.5-2mg cysteine (Sigma)
- 200 units papain suspension (Sigma)

The above reagents were added together in a 15ml Falcon tube and placed in the water bath at 37°C for 15min to dissolve the papain. The solution was then filtered through a 0.22µm Millipore filter.

Electrophysiology

Whole-cell patch-clamp recordings were obtained from isolated neurons found on "microdots" visually identified under a phase contrast microscope (Fig. 2.1, 2.2). All culture electrophysiological recordings have been made in voltage clamp mode using an Axopatch-1C Patch Clamp (Axon Instruments). All command potentials were generated by a software package written by Dr J. M. Bekkers and run on an Osborne 486-25 computer. The patch electrodes were pulled from thin walled borosilicate glass (micro-haematocrit tube, BRI), using a Flaming/Brown micropipette puller (model P-97, Sutter Instruments Co.). Patch electrodes had resistances ranging from 2.0 to 3.5 MΩ and contained (in mM) KMeSO₄ 125, KCl 5, EGTA 10, HEPES 10, Na₂ATP 2, MgCl₂ 2, GTP 0.4, pH 7.3, with osmolarity adjusted to 290mOsm with sorbitol. The usual bath solution contained (in mM) NaCl 135, KCl 5, CaCl₂ 3, glucose 10, HEPES 10, pH 7.3, with osmolarity adjusted to 310mOsm with sorbitol. Salts were from Johnson Matthey or Sigma. A number of variations were made to this

standard external solution and these have been noted in the appropriate Chapter Method section.

Light positive pressure was applied to the patch electrode and it was lowered, using a micromanipulator, onto the cell body of an isolated cultured neuron growing on a microdot. Once contact was made with the cell, light suction was applied until the electrode formed a giga seal with the cell membrane. The fast electrode capacitance was compensated by adjusting the Fast τ and Fast Mag dials, eliminating any transients generated by a repetitive step command potential. A series of sharp suction pulses were made until whole-cell access was obtained. Series resistance (R_S) was routinely monitored and only recordings exhibiting an R_S less than 10 M Ω were analysed. R_S was determined by applying a short 5mV voltage step and measuring the peak of the transient capacitance current. R_S compensation was made in order to: (i) reduce the voltage error due to current flow through the electrode; and (ii) reduce the membrane charging time. The initial current transient generated by the repetitive step command potential was eliminated by adjusting the series resistance and whole-cell capacitance dials. R_S compensation was in the range 80-90%.

Neurons were voltage clamped at -60mV and a 2-3ms voltage step to 0mV was applied via the somatic patch electrode. This voltage step opened voltage activated Na⁺ channels, initiating an action potential which propagated down the unclamped axon and into the presynaptic terminal, causing the release of neurotransmitter. The resultant autaptic current was recorded at the soma under reasonable voltage control (Fig. 2.3). Both excitatory and inhibitory neurons formed "autaptic" connections (Bekkers and Stevens, 1991) (Fig. 2.3). Only neurons exhibiting excitatory postsynaptic currents (EPSCs) were studied in experiments completed for this thesis. At times not all the neurons on a microdot can be visualised. Multiple neurons can give rise to polysynaptic connections. Polysynaptic connections, however, could be easily identified by a multicomponent postsynaptic current and were not analysed. All experiments were performed at room temperature (20-24°C).

Figure 2.3

Figure 2. 3 Both excitatory and inhibitory neurons form autapses.

A, Excitatory autaptic currents exhibit both a fast AMPA and slow NMDA component.

B, AMPA EPSCs can be isolated by blocking NMDA receptors with the addition of Mg^{2+} (10mM) to the bath solution.

C, NMDA EPSCs can be isolated by blocking AMPA receptors with the addition of CNQX (10 μ M) to the bath solution.

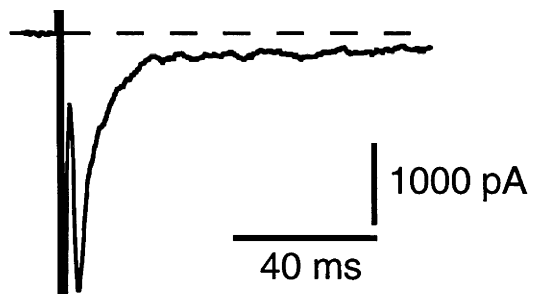
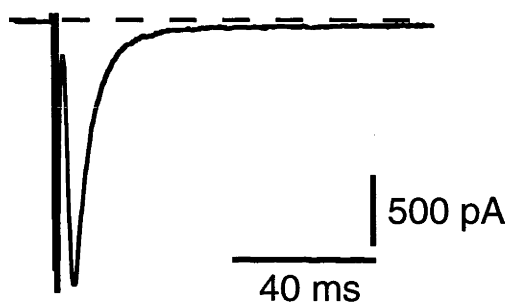
D, Inhibitory autaptic currents exhibit a positive current at negative holding potentials.

Holding potential was -60mV for all cells. Traces represent the average of 5-10 traces.

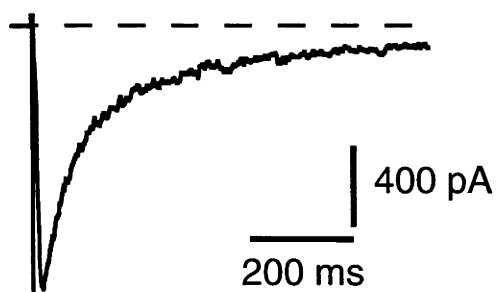
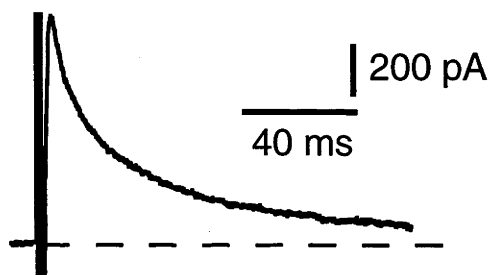
Recordings were from cells grown in culture for 10-14 days.

A

AMPA and NMDA

**B**AMPA (+Mg²⁺)**C**

NMDA (+CNQX)

**D**GABA_A

Data acquisition and analysis

The data acquisition program was written by Dr J. M. Bekkers and was run on an Osborne 486-25 computer. Individual records were filtered at 0.5 or 5kHz using a 4-pole Bessel filter. Data was digitised using a TL-1 DMA Interface board (Axon Instruments) and stored on disk. Data was analysed off-line using the analysis program Axograph (Axon Instruments).

Solution exchange

Solutions were applied via a series of glass flow pipes (Fig 2.2 A), the internal diameters of which (500 μ m) were larger than the diameters of the microdots; this ensured a uniform drug concentration at all autaptic contacts. Solution exchanges were made by quickly moving the flow pipes, through which solutions flowed continuously at \sim 0.1 ml/min, between autaptic stimuli. All drug solutions were gravity fed.

Characterisation of autaptic synaptic currents

Excitatory glutamatergic autapses exhibited both a fast AMPA and a slower NMDA receptor mediated component to the EPSC (Fig. 2.3A). The AMPA receptor mediated current could be isolated by blocking the NMDA component by the addition of either D-2-amino-5-phosphonovaleric acid (50-100 μ M, APV; RBI) or higher concentrations of Mg²⁺ (10mM, Fig. 2.3B) to the bath solution. NMDA receptor mediated currents can be isolated by the addition of 6-cyano-7-nitroquinoxaline-2,3-dione (10 μ M, CNQX; RBI) to the bath solution to block AMPA receptors (Fig. 2.3C). Inhibitory autapses generate an outward current at -60mV holding potential (Fig. 2.3D). Inhibitory currents have been shown to be blocked reversibly by picrotoxin (50 μ M) consistent with a GABA_A receptor mediated current (Bekkers and Stevens, 1991).

II. Hippocampal Slice Experiments

Slice procedure

Wistar rats (17-21 day old) were decapitated on a guillotine, their brains rapidly removed and placed into ice cold artificial cerebrospinal fluid (ACSF). The ACSF contained (in mM) NaCl, 125; KCl, 3; NaHCO₃, 25; NaH₂PO₄, 1.25; MgCl₂, 1; CaCl₂, 2; glucose, 11 and was gassed with 95% O₂/5% CO₂ (pH 7.4). The brain was hemisected along the midline and the cut surface was glued to the stage of a vibratome (Camden) with cyanoacrylic glue. The stage was immersed in ice-cold ACSF and 300µm parasagittal slices were cut. The overlying cortex was removed and the hippocampal sections transferred to a Gibb-type holding chamber (Edwards *et al.*, 1989) containing gassed ACSF. The slices were held at 34°C for 1 hour and then maintained at room temperature until recordings were made. An example of a hippocampal slice is shown in Fig. 2.4 A.

Electrophysiology

The slices were transferred to a recording chamber where they were superfused with gassed ACSF which contained 10µM bicuculline methiodide (Sigma). All slice electrophysiological recordings were made in voltage clamp mode using an Axopatch-200A Patch Clamp (Axon Instruments). All command potentials were generated by the software package pClamp (Axon Instruments) run on an Osborne 486-25 computer. The patch electrodes were pulled from thin walled borosilicate glass (micro-haematocrit tube, BRI) using a Flaming/Brown micropipette puller (model P-97, Sutter Instrument Co.). Patch electrodes had resistances ranging from 3.0 to 5MΩ. Patch electrodes contained (in mM) CsCl, 125; EGTA, 0.5; TES buffer, 10; ATP, 3; GTP, 0.4 and MgCl₂, 3. The pH was adjusted to 7.3 using CsOH and osmolarity was adjusted to between 270 and 290mOsm with sorbitol. Whole cell voltage clamp recordings were made using the "Blind" patch-clamp technique from dentate granule cells (Blanton *et al.*, 1989). Briefly, positive pressure was applied to the patch electrode and it was lowered onto the cell body layer identified in the dentate region of

Figure 2. 4

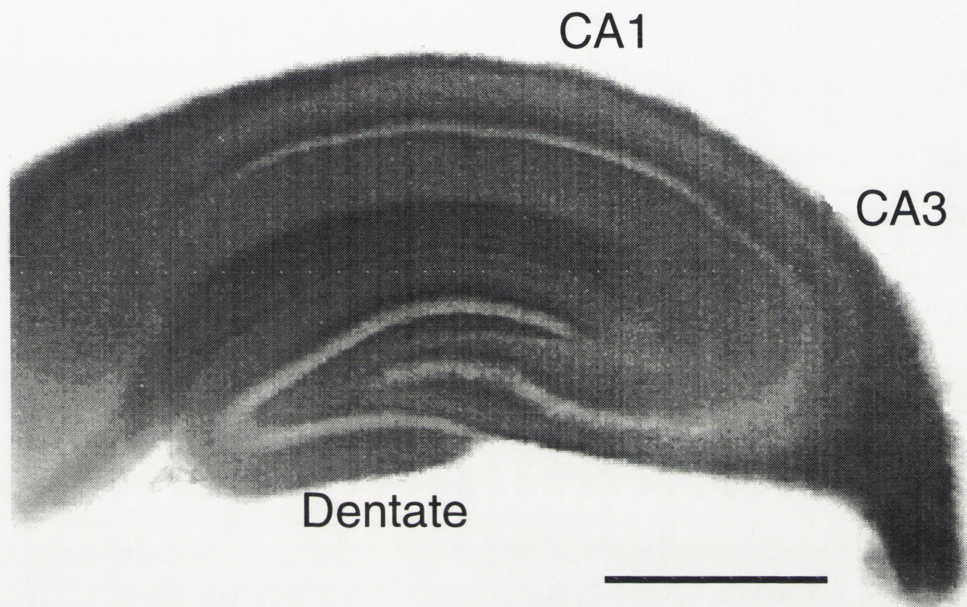
Figure 2.4 The hippocampal slice preparation.

A, A photograph of a hippocampal slice showing CA1, CA3 and the dentate regions.

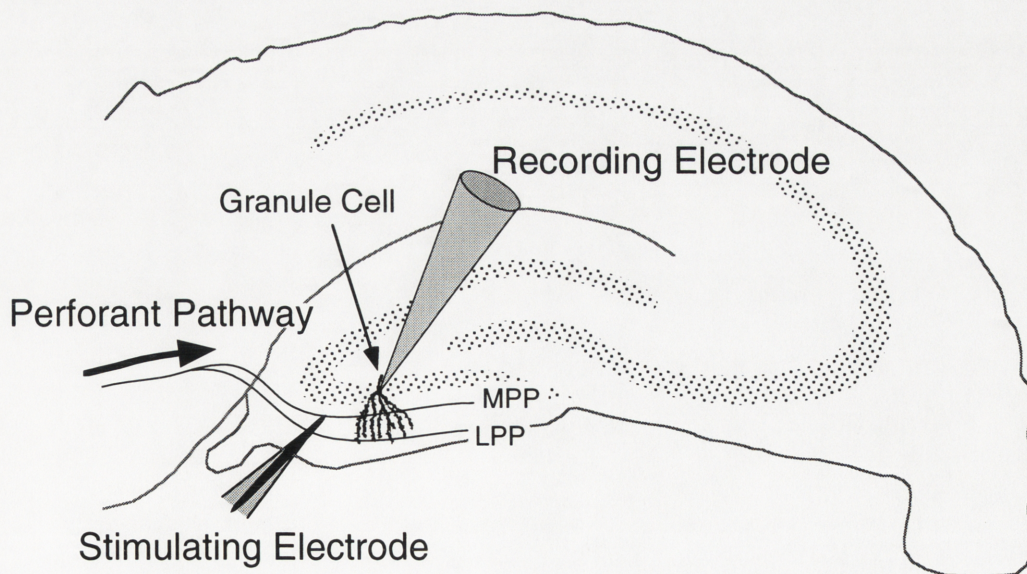
B, A cartoon of the hippocampus illustrating the stimulating and recording electrodes in the dentate region of the hippocampus. The stimulating electrode was positioned in the central third of the dentate gyrus molecular layer. This preferentially stimulated the medial perforant path (MPP). The lateral perforant path (LPP) runs along the outer third of the molecular layer.

Bar = 300 μ m.

A



B



the hippocampal slice viewed through a binocular dissecting microscope. Contact with a cell was indicated by the sudden increase in resistance which was monitored by a repetitive test pulse. Light suction was applied until a giga-seal was formed between the electrode tip and the cell membrane. The fast electrode capacitance was compensated by adjusting the Fast τ and Fast Mag dials. A series of sharp suction pulses were made until whole-cell access was obtained. R_s was monitored from the peak of the capacitance transient evoked by a voltage step and ranged between 10 and 27 M Ω . No R_s compensation was used.

EPSCs were evoked every 3s using low intensity, constant current stimulation through a concentric bipolar tungsten stimulating electrode. During synaptic stimulation cells were voltage clamped at between -60 and -70mV. The stimulating electrode was positioned in the central third of the dentate gyrus molecular layer, preferentially stimulated the medial perforant path (Fig. 2.4B) (McNaughton, 1980). Experiments were conducted at room temperature (20-24°C). External solutions were changed by perfusing the bath with > 10 times its volume.

Data acquisition and analysis

The software package pClamp (Axon Instruments) was used for data acquisition and was run on an Osbourne 486-25 computer. Individual records were filtered at 5kHz using a 4-pole Bessel filter. Data was digitised using a TL-1 DMA Interface board (Axon Instruments) and stored on disk. Data was analysed off-line using the analysis program Axograph (Axon Instruments).

Appendix

List of suppliers of materials and equipment:

Alomone Labs;	Jerusalem, Israel.
Axon Instruments;	Foster City, CA, USA.
BRI;	Herlev, Denmark.
Camden;	Leistersire, UK.
Collaborative Research;	Bedford, Mass, USA.
CSL;	Melbourne, Australia.
Fisher Scientific;	Loughborough, UK.
Forma Scientific;	Marietta, OH, USA.
Gibco BRL;	Gaithersburg, MD, USA.
Johnson Matthey;	Karlsruhe, Germany.
Millipore;	Sydney, Australia.
Pfizer Central Research;	Groton, CT, USA.
RBI;	Natick, MA, USA.
Sigma;	St. Louis, MO, USA.
Sutter Instruments Co.;	San Rafael, CA, USA.

Chapter 3

A Non-uniform Distribution of Ca²⁺ Channel Subtypes on Presynaptic Terminals

Introduction

Several different types of presynaptic Ca²⁺ channel are involved in the support of neurotransmitter release at central synapses. Among them are the two pharmacologically defined classes of Ca²⁺ channel subtype, the ω -CTx-sensitive (N-type) and the ω -Aga-sensitive (P/Q-type) Ca²⁺ channel. Both N-type and P/Q-types of Ca²⁺ channel support the release of glutamate at excitatory synapses in the hippocampus (see Chapter 1, Part I). The question of how these Ca²⁺ subtypes are distributed relative to each other on presynaptic terminals remains unresolved. Ca²⁺ channels could be distributed in one of three possible ways: (i) the subtypes are uniformly distributed with all presynaptic terminals containing both subtypes; (ii) some terminals contain only N-type while others have only P/Q-type Ca²⁺ channels; or (iii) is there a non-uniform distribution where some terminals only have N-type, others only P/Q-type, while others have a mixture of both.

Several lines of evidence suggest that Ca²⁺ channel subtypes are co-localised on excitatory presynaptic terminals and jointly contribute to the Ca²⁺ influx that triggers neurotransmitter release. This evidence includes: the supra-additive sum of ω -CTx and ω -Aga block; an increase in PPF by both toxins; and the partial relief of toxin block by increasing Ca²⁺ influx into presynaptic terminals (see Chapter 1, Part I). This evidence has led to the proposal that the Ca²⁺ channel subtypes are uniformly distributed, with all presynaptic terminals containing both subtypes. However, few studies have attempted to set limits on the degree of co-localisation of Ca²⁺ channel subtypes. By monitoring exocytosis, using the vital dye FM1-43, Reuter (1995) showed that ω -CTx completely blocked release in ~45% of terminals in hippocampal

culture. This suggested that N-type Ca^{2+} channels were solely responsible for neurotransmitter release at these synaptic terminals. In contrast, a different study found that ω -CTx block was only about 9% when Ca^{2+} entry into the presynaptic terminal was maximised by the addition of 4-AP in hippocampal slice (Wheeler *et al.*, 1996). Therefore, a significant fraction of terminals cannot rely solely on N-type channels for neurotransmitter release at hippocampal neurons.

N-type and P/Q-types of Ca^{2+} channel are differentially influenced by neuromodulators such as adenosine, GABA and glutamate (Wu and Saggau, 1994a; Wu and Saggau, 1995b; Qian and Saggau, 1997; Vazquez and Sanchez-Prieto, 1997; Huang *et al.*, 1998) (see Discussion). The way in which Ca^{2+} channels are distributed across presynaptic terminals will have important implications for how synaptic transmission is modulated. For instance, a non-uniform distribution of Ca^{2+} channel subtypes could permit selective alteration of transmitter release at a subset of terminals on a single afferent. Experiments presented in this chapter address the question of how Ca^{2+} channel subtypes are distributed across presynaptic terminals. The probability of transmitter release (P_T) was measured by analysing the progressive block of the NMDA receptor mediated EPSC using the irreversible open-channel blocker MK-801 (Hessler *et al.*, 1993; Rosenmund *et al.*, 1993). N-type or P/Q-type Ca^{2+} channels were selectively blocked and the changes in P_T were measured. Changes in P_T provided clues as to how Ca^{2+} channel subtypes are distributed across excitatory autaptic terminals in hippocampal cultures.

Methods

Whole-cell patch-clamp recordings were obtained from isolated hippocampal pyramidal cells as described in Chapter 2. The usual bath solution contained (in mM) NaCl 135, KCl 5, CaCl_2 3, glucose 10, HEPES 10, glycine 0.01, pH 7.3, with osmolarity adjusted to 310mOsm with sorbitol. NMDA-mediated currents were isolated by adding 10 μ M CNQX to all bath solutions. Ultra-pure NaCl and KCl salts (Johnson Matthey) were used for bath solutions to reduce possible Mg^{2+}

contamination. Currents were low pass filtered at 0.5kHz and digitally sampled at 1kHz.

The progressive block of the NMDA EPSC in the presence of MK-801 was fitted with a double exponential curve using a simplex fitting algorithm to minimise χ^2 .

$$\chi^2 = \sum (\text{experimental amplitude} - \text{predicted amplitude})^2 / \text{experimental amplitude}$$

This is not a true measure of χ^2 but is used because the standard deviation (SD) of each data point is not known. However, this form of χ^2 estimates the true χ^2 , based on the assumption that the SD at each data point is proportional to the amplitude of that data point. The quantal model of synaptic transmission predicts that the SD of the synaptic response is approximately proportional its amplitude at low P_r (Chapter 5). Implicit in the sum of squared errors (SSE) minimisation is the assumption that the SD of each point is constant. Therefore, χ^2 minimisation provides a more accurate estimate of the free parameters in the fit than the minimisation of SSE. In order to improve the signal-to-noise ratio in fits to the progressive block, NMDA EPSC currents were usually measured by averaging the amplitude over a 280 ms-long window starting 20ms after the stimulus (Rosenmund *et al.*, 1993). Residual non-NMDA current, measured in the same way in the presence of 100 μ M D-APV at the end of each experiment, was subtracted from all EPSC amplitude measurements.

In the paired-pulse experiments (Fig. 3.6), ten traces were averaged in each condition (with or without the second pulse) and EPSC amplitudes were measured by averaging over the range 20-40ms after the stimulus. The amplitude of the second EPSC was found by subtracting the averaged trace without the second stimulus from that with the second stimulus. Block by toxin after 30 stimuli in MK-801 (Fig. 3.7) was measured by fitting exponential curves to the progressive block time courses before and after addition of toxin, and finding the difference between these fitted curves extrapolated to the point at which toxin was first added. ω -CTx was obtained from Alomone Labs and ω -Aga was a gift from Pfizer Central Research. MK-801 was from RBI. ω -Aga experiments were done in bath solutions containing cytochrome-c (Sigma) at 1mg/ml

in order to reduce non-specific binding of the toxin. Control experiments showed that cytochrome-c alone had no effect ($98 \pm 2\%$, $n = 3$). Statistical comparisons were made using the t test.

Results

Progressive block of NMDA EPSCs by MK-801 yields P_T

MK-801 is an open-channel blocker of NMDA channels that is irreversible under the conditions of these experiments (Huettner and Bean, 1988). When autaptic NMDA EPSCs were repeatedly evoked at 0.1Hz in solution lacking MK-801, their amplitudes were stable (Fig. 3.1A, triangles; $n = 3$). When $2\mu\text{M}$ MK-801 was added to the external solution, stimulation at 0.1Hz caused a progressive reduction in the amplitudes of the EPSCs (Fig. 3.1A, filled circles; $n = 9$). Examples of individual NMDA EPSCs at different time points in a typical experiment are shown in Fig. 3.1B (normalised amplitudes on right). If the MK-801 was removed after 30 stimuli the EPSC amplitudes were stable (Fig. 3.1A, open circles; $n = 4$), confirming the irreversibility of the block under these recording conditions. The rate of the progressive block in MK-801 is proportional to transmitter release probability, P_T , because when P_T is high, synaptic terminals will be more likely to release glutamate and open postsynaptic NMDA channels, which will therefore be blocked more quickly. The utility of this technique has already been established (Hessler *et al.*, 1993; Rosenmund *et al.*, 1993; Manabe and Nicoll, 1994; Weisskopf and Nicoll, 1995).

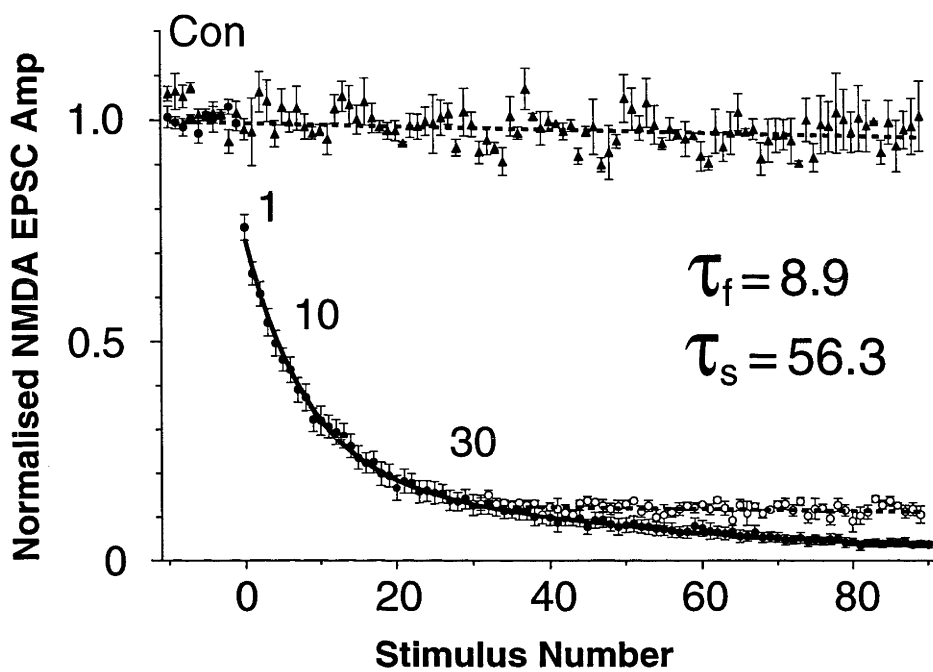
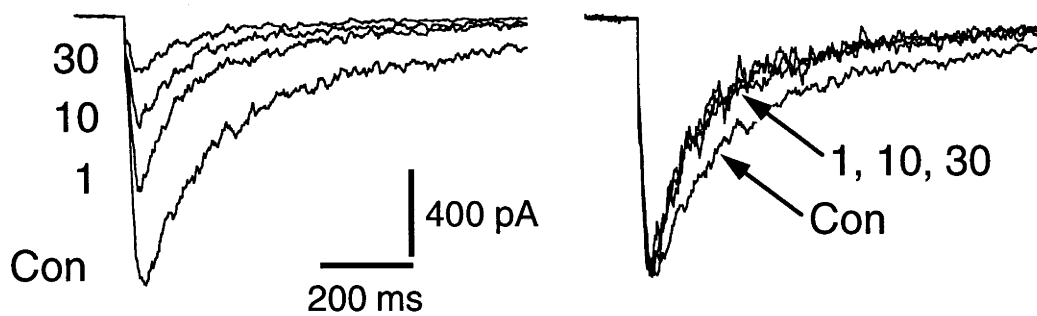
The time course of the progressive block of the evoked NMDA EPSC by MK-801 is well-fitted by a sum of two exponentials (Fig. 3.1A), suggesting that the population of synaptic terminals can be divided into two classes, one with a high P_T , the other with a low P_T (Hessler *et al.*, 1993; Rosenmund *et al.*, 1993). It is likely that terminals have a continuous range of P_T values (Huang and Stevens, 1997) and the criterion used to divide them into high- and low- P_T categories is somewhat arbitrary. However, the general conclusions are not dependent on this classification scheme and the double

Figure 3. 1

Figure 3. 1 Progressive block of NMDA EPSCs by the use-dependent open-channel blocker, MK-801, can be used to estimate the probability of glutamate release, P_r .

A, Averaged normalised NMDA EPSC amplitudes plotted against stimulus number, for three different kinds of experiment (different symbols). Each point is the ensemble average (\pm SEM) across different cells. *Triangles*: EPSC amplitude timecourse in normal bath solution without MK-801, showing the stability of the EPSCs over the duration of a typical experiment ($n = 3$ cells). *Filled circles*: EPSC amplitude timecourse in bath solution containing $2\mu\text{M}$ MK-801, applied at stimulus 0 and maintained until the end of the recording ($n = 9$). The superimposed solid line is a double exponential fit, suggesting the existence of at least two groups of terminals, one with a high P_r and the other with a low P_r . *Open circles*: EPSC amplitude timecourse after the removal of MK-801 after 30 stimuli, showing that the MK-801 block is irreversible under our conditions ($n = 4$).

B, **Left**: representative NMDA EPSCs recorded from one cell in control solution (trace labelled Con) and at 1, 10 and 30 stimuli after adding $2\mu\text{M}$ MK-801. Stimulus artefacts have been blanked. **Right**: the same EPSCs normalised at their peaks, showing that their decay is faster in the presence of MK-801 and does not change with stimulus number. This confirms that a homogeneous population of NMDA channels is being activated.

A**B**

exponential fit provides a useful estimate of the range and distribution of P_r values (see Discussion).

A heterogeneity in the open probability (P_o) of NMDA receptors could also be expected to give a double exponential progressive block of NMDA EPSC in the presence of MK-801. If two classes of NMDA receptors existed on the postsynaptic membrane, one with a high P_o and another with a low P_o , then the fast component of the MK-801 progressive block could be due to the preferential block of the high P_o NMDA receptors with the slower progressive block due to the low P_o receptors. This possibility is ruled out by observing the decay time course of the NMDA mediated EPSC at different sweep numbers in MK-801 (Fig. 3.1B). If glutamate activated a mixed population of NMDA channels, then those with a higher P_o will be preferentially blocked. This will bias the population towards low P_o NMDA channels as more channels are blocked by successive stimuli. MK-801 irreversibly blocks open channels early in the synaptic event preventing re-opening and thus accelerates the EPSC decay. This acceleration is expected to decrease with decreasing P_o (Rosenmund *et al.*, 1993). There is no change in the NMDA decay time course after successive stimuli in the presence of MK-801 (Fig. 3.1B) consistent with a uniform population of NMDA receptor P_o . This implies that the double exponential nature of the progressive block in MK-801 is not a function of postsynaptic NMDA receptor heterogeneity (Hessler *et al.*, 1993; Rosenmund *et al.*, 1993).

The rate constants of progressive block in $2\mu\text{M}$ MK-801 at 3mM Ca^{2+} were $\tau_{\text{fast}} = 8.9 \pm 1.1$ stimuli and $\tau_{\text{slow}} = 56.3 \pm 5.1$ stimuli (mean \pm SEM; $n = 9$). It is possible to get a quantitative estimate of P_r using the MK-801 progressive block time constants (Hessler *et al.*, 1993; Rosenmund *et al.*, 1993). However, this was not done here. The progressive block rate constants provide an index of changes in P_r and conclusions made from experiments in this chapter do not require the quantitative estimate of P_r .

The areas under each of the two fitted exponentials give the relative number of terminals in the high- and low- P_T categories (Hessler *et al.*, 1993; Rosenmund *et al.*, 1993). The area is proportional to the numbers of terminals (N) because the progressive block time constant of the exponential is proportional to $1/P_T$ while the exponential amplitude is proportional to the number of terminals times P_T . The area is therefore independent of P_T .

$$\begin{aligned} \text{Area} &= \text{Amplitude} \cdot \tau \\ &\propto N \cdot P_T \cdot 1/P_T \\ &\propto N \end{aligned}$$

In control conditions high- P_T terminals constituted $36.1 \pm 6.2\%$ of the total ($n = 9$).

Three lines of evidence confirm that the progressive block of NMDA EPSCs by MK-801 provides an index of P_T :-

(i) Adding Cd^{2+} ($3.5\mu\text{M}$) to the bath reduced NMDA EPSC amplitudes by $52 \pm 2.4\%$ ($n = 8$), presumably by non-selectively blocking presynaptic voltage-activated Ca^{2+} channels (Fig. 3.2A left) (Sather *et al.*, 1993; Sabatini and Regehr, 1995), although there is also a small postsynaptic blocking effect on the NMDA channel ($\sim 7\%$) (Mayer *et al.*, 1989). Progressive block rates in MK-801 were slowed approximately two-fold by Cd^{2+} : $\tau_{\text{fast}} = 19.1 \pm 2.7$, $\tau_{\text{slow}} = 96.5 \pm 12.4$ ($n = 8$) (Fig. 3.2A, right). This corresponds to a reduction of P_T by 53% and 42% at high- and low- P_T terminals, respectively. The percentage of high- P_T terminals was unchanged at $34.9 \pm 6.0\%$ (*cf.* 36.1% in control).

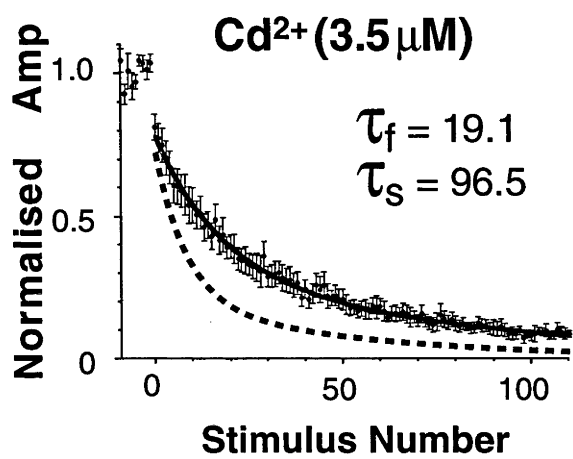
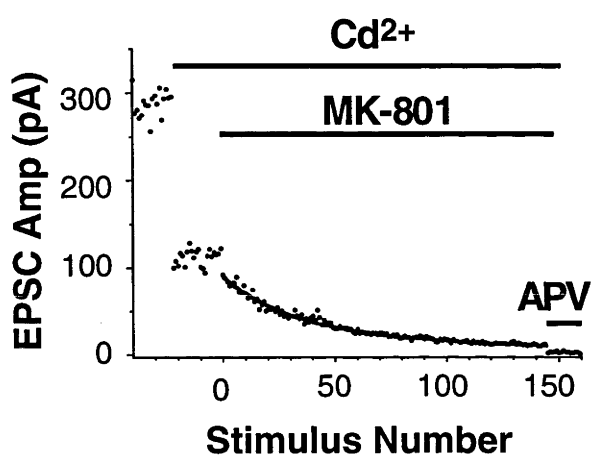
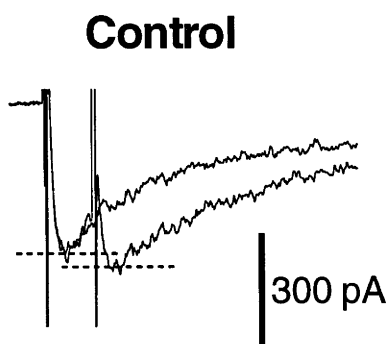
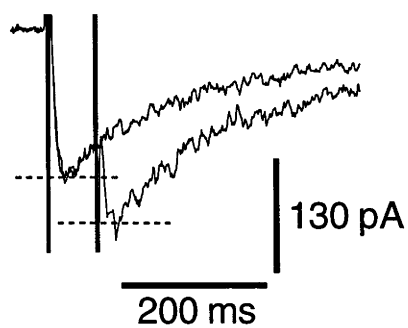
(ii) Reducing the external calcium concentration to 1.5mM reduced NMDA EPSC amplitudes by $38 \pm 3\%$ ($n = 5$) and slowed the progressive block rates: $\tau_{\text{fast}} = 14.9 \pm 1.0$, $\tau_{\text{slow}} = 77.2 \pm 10.0$ ($n = 5$). This corresponds to a reduction of P_T by 40% and 28% at high- and low- P_T terminals, respectively. The percentage of high- P_T terminals was unchanged at $37.2 \pm 3.7\%$ (*cf.* 36.1% in control). This data confirms previous results (Rosenmund *et al.*, 1993; Manabe and Nicoll, 1994).

Figure 3. 2

Figure 3.2 Control experiments confirm that MK-801 block measures P_T .

A, Non-selective partial blockade of presynaptic Ca^{2+} currents by Cd^{2+} uniformly reduces P_T at both high- and low- P_T terminals. **Left:** representative timecourse plot for one experiment, showing the block due to Cd^{2+} ($3.5\mu M$) and MK-801 ($2\mu M$). Periods of drug application are indicated by horizontal bars. At the end of the experiment $100\mu M$ D-APV was added, completely blocking the current and confirming that these were pure NMDA EPSCs. **Right:** normalised progressive block plots averaged as in Fig. 3.1A ($n = 8$ cells). The superimposed solid line is a double exponential fit with time constants shown in the inset; the dashed line is the control fit from Fig. 3.1A. Both block time constants are twice the corresponding control values (Fig. 3.1A), indicating a uniform halving of P_T by this concentration of Cd^{2+} .

B, Paired-pulse depression, which reflects P_T averaged across functioning terminals, is reduced after most high- P_T terminals have been masked by applying 30 stimuli in $2\mu M$ MK-801. All traces are averages of 10 sweeps and were obtained from the same cell in drug-free external solution before (**left**) and after (**right**) the stimuli in MK-801. The interstimulus interval was 70ms. Stimulus artefacts were not blanked.

A**B****After MK-801**

(iii) A standard way to detect a modulation of average P_T is to measure a change in paired-pulse facilitation or depression (Martin, 1977). After 30 stimuli in MK-801 most high- P_T terminals should be masked (Fig. 3.1A), thereby reducing the P_T averaged across all terminals contributing to the EPSC. Paired-pulse depression (70ms interstimulus interval) was measured in drug-free external solution before and after 30 stimuli had been applied in MK-801. The amount of depression was reduced by $31.3 \pm 7.5\%$ after MK-801 application ($p < 0.05$; $n = 7$) (Fig. 3.2B). This confirms the expected reduction in average P_T .

ω -CTx and ω -Aga affect P_T non-uniformly

Having shown that non-specific reduction of Ca^{2+} currents uniformly decreased P_T , the effect of selective blockade of calcium channel subtypes by ω -CTx or ω -Aga were explored next. When N-type calcium channels were irreversibly blocked by ω -CTx (1 μ M) (Williams *et al.*, 1992a; Fujita *et al.*, 1993) the NMDA EPSC amplitude was reduced by $41.2 \pm 4.7\%$ (Fig. 3.3A, left; $n = 9$) but there was no change in the time constants for the progressive block in 2 μ M MK-801: $\tau_{fast} = 7.3 \pm 1.3$, $\tau_{slow} = 50.1 \pm 4.9$ (Fig. 3.3A, right; $n = 8$). A postsynaptic effect of ω -CTx was excluded by Pfrieger *et al.* (1992) who showed that ω -CTx had no effect on the amplitude distribution of miniature EPSCs. Also the current generated by the application of exogenous AMPA to hippocampal pyramidal cells was unaltered in the presence of ω -CTx (Luebke *et al.*, 1993). By observing no change in the fibre volley on application of ω -CTx, a presynaptic effect on the action potential has been ruled out by Wheeler *et al.* (1995).

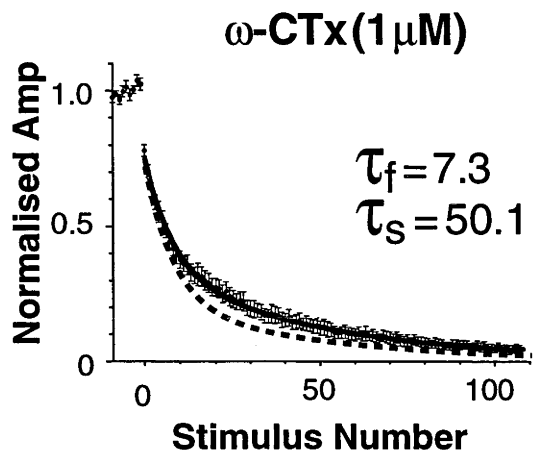
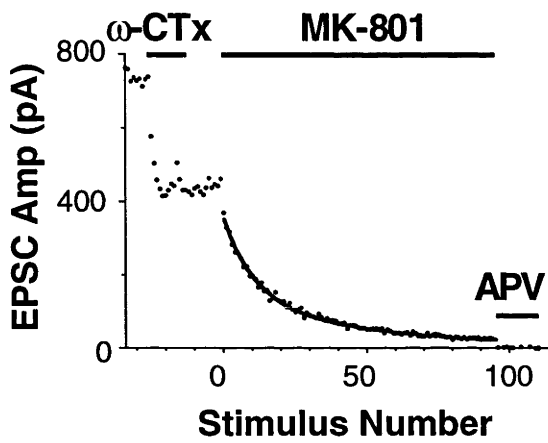
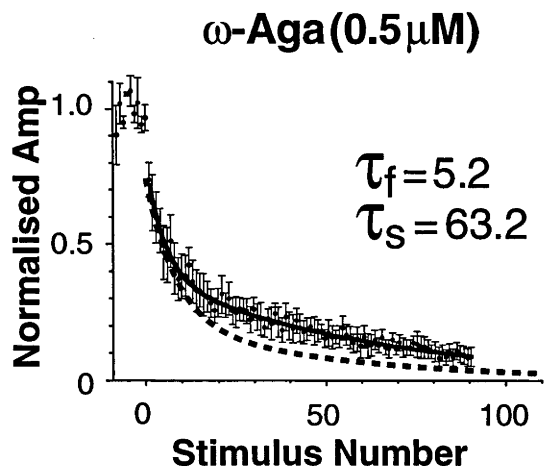
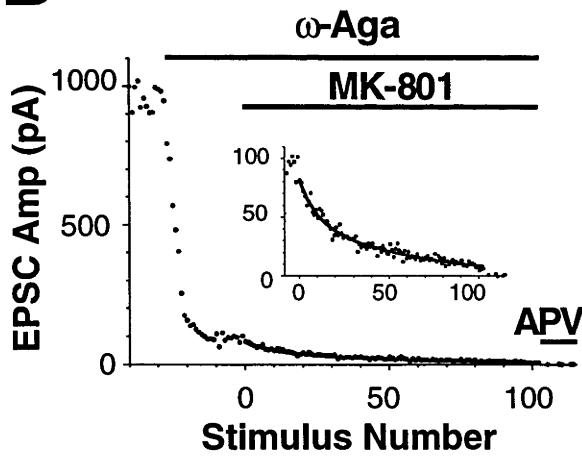
Since τ_{fast} was unchanged by ω -CTx, some functional high- P_T terminals remained after ω -CTx block. However, the percentage of these terminals was reduced to $19.2 \pm 4.7\%$ (*cf.* 36.1% in control), suggesting that some were shifted from the high- to low- P_T class. Can this shift from high- to low- P_T terminals explain the 41.2% average EPSC amplitude reduction in ω -CTx? The mean EPSC amplitude, I_{EPSC} , due to a fraction f_H of terminals with high P_T ($P_{T,H}$) and a fraction f_L ($= 1 - f_H$) of terminals

Figure 3.3

Figure 3. 3 Selective blockade of different Ca²⁺ channel subtypes by ω-CTx (**A**) or ω-Aga (**B**) has little effect on progressive block time constants, but reduces the proportion of high-P_r terminals.

Lefthand panels: representative timecourse plots for individual experiments. Horizontal bars show the periods of application of ω-CTx (1μM), ω-Aga (0.5μM), MK-801 (2μM) and D-APV (100μM). The progressive block in panel B (left) is shown expanded in the inset.

Righthand panels: normalised progressive block plots averaged as in Fig. 3.1A (n = 8 in A; n = 4 in B). The superimposed solid line in each panel is a double exponential fit with time constants shown in the inset; the dashed line is the control fit from Fig. 3.1A. The fitted time constants are similar to control, but the area under the fast component, which gives the proportion of high-P_r terminals, is reduced.

A**B**

with low P_r ($P_{r,L}$) is given by $I_{EPSC} = Ni(f_H P_{r,H} + f_L P_{r,L})$, where N is the total number of functional terminals and i is the unitary current. If N and i are unaffected by ω -CTx, then substitution of the values for $P_{r,H}$, $P_{r,L}$, f_H and f_L measured before and after ω -CTx predicts an amplitude reduction by the toxin of only 30%. Since ω -CTx does not have a postsynaptic effect on i , the additional 10% of block must be due to a reduction in N . Thus, a shift from the high- to low- P_r class cannot alone account for the observed amplitude reduction, and ω -CTx must completely block transmitter release from some terminals. This means that some terminals must contain only functional N-type Ca^{2+} channels.

ω -Aga at higher concentrations ($> 100nM$) is thought to block both P- and Q-type Ca^{2+} channels in the hippocampus (Wheeler *et al.*, 1994; Randall and Tsien, 1995; Scholz and Miller, 1995; Wheeler *et al.*, 1996). The toxin was used at $0.5\mu M$, and therefore ω -Aga-sensitive channels are referred to as P/Q-type channels. In the autaptic culture preparation the block by ω -Aga was reversible, so the toxin had to be present throughout the experiment (Fig. 3.3B, left). ω -Aga ($0.5\mu M$) blocked the NMDA EPSC amplitude by $81.2 \pm 3.2\%$ ($n = 5$) with no significant change in the progressive block time constants in $2\mu M$ MK-801: $\tau_{fast} = 5.2 \pm 1.6$, $\tau_{slow} = 63.2 \pm 15.8$ ($n = 4$; Fig 3.3B, right). Again, this suggests that release probability was unaltered at some terminals. The percentage of high- P_r terminals was reduced by ω -Aga to $8.4 \pm 2.4\%$ (*cf.* 36.1% in control). This reduction predicts a block by ω -Aga of about 50%, compared with the observed 81% block. So, by the same argument that was used for ω -CTx, transmitter release from some terminals must be completely blocked by ω -Aga. Thus, some terminals contain only functional P/Q-type channels.

ω -Aga-sensitive and ω -CTx-sensitive Ca^{2+} channels play a predominant role in the release of glutamate at excitatory synapses in the central nervous system including the hippocampus (see Chapter I, Part I). Many central synapses exhibit a component of release which is resistant to both ω -CTx and ω -Aga (Mintz *et al.*, 1995; Wu and Saggau, 1995a). Wheeler *et al.* (1996) suggest that this resistant channel plays a minor

role at hippocampal synapses. The co-application of ω -CTx (1 μ M) and ω -Aga (0.5 μ M) blocked NMDA EPSCs at autapses by $98.6 \pm 0.4\%$ ($n = 5$), confirming that N-, P- and Q-type Ca^{2+} channels are predominant in mediating excitatory synaptic transmission in hippocampal cultures (Fig. 3.4). However, a role of a resistant Ca^{2+} channel cannot be entirely ruled out.

Results for selective and non-selective Ca^{2+} channel blockers are summarised and compared in Fig. 3.5. Non-selective block by Cd^{2+} reduced release probability at all terminals (Fig. 3.5A, B) but did not alter the fraction of high- and low- P_r terminals (Fig. 3.5C). In contrast, selective block by ω -CTx or ω -Aga did not alter release probability at some terminals (Fig. 3.5A, B) but reduced the percentage of high- P_r terminals (Fig. 3.5C). These results suggest that the selective toxins completely blocked release from some terminals, converted some terminals from the high- to low- P_r class, and left the remainder unaffected. This implies a non-uniform distribution of N- and P/Q-type channels across presynaptic terminals.

Paired-pulse depression gives an average measure of P_r

Paired-pulse facilitation (PPF) and depression reflect the average P_r of all terminals contributing to an EPSC (Martin, 1977) (see Chapter 1, Part II). Cd^{2+} (3.5 μ M) reduced paired-pulse depression by $30.0 \pm 5.1\%$ compared to control ($n = 10$, Fig. 3.6B, D), while ω -CTx reduced it by $26.0 \pm 7.0\%$ ($n = 5$, Fig 3.6C, D). Thus, the average measure of P_r provided by paired-pulse depression was similar for both Cd^{2+} and ω -CTx, consistent with their similar reduction of EPSC amplitude (52% and 41%, respectively). In contrast, the MK-801 technique revealed very different effects of Cd^{2+} and ω -CTx on high- and low- P_r terminals (Fig. 3.5). This highlights the fact that gross measures of P_r , like PPF, obscure details about P_r at subclasses of terminals that can be revealed by the MK-801 technique.

Figure 3. 4

Figure 3. 4 N- and P/Q-type Ca^{2+} channels support glutamate release at excitatory autaptic synapses.

A, An evoked autaptic NMDA EPSC is significantly reduced in the presence of ω -CTx and is blocked by the co-application of ω -CTx and ω -Aga. All traces are averages of 5 sweeps and were obtained from the same cell. The residual non-NMDA current has been subtracted from the average traces.

B, A summary of experiments shown in A. NMDA receptor mediated EPSCs were measured by averaging the amplitude over a 280ms-long window starting 20ms after the stimulus. Bars represent mean \pm SEM (ω -CTx; n = 9, ω -Aga; n = 5 and co-application; n = 5).

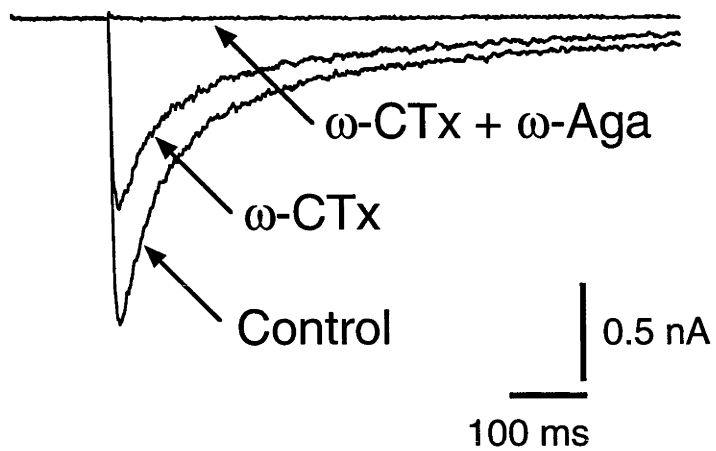
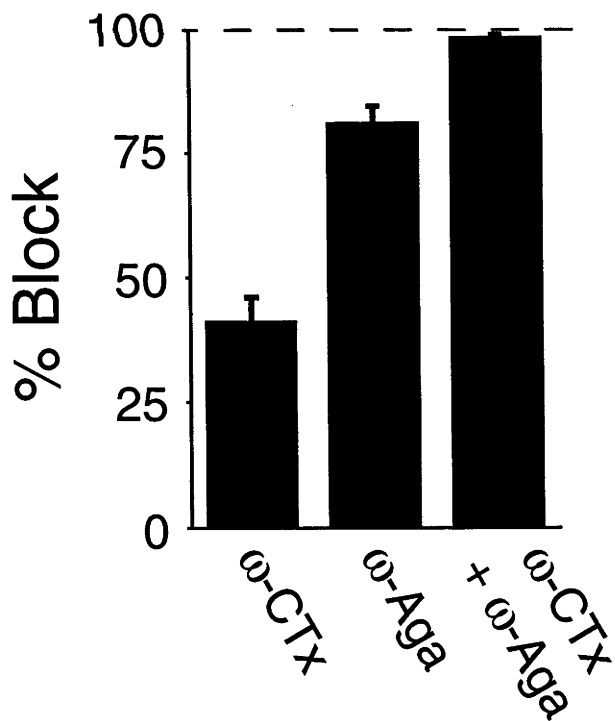
A**B**

Figure 3.5

Figure 3. 5 Summary of the progressive block experiments. Bars represent mean \pm SEM; stars indicate a statistically significant difference from control (one star, $p < 0.05$; two stars, $p < 0.02$). The progressive block time constants are increased by Cd^{2+} but are unaffected by the toxins (**A**, **B**). The percentage of high- P_r terminals is unaffected by Cd^{2+} but is reduced by the toxins (**C**), implying that the toxins cause a population shift from high- P_r to low- P_r terminals.

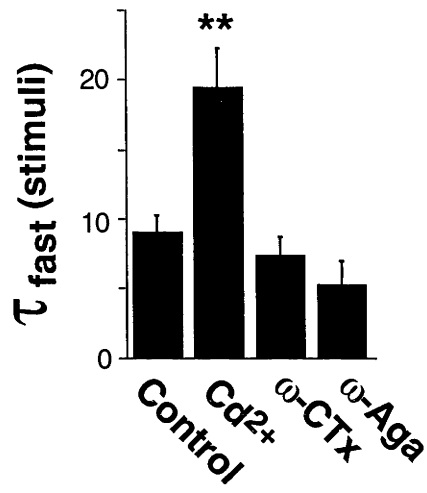
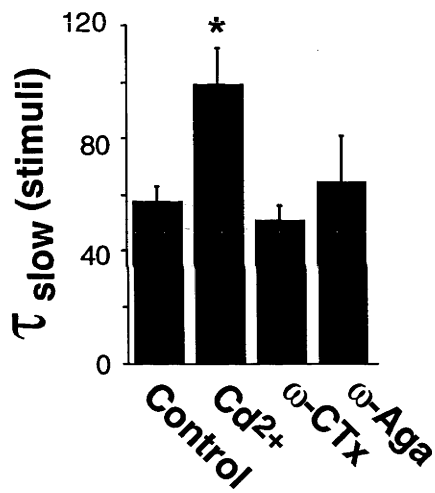
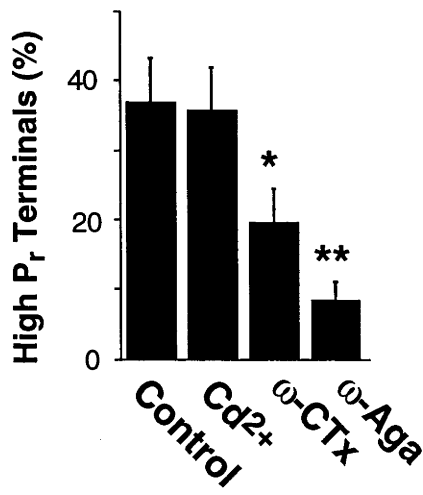
A**B****C**

Figure 3. 6

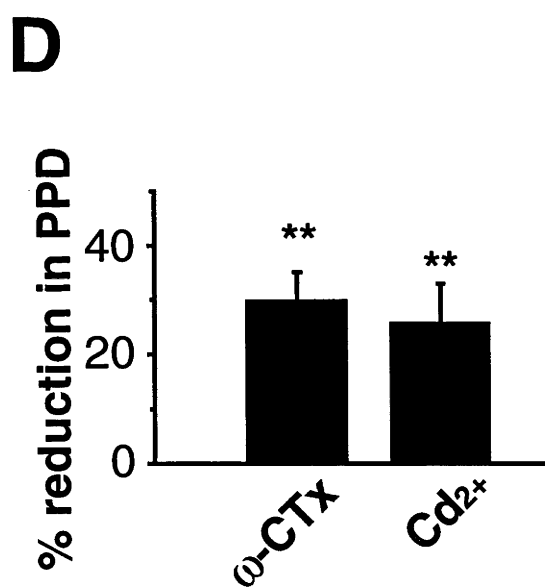
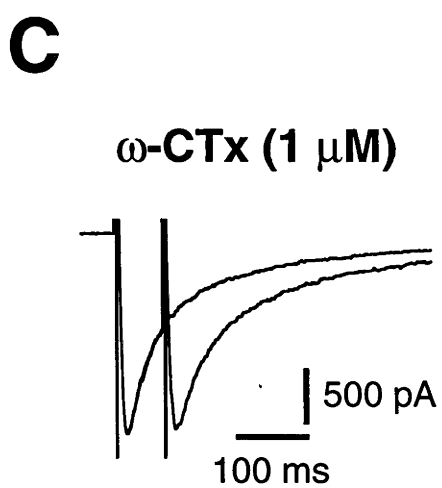
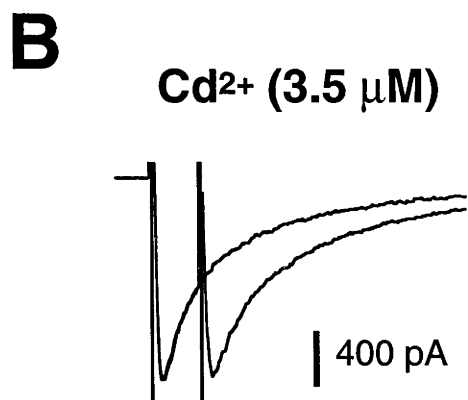
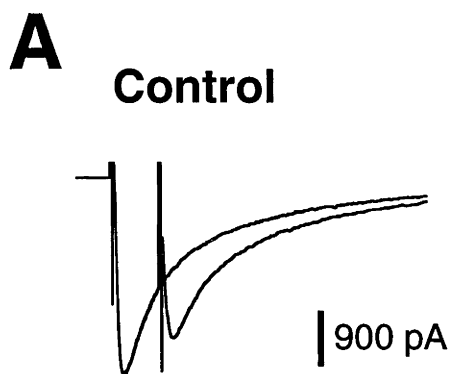
Figure 3. 6 Paired-pulse depression (PPD) reflects the average P_r of all terminals contributing to an EPSC.

A, A paired pulse, with an interstimulus interval of 70ms, results in a depression of the second evoked NMDA EPSC at autaptic excitatory synapses.

B, Cd^{2+} , a non-selective blocker of Ca^{2+} channels, reduces the amount of PPD consistent with a reduction in P_r .

C, ω -CTx, selective for N-type Ca^{2+} channels, reduces the amount of PPD consistent with a reduction in average P_r .

D, Summary of the PPD experiments. Bars represent mean \pm SEM; stars indicate a statistically significant difference from control (two stars, $p < 0.02$, Cd^{2+} ; $n = 10$, ω -CTx; $n = 5$).



High- P_r and low- P_r terminals do not correlate with Ca^{2+} channel subtypes

After 30 stimuli in $2\mu M$ MK-801, approximately 97% of high- P_r terminals are masked (Fig. 3.1A), leaving a residual EPSC generated by an almost pure population of low- P_r terminals. If transmitter release at these low- P_r terminals was mediated preferentially by N-type Ca^{2+} channels, the residual EPSC would be more sensitive to block by ω -CTx than the control EPSC. The converse would be true if N-type channels were preferentially found on high- P_r terminals. A similar argument applies for P/Q-type Ca^{2+} channels. After 30 stimuli in MK-801 the amount of block was not significantly different from control for both ω -CTx ($53.1 \pm 6.5\%$, $n = 6$; *cf.* $41.2 \pm 4.7\%$ for control, $n = 9$) and ω -Aga ($85.5 \pm 4\%$, $n = 6$; *cf.* $81.2 \pm 3.2\%$ for control, $n = 5$) (Fig. 3.7). Thus, Ca^{2+} channel subtypes are similarly distributed on both high- and low- P_r terminals.

Discussion

Modelling the effect of toxins on P_r

How is it possible to maintain P_r in a proportion of synaptic terminals after blocking a subset of Ca^{2+} channels with either ω -CTx or ω -Aga? One mechanism is that each terminal contains only N- or only P/Q-type channels. In this case application of a toxin would completely remove selected terminals, reducing EPSC amplitude but not altering P_r for the terminals that remain. This can be ruled out because of supra-additivity of blockade of neurotransmission by ω -CTx and ω -Aga. The amplitude reduction produced by each toxin sums to 122% (see above), consistent with previous observations (Mintz *et al.*, 1995; Wheeler *et al.*, 1996) and suggesting that at some terminals N-type and P/Q-type channels co-operate to support transmitter release. To account for both supra-additivity and the maintenance of P_r in the presence of toxins, some terminals must contain mixtures of Ca^{2+} channel subtypes, but others must contain only one or the other subtype. This model is shown schematically in Fig. 3.8. The fraction of terminals in each class was estimated from the experimental results.

Figure 3.7

Figure 3. 7 Block of NMDA EPSCs by toxin is similar in control cells (i.e. with both high- and low- P_r terminals contributing; panel **A**) or following 30 stimuli in $2\mu\text{M}$ MK-801 (i.e. after most high- P_r terminals have been masked; panel **B**). This suggests that both high- P_r and low- P_r terminals contain, on average, the same mix of presynaptic Ca^{2+} channel subtypes.

A, B, The above experiment performed using $1\mu\text{M}$ $\omega\text{-CTx}$ ($\omega\text{-CTx}$). Each panel was obtained from a different cell. A similar protocol was used for $0.5\mu\text{M}$ $\omega\text{-Aga}$.

C, Summary of experiments of the type shown in **A** and **B**. Bars represent mean \pm SEM. The amount of block by each toxin is not significantly different in control or after 30 stimuli in $2\mu\text{M}$ MK-801.

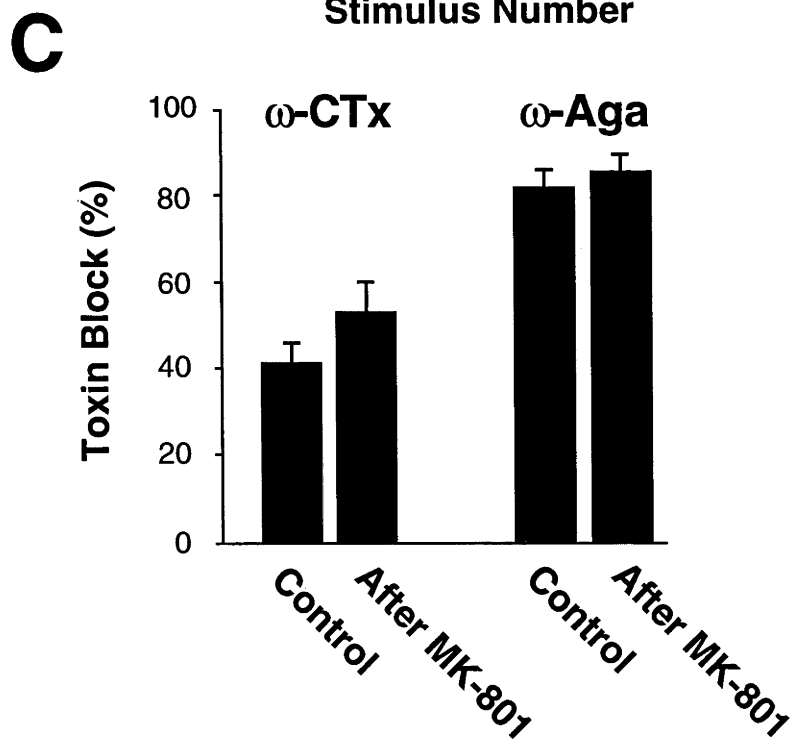
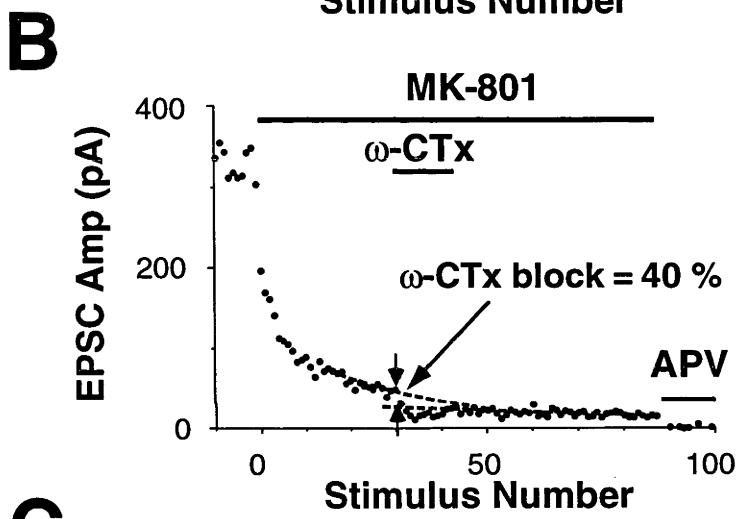
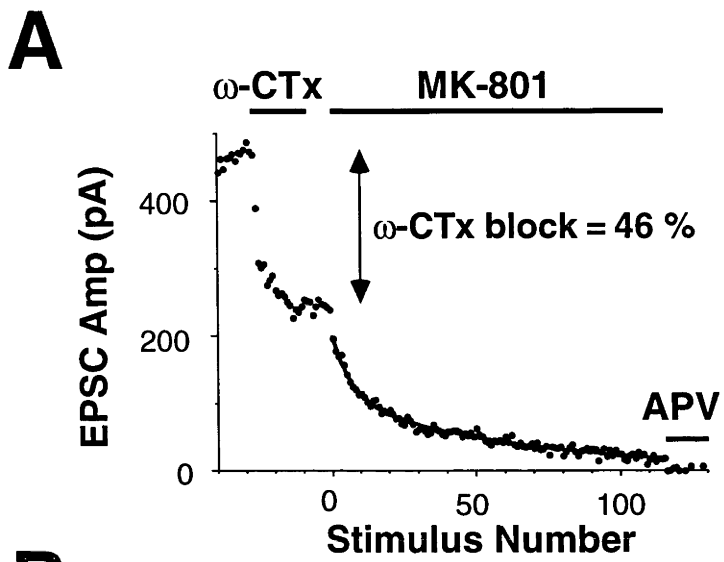
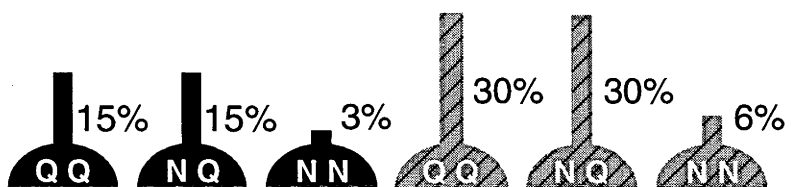


Figure 3. 8

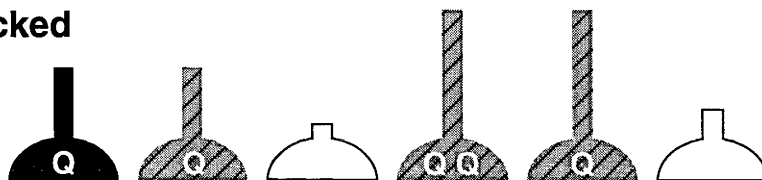
Figure 3. 8 A simple model of a non-uniform distribution of presynaptic Ca^{2+} channel subtypes accounts for our data. Presynaptic terminals are assumed to be either high- P_r or low- P_r , and to contain only P/Q-type Ca^{2+} channels (QQ), only N-type (NN) or a mixture of the two (NQ), in the same relative proportions for both high- and low- P_r sites. When N-type channels are blocked by adding ω -CTx, NN-type terminals are completely blocked, QQ-type terminals are unaltered, and NQ-type terminals have their P_r either reduced or unaffected, depending on the initial P_r . A similar argument applies to block of P/Q-type channels by ω -Aga. For further details see Discussion. The percentages shown above the control terminals are the estimated relative number of terminals in each category when the model was optimised to fit the data (Table 3.1). The pie graphs give the percentages of functional high- and low- P_r terminals in each condition.



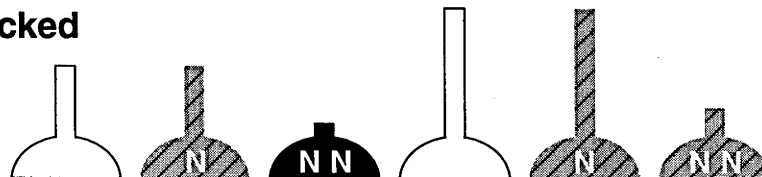
Control



N-Type Blocked



Q-Type Blocked



The distribution of Ca²⁺ channel subtypes across autaptic terminals was modelled with a number of simplifying assumptions. Terminals were divided into three classes: those with only P/Q-type channels (QQ), those with only N-type channels (NN) and those with both classes (NQ) (Fig. 3.8). Each class was further divided into two sub-classes with high P_T or low P_T. The behaviour of these terminals in the presence of the toxins are based on three assumptions:- (i) When ω-CTx is applied, pure N-type terminals in both the high-P_T and low-P_T categories will be completely blocked because no Ca²⁺ can enter. Similarly, pure P/Q-type terminals will be completely blocked by ω-Aga. (ii) When ω-CTx is applied, high-P_T terminals that contain both N- and P/Q-type channels will be shifted to the low-P_T class, because blockade of N-type channels will reduce the net presynaptic Ca²⁺ influx. A similar situation applies for ω-Aga. (iii) Low-P_T terminals that contain both N- and P/Q-type channels will not be completely blocked by either toxin, but will remain in the low-P_T class, although perhaps with reduced P_T (see below).

Two experimental observations constrained the distribution of terminal classes: the percentage of high- and low-P_T terminals measured under control conditions (Fig. 3.5), and the finding that Ca²⁺ channel subtypes were similarly distributed on high- and low-P_T terminals (Fig. 3.7). These constraints meant that the model had only two free parameters: the fraction of NN terminals, and the fraction of QQ terminals. The relative numbers of terminals in the 6 classes were used to fit four key experimental results: (i) amount of ω-CTx block of the EPSC, (ii) amount of ω-Aga block of the EPSC, (iii) percentage of high P_T terminals after ω-CTx block and (iv) the percentage of high P_T terminals after ω-Aga block. The two free parameters were adjusted to give the best fit between the model and the corresponding experimental parameters (Table 3.1) by a simplex optimisation procedure minimising the sum of squared errors (SSE, see Appendix).

A Monte Carlo simulation was performed to examine the sensitivity of the model predictions to errors in the exponential fits to the progressive block data. This was

Table 3. 1 Comparison of predicted and experimental data for the model illustrated in Fig. 3.8. The percentage of terminals in each category of terminal in Fig. 3.8 was estimated as described in Discussion, and the optimal values are shown in Fig. 3.8 for the control condition, after rounding each value by 1-2%. The unrounded optimal values were used to calculate the Predicted values in the Table.

	Predicted (%)	Observed (%)
Amount of ω -CTx Block	38.5	41.2 \pm 4.7
Amount of ω -Aga Block	75.2	81.2 \pm 3.2
Percent of high P_r after ω -CTx	18.4	19.2 \pm 4.7
Percent of high P_r after ω -Aga	6.4	8.4 \pm 2.4

done by drawing random samples from a set of gaussian distributions with the same means and standard deviations as each of the experimental parameters (high and low P_r ; percent of terminals with high P_r before and after ω -CTx or ω -Aga block; amplitude reduction following ω -CTx and ω -Aga block). The two free parameters in the model (fractions of NN and QQ terminals) were optimised for each set of sampled parameters. One thousand sample sets were drawn, and the means and standard deviations of the optimum parameters were calculated. The Monte Carlo fit of the model to the data gave the following values for the fractions of different terminal types (mean \pm SD): $8.2 \pm 3.6\%$ (NN), $46.9 \pm 6.2\%$ (QQ), $44.8 \pm 8.6\%$ (QN).

The model incorporating the above assumptions (Fig. 3.8) gives an accurate quantitative description of all aspects of the data. The model explains the amount of block produced by ω -Aga and ω -CTx, and their supra-additivity (Table 3.1). It also explains how the toxins reduce the percentage of high- P_r sites, while leaving release probabilities unaltered. Together these results suggest that about 10% of terminals contain only functional N-type channels, about 45% only functional P/Q-type channels, and the remaining 45% a mixture of both types.

Exploring the model

The way in which the NQ low- P_r class of terminal acts in the presence of the toxins was examined. Simulations in which the NQ low- P_r terminal class were completely blocked by the addition of either toxins did not provide a good match between the predicted and experimental values. Similarly, when NQ low- P_r terminals were completely blocked by ω -CTx but not ω -Aga the fit was poor. A better fit to the data was seen if ω -Aga blocked the NQ low- P_r class but ω -CTx did not. The best fit of the data was achieved if neither toxin blocked release from the NQ low- P_r class of terminals (Table 3.2). This finding probably reflects the complex shift in distribution of P_r within the low P_r class of terminals following the application of either toxin. Experimentally, no reduction in P_r at terminals in the low- P_r class was seen after the application of either toxin. However, a small shift may have been obscured by the

Table 3. 2 The way in which the NQ low- P_r class of terminal acts in the presence of the toxins was examined. The comparison of predicted and experimental data for the different model assumptions described are shown. The best fit was achieved if NQ low- P_r terminals were resistant to both ω -CTx and ω -Aga block.

	% ω -CTx Block	% ω -Aga Block	% High P_r after ω -CTx	% High P_r after ω -Aga
Observed	41.2	81.2	19.2	8.6
NQ low- P_r terminals blocked by both toxins	45.7	86.5	27.4	12.46
NQ low- P_r terminals blocked by ω -CTx only	43.4	78.3	28.0	5.7
NQ low- P_r terminals blocked by ω -Aga only	41.8	84.0	16.6	13.1
NQ low- P_r terminals blocked by neither toxin	38.5	75.2	18.4	6.4

high- P_r terminals that switched to the low- P_r class following toxin block. The analytical approach estimates the average P_r for each class, and lacks the resolution to detect an altered distribution within the low- P_r class.

The model could be made more realistic by postulating a continuum of P_r values and Ca^{2+} channel ratios, and a graded effect of toxin blockade on each terminal. However, attempts at increasing the number of terminal classes and grading the toxin effect on each did not greatly improve the fit to the data. Recently a mathematical relationship between MK-801 progressive block and a continuum of P_r values has been derived (Huang and Stevens, 1997). It would be possible to develop a model in which a continuum of P_r was incorporated. However, this would add further degrees of freedom to the model making interpretation more difficult. The qualitative conclusions are not dependent on the assumption of two classes of P_r . For example, it can be concluded unambiguously that Ca^{2+} channels are distributed non-uniformly on presynaptic terminals, because both toxins leave some terminals unaffected. The double exponential fit to the progressive block provides a useful analytical measure of the range and distribution of P_r across presynaptic terminals and the simple model predicts the details of a non-uniform distribution that is consistent with all the data.

Developmental change in Ca^{2+} channel subtype supporting transmitter release

A developmental change in Ca^{2+} channel subtype composition supporting transmitter release has been demonstrated at excitatory hippocampal neurons grown in culture (Scholz and Miller, 1995). At immature synapses (< 15 days in culture) ω -CTx blocked synaptic transmission by more than 80% while ω -Aga was less effective. In contrast, in older cultures (>15 days in culture) ω -Aga was shown to be more effective (~65%) than ω -CTx (~30%) at blocking transmission. Therefore, the proportions of terminal classes (NN, QQ and QN) would be expected to alter in a developmental fashion. All experiments described here used neurons that had been maintained for 10-14 days *in-vitro*. A direct developmental comparison between results presented here and those of (Scholz and Miller, 1995) is difficult because of the differences in

the culture preparation method. Scholz and Miller (1995) remove the hippocampi from embryonic rats (day 17) while cultures used here are from newborn rat hippocampi. Differences in rat species (Wistar vs Sprague-Dawley) between the two studies may also complicate developmental comparisons. However, the developmental trend observed by Scholz and Miller (1995) may still be valid in our preparation. Technical difficulties made the use of the MK-801 technique unreliable when addressing developmental changes in Ca²⁺ channel subunit distribution. In immature cultures (< 10 days) the NMDA EPSC is small and fitting exponentials to the noisy data proved difficult. Older cultures had very large NMDA EPSC which were less well voltage clamped and exhibited rundown compromising the progressive block analysis.

Other evidence for a non-uniform distribution of Ca²⁺ channels

Reuter (1995) has shown that the distribution of presynaptic N-type channels is non-uniform in culture, by using the dye FM1-43 to monitor exocytosis. At some terminals exocytosis was entirely blocked by ω -CTx, while at others it was only partially blocked. ω -Aga did not show this heterogeneity, partially blocking all terminals to a small extent. These results qualitatively agree with ours for ω -CTx but not for ω -Aga. There are two possible explanations for the discrepancy. First, Reuter (1995) used a lower concentration of ω -Aga (80nM), which completely blocks P-type channels (Mintz *et al.*, 1992a) but is much less effective at blocking the Q-type channel (Wheeler *et al.*, 1994; Scholz and Miller, 1995). ω -Aga was used at 500nM in these experiments, which blocks both P- and Q-type channels effectively. It is possible that the altered progressive block observed in ω -Aga is due primarily to Q-type channels, which Reuter would not have observed. Second, Reuter's experiments gave no information about possible differences between inhibitory and excitatory terminals, whereas the autapse experiments ensured that a pure population of excitatory terminals was studied. A recent study detailed below shows that GABA release can be supported by either N-type alone or P/Q-type alone (Poncer *et al.*, 1997).

Wheeler *et al.* (1996) have taken a different approach to this question. When presynaptic Ca^{2+} influx was increased by prolonging the action potential with 4-aminopyridine (4-AP), they found that block of synaptic transmission by ω -CTx was reduced from 46% in control to 9%. From this they concluded that a significant fraction of terminals cannot rely solely on N-type channels for neurotransmitter release. Although they did not set quantitative limits on this statement, their conclusion is in general agreement with the result presented here, which suggests that there are about 10% pure N-type terminals (Fig. 3.8). Presumably this 10% of terminals is involved in the residual 9% block by ω -CTx in 4-AP (Wheeler *et al.*, 1996). Wheeler *et al.* (1996) found that 4-AP was less effective at reducing the block of transmission by ω -Aga (from 95% to 74%). Although they did not discuss this result, it is consistent with the suggestion that there are many more pure P/Q-type than pure N-type terminals.

Synapse specific expression of different Ca^{2+} channel subtypes has been demonstrated at two distinct inhibitory pathways onto CA1 pyramidal neurons (Poncer *et al.*, 1997). Interneurons originating in *Str. radiatum* were shown to support GABA release by the N-type Ca^{2+} channel alone, while interneurons originating in *Str. lucidum* and *Str. oriens* supported release via the P/Q-type channel. A heterogeneity of Ca^{2+} channel distribution has also been demonstrated in the preoptic region of the brain. Potassium induced GABA release from acutely dissociated medial preoptic neurons with co-isolated synaptic boutons was blocked in a heterogenous way by ω -CTx or ω -Aga (Haage *et al.*, 1998).

In summary, our data for a non-uniform distribution of Ca^{2+} channel subtypes across presynaptic terminals is qualitatively consistent with other findings in the CNS.

Functional implications of a non-uniform distribution of Ca²⁺ channels

N-type and P/Q-type Ca²⁺ channels are presumably synthesised in the cell body, transported along the axon to presynaptic terminals, then inserted into the membrane close to vesicle release sites. If this process is random and there are many Ca²⁺ channels per terminal, then all terminals should have both channel subtypes. The existence of terminals where only one type of Ca²⁺ channel is functional may be explained in two ways. The first possibility is that Ca²⁺ channel subtypes are targeted to specific terminals, either by directed transport along the axon or by selective insertion at the terminal. The second possibility is that all terminals are non-selective and Ca²⁺ channel subtypes are inserted randomly, but only a few Ca²⁺ channels are functional at a given terminal (Stanley, 1993). The resultant binomial distribution of channels would automatically produce some terminals with exclusively N-type or P/Q-type channels. For example, if there were two functional Ca²⁺ channels per terminal, and these were inserted randomly from a population of 70% P/Q-type and 30% N-type channels, the resulting terminals would be 9% N-type, 49% P/Q-type and 42% mixed. These experiments have shown that excitatory synaptic terminals arising from a single axon have a non-uniform distribution of Ca²⁺ channel subtypes. What could be the physiological importance of this heterogeneity? Neuromodulators differentially modulate specific Ca²⁺ channel subtypes (see below). One possibility, therefore, might be to enable terminal-specific modulation.

Differential modulation of Ca²⁺ channel subtypes

Synaptic transmission can be regulated by neurotransmitter modulation of Ca²⁺ channels via a G-protein mediated mechanism (Mintz and Bean, 1993; Hille, 1994). There is general consensus that the inhibition involves the direct effect of the activated G-protein subunit or subunits on the Ca²⁺ channel itself, with recent evidence indicating a key role for the G-proteins $\beta\gamma$ subunits (Herlitze *et al.*, 1996; Ikeda, 1996). Similar mechanisms of inhibition have been proposed for both N- and P/Q-type Ca²⁺ channels (Mintz and Bean, 1993). However, a few studies have reported that the N-type Ca²⁺ current is inhibited to a greater extent than the P/Q-type Ca²⁺ current.

Imaging studies which allow the simultaneous recording of the presynaptic Ca^{2+} transient and the field excitatory postsynaptic potential (EPSP), show that GABA_B , adenosine (A1) and muscarinic receptors preferentially block the N-type Ca^{2+} channel at CA3 to CA1 synapses (Wu and Saggau, 1994a; Wu and Saggau, 1995b; Qian and Saggau, 1997). Similarly, presynaptic inhibition of EPSCs by adenosine in cultured hippocampal neurons was preferentially mediated by the N-type Ca^{2+} channel (Scholz and Miller, 1996). The degree of presynaptic inhibition reduced with synaptic maturation, consistent with a developmental reduction in the N-type Ca^{2+} channel (Scholz and Miller, 1995). Vazquez and Sanchez-Prieto (1997), using a synaptosomal preparation from cerebrocortical neurons, have also demonstrated that modulation of release by adenosine (A1) and the metabotropic glutamate receptor is dominated by action on the N-type Ca^{2+} channel. In contrast, presynaptic modulation by the metabotropic glutamate receptor was shown to preferably target ω -CTx-insensitive channels for both inhibitory and excitatory pathways in the rat medulla (Glaum and Miller, 1995). This raises the issue of whether the selective modulation is a function of the physical location of the Ca^{2+} channels and the presynaptic modulating receptor, or whether there are fundamental differences in the modulation pathways between N- and P/Q-type Ca^{2+} channels. Differential enhancement of Ca^{2+} currents have also recently been demonstrated in rat amygdala neurons (Huang *et al.*, 1998). The β -adrenergic agonist, isoproterenol, acting through an cyclic AMP cascade was shown to selectively increase the Ca^{2+} current through P/Q-type Ca^{2+} channels in these neurons.

A comparison of G-protein mediated inhibition of the N- and P/Q-type Ca^{2+} channels has been completed in adrenal chromaffin cells (Currie and Fox, 1997). G-protein inhibition of Ca^{2+} channels produces a slowing of activation kinetics, a reduction of the inhibition at positive membrane potentials, and partial relief from inhibition by depolarising prepulse (Bean, 1989; Elmslie *et al.*, 1990; Penington *et al.*, 1991; Currie and Fox, 1997). The inhibition can be divided into either voltage-sensitive (relieved by a conditioning prepulse) or voltage-insensitive inhibition (present after conditioning

prepulse). Only the voltage-sensitive component of inhibition was larger for N-type channels. Currie and Fox (1997) suggest that this difference in kinetics cannot alone account for the observed differences between N- and P/Q-type Ca^{2+} channel modulation. Differential G-protein inhibition may be, in part, due to the spatial organisation of the Ca^{2+} channel subtypes and the modulating receptor on presynaptic terminals.

In summary, Ca^{2+} channel subtypes may be differentially modulated. Therefore, modulators that are diffusely present in the brain could acquire specificity because of the non-uniform distribution of the channels they modulate.

What determines P_T at a given synaptic terminal?

The progressive block of the NMDA EPSC in the presence of MK-801 is best fit by at least a double exponential, suggesting a non-uniform distribution of P_T across synaptic terminals (Hessler *et al.*, 1993; Rosenmund *et al.*, 1993). Results presented here confirm the heterogeneity of P_T at excitatory synapses in dissociated hippocampal cultures. The hypothesis that different Ca^{2+} channel subtypes may be preferentially found on either high or low P_T terminals was tested. After 30 stimuli in MK-801 the majority of high P_T terminals are blocked leaving an EPSC generated by low P_T terminals. The amount of block by either ω -CTx or ω -Aga was the same for an EPSC generated by all terminals and an EPSC generated by low P_T terminals only. This argues against any relationship between P_T and Ca^{2+} channel subtype (see Results).

An anatomical basis for non-uniform P_T has been postulated. Serial electron microscopy was used to reconstruct entire presynaptic boutons and the size, number and location of docked vesicles were measured (Harris and Sultan, 1995). A large variation in the number of docked vesicles per terminal was found. This distribution may provide a basis for non-uniform P_T across hippocampal synapses. Additional evidence supporting an anatomical basis of the non-uniform P_T has come from studies using FM1-43. This technique allows an estimate of the size of the "recycling pool" of

synaptic vesicles as well as P_T for a given synaptic terminal. Murthy *et al* (1997) found a strong correlation between the P_T of an individual terminal and the number of synaptic vesicles. An estimate of a "readily releasable pool" of synaptic vesicles and P_T has also been made at putative individual synapses in hippocampal slice (Dobrunz and Stevens, 1997). They also showed a strong correlation between P_T and the number of synaptic vesicles available for release. A biochemical basis may also underlie the difference between P_T at different synaptic terminals. Changes in the phosphorylation state of synapsin 1 has been shown to control the fraction of synaptic vesicles available for release (Greengard *et al.*, 1993). The availability of additional synaptic vesicles for release would presumably increase the P_T of a given terminal. Despite evidence correlating the size of the releasable pool with P_T the underlying mechanism generating the heterogeneity in P_T remains unresolved.

Conclusion

The analysis of the progressive block of NMDA EPSCs in the presence of MK-801 is a powerful technique for demonstrating changes in P_T . This Chapter has investigated the pattern of co-localisation of Ca^{2+} channel subtypes on presynaptic terminals in hippocampal cultures. N-type or P/Q-type Ca^{2+} channels were selectively blocked and the changes in P_T were measured using MK-801. The antagonists completely blocked release at some terminals, reduced P_T at others, and failed to affect the remainder. In contrast, non-selective reduction of presynaptic Ca^{2+} influx by adding Cd^{2+} or lowering external Ca^{2+} reduced P_T uniformly at all terminals. It was concluded from these results that the mixture of N-type and P/Q-type channels varies markedly between terminals on the same afferent. A model was developed incorporating a non-uniform distribution of Ca^{2+} channel subtypes across presynaptic terminals. The model accounted for all the experimental data and suggests that about 10% of terminals have only N-type channels, about 45% of terminals have only P/Q-type channels and the remaining 45% have a mixture of subtypes. The amount of block by ω -CTx and ω -Aga was unaltered after most of the high- P_T sites were masked by MK-801, suggesting that the pattern of co-localisation of Ca^{2+} channel subtypes is similar

for high- and low- P_r terminals. Thus, the functional distinction between high- and low- P_r terminals cannot be explained by the non-uniform distribution of Ca^{2+} channel subtypes, and may instead have a structural or biochemical basis. Given that Ca^{2+} channel subtypes are differentially affected by neuromodulators, these findings lead to the possibility of terminal-specific modulation of synaptic function. This may have important ramifications for synaptic modulation and plasticity.

Appendix

The function "MK-801 model" was used to search for the optimum distribution of terminal classes to explain average experimental results. The function predicts four main results for a given distribution of terminal types. It calculates the SSE between the predictions and the observed results.

Observed experimental results:

- 1) Percentage block by ω -CTx (Observed_CTX_Block = 41.2%)
- 2) Percentage block by ω -Aga (Observed_Aga_Block = 81.2%)
- 3) Percentage of high P_r terminals after ω -CTx block
(Observed_CTX_Percent = 19.2%)
- 4) Percentage of high P_r terminals after ω -Aga block
(Observed_Aga_Percent = 8.4%)

Experimental results used to constrain the model:

- 1) Measured P_r for high P_r terminals (High_Pr = 1/8.9)
- 2) Measured P_r for low P_r terminals (Low_Pr = 1/56.3)
- 3) Percentage of high P_r terminal in control conditions
(High_Pr_Percent = 36.1%)
- 4) Percentage of low P_r terminal in control conditions
(Low_Pr_Percent = 63.9%)

The model assumes terminals are divided into three classes:

QQ = only Q-type channels present

NN = only N-type channels present

QN = both Q- and N-type channels present

The computer model:

- Calculate NN fraction from other two fractions

$$\text{NN_Fraction} = 1 - (\text{QQ_Fraction} + \text{QN_Fraction})$$

- Calculate Low P_T and High P_T terminal type sub-fractions

$$\text{QQ_High_Pr_Fraction} = \text{QQ_Fraction} * \text{High_Pr_Percent} / 100$$

$$\text{QN_High_Pr_Fraction} = \text{QN_Fraction} * \text{High_Pr_Percent} / 100$$

$$\text{NN_High_Pr_Fraction} = \text{NN_Fraction} * \text{High_Pr_Percent} / 100$$

$$\text{QQ_Low_Pr_Fraction} = \text{QQ_Fraction} * \text{Low_Pr_Percent} / 100$$

$$\text{QN_Low_Pr_Fraction} = \text{QN_Fraction} * \text{Low_Pr_Percent} / 100$$

$$\text{NN_Low_Pr_Fraction} = \text{NN_Fraction} * \text{Low_Pr_Percent} / 100$$

- Percent of High P_T terminals after ω -CTx blocks N-type channels. Assumes that ω -CTx block of N-type channels totally blocks release from NN terminals, converts QN terminals with High P_T to Low P_T , but leaves QN terminals with Low P_T unaffected.

$$\text{CTX_Total_High_Pr} = \text{QQ_High_Pr_Fraction}$$

$$\begin{aligned} \text{CTX_Total_Low_Pr} &= \text{QQ_Low_Pr_Fraction} + \text{QN_Low_Pr_Fraction} \\ &\quad + \text{QN_High_Pr_Fraction} \end{aligned}$$

$$\begin{aligned} \text{CTX_High_Pr_Percent} &= 100 * \text{CTX_Total_High_Pr} / (\text{CTX_Total_High_Pr} \\ &\quad + \text{CTX_Total_Low_Pr}) \end{aligned}$$

- Percent of High P_r terminals after ω -Aga blocks Q-type channels. Assumes that ω -Aga block of Q-type channels totally blocks release from QQ terminals, and converts QN terminals with High P_r to Low P_r , but leaves QN terminals with Low P_r unaffected.

$$\text{Aga_Total_High_Pr} = \text{NN_High_Pr_Fraction}$$

$$\begin{aligned} \text{Aga_Total_Low_Pr} &= \text{NN_Low_Pr_Fraction} + \text{QN_Low_Pr_Fraction} \\ &+ \text{QN_High_Pr_Fraction} \end{aligned}$$

$$\begin{aligned} \text{Aga_High_Pr_Percent} &= 100 * \text{Aga_Total_High_Pr} / (\text{Aga_Total_High_Pr} \\ &+ \text{Aga_Total_Low_Pr}) \end{aligned}$$

- Part I of SSE calculation

$$\begin{aligned} \text{SSE} &= (\text{CTX_High_Pr_Percent} - \text{Observed_CTX_Percent})^2 \\ &+ (\text{Aga_High_Pr_Percent} - \text{Observed_Aga_Percent})^2 \end{aligned}$$

- Predicted block of transmission by ω -CTx and ω -Aga

$$\text{Control_Release} = \text{High_Pr} * \text{High_Pr_Percent}/100 + \text{Low_Pr} * \text{Low_Pr_Percent}/100$$

$$\text{CTX_Release} = \text{High_Pr} * \text{CTX_Total_High_Pr} + \text{Low_Pr} * \text{CTX_Total_Low_Pr}$$

$$\text{Aga_Release} = \text{High_Pr} * \text{Aga_Total_High_Pr} + \text{Low_Pr} * \text{Aga_Total_Low_Pr}$$

$$\text{CTX_Block} = 100 * (1 - \text{CTX_Release} / \text{Control_Release})$$

$$\text{Aga_Block} = 100 * (1 - \text{Aga_Release} / \text{Control_Release})$$

- Part II of SSE calculation

$$\begin{aligned} \text{SSE} &= \text{SSE} + (\text{CTX_Block} - \text{Observed_CTX_Block})^2 \\ &+ (\text{Aga_Block} - \text{Observed_Aga_Block})^2 \end{aligned}$$

- Minimise SSE with respect to variables, QQ_Fraction and QN_Fraction

- Write results:

QQ Fraction	QN Fraction	NN Fraction
0.4667	0.4534	0.07988

	Predicted	Observed
ω -CTx Block	38.5	41.2
ω -Aga Block	75.2	81.2
% High P_r after ω -CTx	18.4	19.2
% High P_r after ω -Aga	6.4	8.4

Chapter 4

Ca²⁺ Cooperativity of Release and Ca²⁺ Channel Subtypes

Introduction

The relationship between transmitter release and $[Ca^{2+}]_o$ is steeply non-linear at central synapses. This non-linear relationship implicates the cooperative involvement of multiple Ca²⁺ ions in the release of each vesicle of transmitter (Chapter 1, Part I). The Dodge-Rahamimoff equation provides a model of the relationship between $[Ca^{2+}]_o$ and transmitter release at the frog neuromuscular junction (Dodge and Rahamimoff, 1967). The Dodge-Rahamimoff equation, however, assumes that there is a linear relationship between $[Ca^{2+}]_o$ and intra-terminal Ca²⁺ concentration ($[Ca^{2+}]_{it}$). This relationship is known to be sublinear at higher $[Ca^{2+}]_o$ at central synapses (Mintz *et al.*, 1995; Borst and Sakmann, 1996). This chapter examines the relationship between $[Ca^{2+}]_o$ and transmitter release at excitatory autaptic synapses in hippocampal culture. A modified version of the Dodge-Rahamimoff equation incorporating a non-linear relationship between $[Ca^{2+}]_o$ and $[Ca^{2+}]_{it}$ is developed to explain the dose-response relationship at these synapses.

Several Ca²⁺ channels subtypes, including the N-type and the P/Q-type, support the release of neurotransmitter at central synapses (Chapter 1, Part I and Chapter 3). It has been suggested that different Ca²⁺ channel subtypes mediate transmitter release with different cooperativities but this finding remains controversial. Mintz *et al.* (1995) observe that release is more steeply dependent on $[Ca^{2+}]_{it}$ for P/Q- than for N-type Ca²⁺ channels at granule cell to Purkinje cell synapses in the cerebellum. In contrast, Wu and Saggau (1994) see no significant difference in cooperativity for Ca²⁺ entering via either N- or P/Q-type Ca²⁺ channels for CA3 - CA1 synapses in the hippocampus. Both these studies used Ca²⁺ sensitive dyes to measure $[Ca^{2+}]_{it}$ before and after

selective block of each Ca^{2+} channel subtype. Mintz *et al.* (1995) estimate cooperativity from only two data points, one recorded before and one after selective block. These two points spanned a different $[\text{Ca}^{2+}]_{\text{it}}$ range for each channel subtype. By measuring $[\text{Ca}^{2+}]_{\text{it}}$ at several time points after the application of the toxins Wu and Saggau (1994) explore the $[\text{Ca}^{2+}]_{\text{it}}$ range more thoroughly and see no significant difference in cooperativity for the two channel subtypes.

In the present study selective Ca^{2+} channel blockers and traditional dose-response analysis were used to investigate the Ca^{2+} cooperativity associated with influx through different Ca^{2+} channel subtypes. An empirical comparison, using the Hill equation or a power function fit (at low $[\text{Ca}^{2+}]_0$), was made between Ca^{2+} dose-response curves generated in the presence of ω -CTx or ω -Aga. The Ca^{2+} dose-response curves were generated over a wide range of $[\text{Ca}^{2+}]_0$ and therefore overcome some of the limitations of the imaging studies.

Methods

Whole-cell patch-clamp recordings were obtained from isolated hippocampal pyramidal neurons which formed autaptic synapses as described in Chapter 2. The bath solution contained (in mM) NaCl 135, KCl 5, MgCl_2 10, glucose 10, HEPES 10, pH 7.3, with osmolarity adjusted to 310mOsm with sorbitol. CaCl_2 was added from stock to a final concentration between 0.4 and 10mM. Currents were low pass filtered at 5kHz and digitally sampled at 10kHz. Series resistance was typically $5\text{M}\Omega$ (range 4 - $7\text{M}\Omega$), and compensation was set at 80-90%. Errors associated with uncompensated series resistance were small under our recording conditions (see Results). EPSCs were evoked every 6s. AMPA EPSCs were measured by averaging the amplitude over a 5 - 10ms range around the peak of the current. Residual non-AMPA current, measured in the same way in the presence of $10\mu\text{M}$ CNQX during each experiment, was subtracted from all EPSC measurements.

All theoretical curves were fit to the data by minimising χ^2 , defined as:

$$\chi^2 = \Sigma (\text{experimental amplitude} - \text{predicted amplitude})^2 / \text{experimental SD}$$

In 3 out of 20 cells a single outlier point was deleted before performing Dodge-Rahamimoff fit to the full dose-response curve. The quality of the fit for the Hill and Dodge-Rahamimoff equations was determined using a χ^2 test. Other statistical comparisons were made using the Student's *t* test.

Approaches used to estimate Ca²⁺ cooperativity

An estimate of the degree of Ca²⁺ cooperativity was obtained by fitting an equation to the EPSC amplitude *vs* [Ca²⁺]_o dose-response curve. The Dodge-Rahamimoff equation, the Hill equation and the power function were used. Each equation contains a parameter related to cooperativity.

The Dodge-Rahamimoff equation

The Dodge-Rahamimoff equation was developed to describe the relationship between the endplate potential amplitude and [Ca²⁺]_o. It is based on the assumption that Ca²⁺ ions bind to several independent sites on a presynaptic protein complex to promote the release of a transmitter vesicle (Dodge and Rahamimoff, 1967). It also assumes that Mg²⁺ ions can bind to the same sites, but do not promote vesicle release.

The standard Dodge-Rahamimoff equation is,

$$E = S \left(\frac{[\text{Ca}^{2+}]_o}{K_1} \right) / \left(1 + \frac{[\text{Ca}^{2+}]_o}{K_1} + \frac{[\text{Mg}^{2+}]_o}{K_2} \right)^{N_D}$$

where:

E is the EPSC amplitude;

K₁ is the affinity for Ca²⁺ binding to the vesicle release complex;

K₂ is the affinity for Mg²⁺ binding to the vesicle release complex;

S is a scaling factor;

N_D is the number of Ca²⁺ ion binding sites that must be occupied to trigger the release of a transmitter vesicle.

The Hill equation

Another method for estimating the degree of cooperativity is to fit a Hill equation. The Hill equation provides a useful empirical description of the dose-response relationship (Weiss, 1997). The equation only provides an estimate of the number of binding sites when extreme positive cooperativity is present between the binding of the first and subsequent ligand molecules. That is, the affinity of binding for the first Ca^{2+} ion has to be much lower than subsequent Ca^{2+} binding affinities. The fit provides an estimate of both cooperativity, N_H , and affinity, EC_{50} , of Ca^{2+} binding to the vesicle release complex.

The Hill equation is,

$$E = S [\text{Ca}^{2+}]_o^{N_H} / (\text{EC}_{50}^{N_H} + [\text{Ca}^{2+}]_o^{N_H})$$

where:

EC_{50} is the Ca^{2+} concentration giving half the maximal synaptic response;

N_H is the Hill coefficient, an empirical value related to the cooperativity underlying the dose-response relationship.

The power function

The shape of the dose-response curve at lower Ca^{2+} concentrations contains the most information about cooperativity. In the limit as $[\text{Ca}^{2+}]_o$ approaches zero the Hill and the Dodge-Rahamimoff equations both reduce to a power function. The power function forms a straight line when plotted in log-log coordinates, and the slope of the line is equal to the cooperativity parameter, N_P .

The power function is,

$$E = S [\text{Ca}^{2+}]_o^{N_P}$$

where:

N_P is an empirical parameter indicating the degree of cooperativity of the dose-response relationship.

Results

Ca²⁺ dose-response curve for autaptic EPSCs

The amplitude of the AMPA EPSC was measured as a function of [Ca²⁺]_o at autaptic synapses on cultured hippocampal neurons (Fig. 4.1A). EPSC amplitude measurements at each [Ca²⁺]_o were bracketed with measurements at 2mM [Ca²⁺]_o to ensure the stability of the recording (Fig. 4.1B). The relationship between EPSC amplitude and [Ca²⁺]_o was highly non-linear (Fig. 4.1C), consistent with the cooperative involvement of several Ca²⁺ ions in transmitter release.

Estimating Ca²⁺ cooperativity

The number of Ca²⁺ ions that cooperate to trigger the release of a vesicle (the degree of cooperativity) was estimated using several approaches. The EPSC amplitude vs [Ca²⁺]_o dose-response curves were fit with the following equations; the Dodge-Rahamimoff equation, the Hill equation and the power function.

The Dodge-Rahamimoff equation was developed to describe the relationship between [Ca²⁺]_o and the endplate potential amplitude at the neuromuscular junction (Dodge and Rahamimoff, 1967). It is based on physically plausible assumptions, in contrast to more empirical approaches such as the Hill equation. It also considers the ion Mg²⁺ which is known to inhibit transmitter release (Dodge and Rahamimoff, 1967).

The standard Dodge-Rahamimoff equation is,

$$E = S \left(\frac{[Ca^{2+}]_o}{K_1} \right) / \left(1 + \frac{[Ca^{2+}]_o}{K_1} + \frac{[Mg^{2+}]_o}{K_2} \right)^{N_D}$$

The two affinity parameters, K₁ and K₂, are expressed in terms of extracellular Ca²⁺ and Mg²⁺ concentrations and were fixed to 2.7 and 4.8mM respectively (Dodge and Rahamimoff, 1967; Donaldson and Stricker, 1996). Therefore only two free parameters the cooperativity, N_D, and the scaling factor, S, are varied to fit the experimental data. This equation did not provide a good description of the data and the fit could be rejected in every case (p < 0.05, n=9, Fig. 4.1C). The fit could also be rejected when either or both K₁ and K₂ were made free parameters (p < 0.05, n=9).

Figure 4. 1

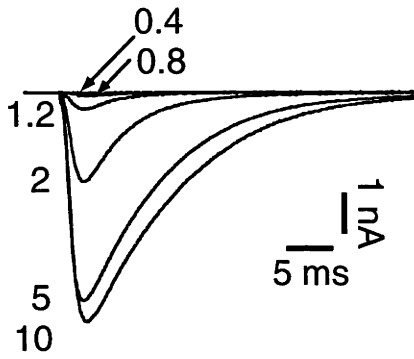
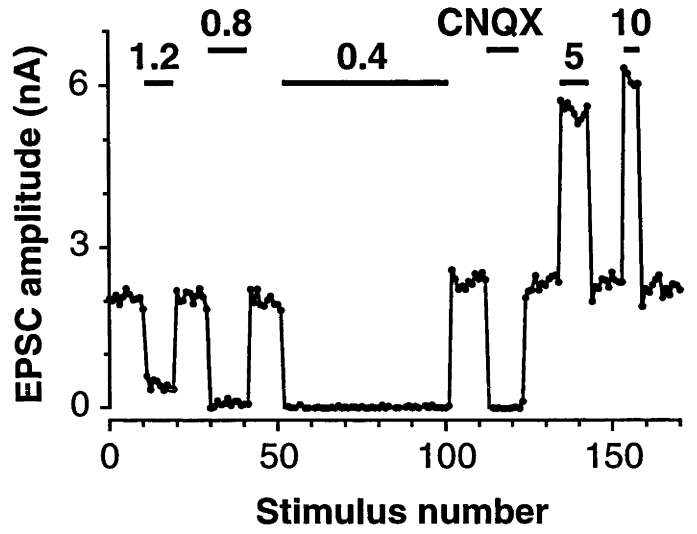
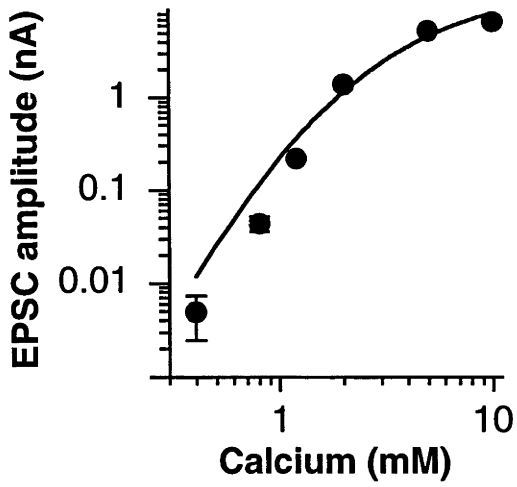
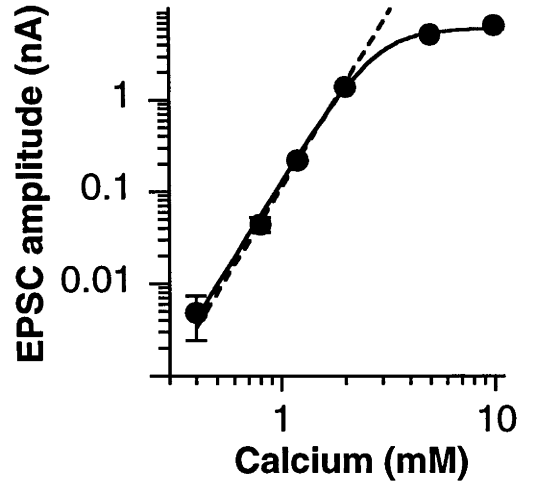
Figure 4. 1 Non-linear relationship between EPSC amplitude and $[Ca^{2+}]_o$. The cooperative involvement of several Ca^{2+} ions in the release of each vesicle of neurotransmitter is demonstrated by the non-linear relationship between $[Ca^{2+}]_o$ and EPSC amplitude.

A, AMPA EPSCs recorded at several different $[Ca^{2+}]_o$. Each trace is the average of 10 - 50 EPSCs.

B, Amplitude of individual EPSCs (same cell as A) plotted against stimulus number. Each $[Ca^{2+}]_o$ is bracketed by an epoch in 2mM $[Ca^{2+}]_o$ to ensure recording stability.

C, Average EPSC amplitude plotted against $[Ca^{2+}]_o$ on log-log axes. Error bars indicate ± 1 SD. The solid line is the optimally fitted Dodge-Rahamimoff equation. The fit was poor, and could be rejected ($p > 0.05$).

D, The same data as C, showing the optimally fitted Hill equation (solid line) with a Hill coefficient of 3.7. This equation provided an adequate fit ($p < 0.05$). The degree of cooperativity was independently estimated at 3.8 by fitting a power function over the 0.4 to 1.2 $[Ca^{2+}]_o$ range (dashed line).

A**B****C****D**

The most likely explanation for the failure of this approach is that the standard Dodge-Rahamimoff equation assumes a linear relationship between $[Ca^{2+}]_{it}$ and $[Ca^{2+}]_o$ whereas it is now known to be sublinear at higher $[Ca^{2+}]_o$ (Mintz *et al.*, 1995; Borst and Sakmann, 1996). This possibility is investigated below using the modified Dodge-Rahamimoff equation which incorporates a sublinear relationship between $[Ca^{2+}]_{it}$ and $[Ca^{2+}]_o$.

The Hill equation provides an empirical description of the dose-response relationship.

The Hill equation is,

$$E = S [Ca^{2+}]_o^{N_H} / (EC_{50}^{N_H} + [Ca^{2+}]_o^{N_H})$$

The fit provides an estimate of both cooperativity, N_H , and affinity, EC_{50} , of Ca^{2+} binding to the vesicle release complex. It permits empirical comparison between dose-response curves recorded under different conditions (Weiss, 1997). The Hill equation gave a good fit to the data in every case ($p > 0.05$, $n=9$). The Hill constant, N_H , was 3.3 ± 0.1 and EC_{50} was 2.3 ± 0.2 mM ($n=9$, solid line, Fig. 4.1D).

The dose-response curve at lower $[Ca^{2+}]_o$ should follow approximately a power function form. A fit at lower Ca^{2+} concentrations would be less affected by inadequate voltage clamp and other non-linearities (see Discussion). A power function fit restricted to this region may therefore provide a more reliable estimate of cooperativity than the Hill equation fit to the entire dose-response curve.

The power function is,

$$E = S [Ca^{2+}]_o^{N_P}$$

The power function forms a straight line when plotted in log-log coordinates, and the slope of the line is equal to the cooperativity parameter, N_P . The degree of cooperativity was estimated at 3.1 ± 0.2 ($n=9$, dashed line, Fig. 4.1D) by fitting the power function over the $[Ca^{2+}]_o$ range from 0.4 to 1.2mM.

Ca²⁺ cooperativity in the presence of Cd²⁺

The effect of non-selective blockade of Ca²⁺ channels on cooperativity was explored. Cd²⁺ is a competitive blocker of Ca²⁺ channels, but is not selective for different Ca²⁺ channel subtypes (Sather *et al.*, 1993; Zhang *et al.*, 1993). As expected, Cd²⁺ increased the Ca²⁺ EC₅₀ in a dose dependent manner: EC₅₀ (2μM Cd²⁺) = 3.5 ± 0.3mM and EC₅₀ (4μM Cd²⁺) = 5.0 ± 0.3mM (n = 5) (*cf.* 2.3 in control, Fig. 4.2A, B). However, Cd²⁺ produced no change in the degree of cooperativity, N_P (2μM Cd²⁺) = 3.1 ± 0.1 and N_P (4μM Cd²⁺) = 3.0 ± 0.1 (*cf.* 3.1 in control, Fig. 4.2C, D). Similarly, N_H was not significantly changed: N_H (2μM Cd²⁺) = 3.0 ± 0.2 and N_H (4μM Cd²⁺) = 3.6 ± 0.3 (n = 5) (*cf.* 3.3 in control). In summary, Cd²⁺ shifted the dose-response curve to the right without changing its steepness at lower Ca²⁺ concentrations.

Ca²⁺ cooperativity in the presence of ω-CTx and ω-Aga

The effect of selective blockade of Ca²⁺ channel subtypes on cooperativity was explored next. ω-CTx or ω-Aga were used to block N-type or P/Q-type channels respectively. N- and P/Q-type Ca²⁺ channels support transmitter release at excitatory synapses in the hippocampus (see Chapter 1, Part I and Chapter 3). N-type Ca²⁺ channels were blocked by ω-CTx (1μM) in an irreversible manner and this reduced the EPSC amplitude by 46.6 ± 4% (n=7, Fig. 4.3A, B) in 2mM Ca²⁺. The Ca²⁺ dependent binding of ω-CTx (Wagner *et al.*, 1988) is not a concern in experiments presented here. ω-CTx was always added in 2mM [Ca²⁺]_o and as the EPSC amplitude was unchanged when the external solution was bracketed back to 2mM Ca²⁺ (Fig. 4.3A) the binding of ω-CTx must be irreversible. ω-Aga (500nM) blocks both P- and Q-type Ca²⁺ channels. The EPSC amplitude reduction produced by ω-Aga was partially reversible in the autaptic culture preparation, therefore, the toxin had to be present throughout the experiment. ω-Aga (0.5μM) reduced the EPSC by 94 ± 0.4% (n=4, Fig. 4.3C, D) in 2mM Ca²⁺.

Figure 4. 2

Figure 4. 2 Cd^{2+} does not change the steepness of the Ca^{2+} dose-response curve. The competitive Ca^{2+} channel antagonist, Cd^{2+} , shifts the Ca^{2+} dose-response curve to the right in a dose-dependent manner.

A, Linear-log plot of the normalised EPSC amplitude vs $[\text{Ca}^{2+}]_o$ for three individual cells recorded in normal bath solution (*filled circles*), in the presence of $2\mu\text{M}$ Cd^{2+} (*open squares*) and $4\mu\text{M}$ Cd^{2+} (*open triangles*). Each point is the ensemble average amplitude ± 1 SD. The solid lines are Hill equation fits to the data.

B, Cd^{2+} increased the EC_{50} for Ca^{2+} . Average EC_{50} 's are shown in control solution ($n=9$) and in the presence of Cd^{2+} (2 and $4\mu\text{M}$, $n=5$). Error bars indicate SEM.

C, Cd^{2+} , did not broaden or change the steepness of the dose-response curve. Log-log plot of normalised EPSC amplitude vs $[\text{Ca}^{2+}]_o$ is shown for the same three cells as A. Solid lines show power function fits to the data.

D, Cd^{2+} had no effect on cooperativity. Average cooperativity (N_p) over the 0.4 to 1.2mM $[\text{Ca}^{2+}]_o$ range in control solution ($n=9$) and 0.8 to 2mM $[\text{Ca}^{2+}]_o$ range in the presence of Cd^{2+} (2 and $4\mu\text{M}$, $n=5$). Error bars indicate SEM.

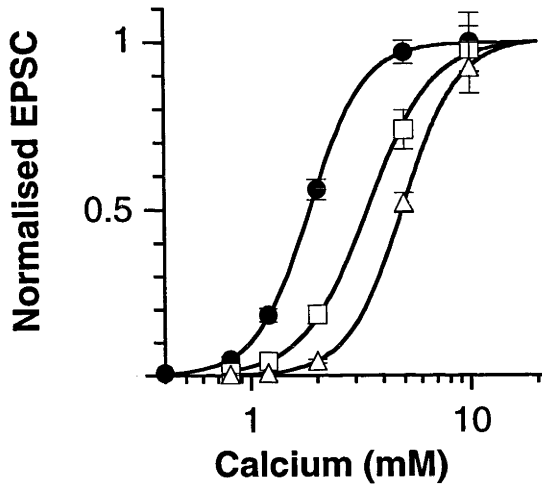
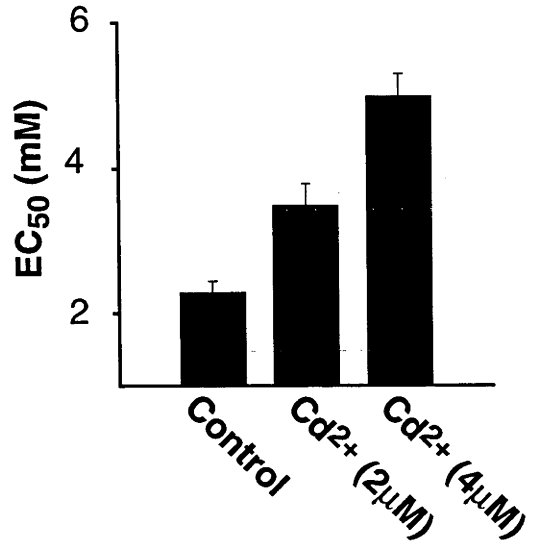
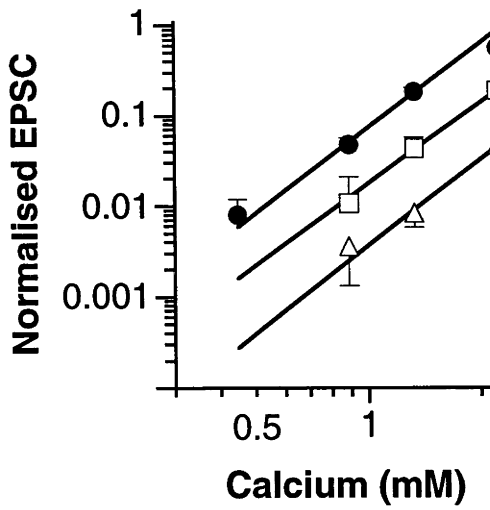
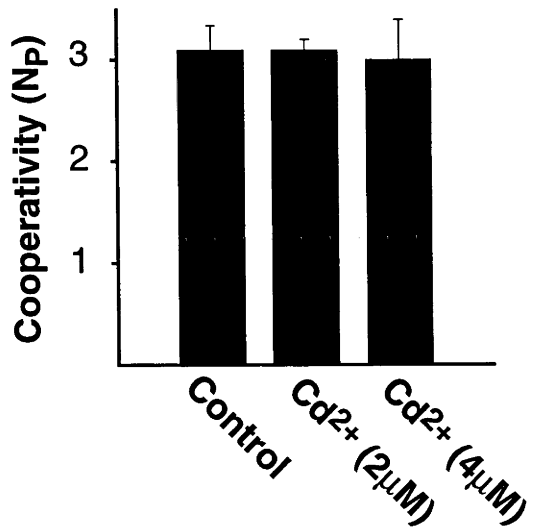
A**B****C****D**

Figure 4.3

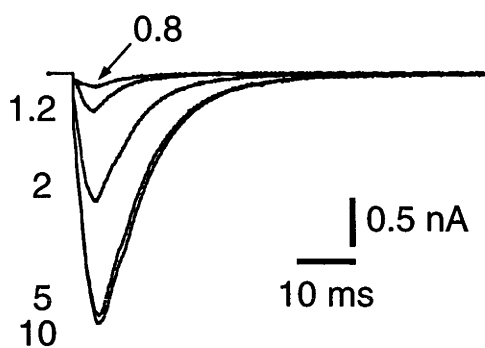
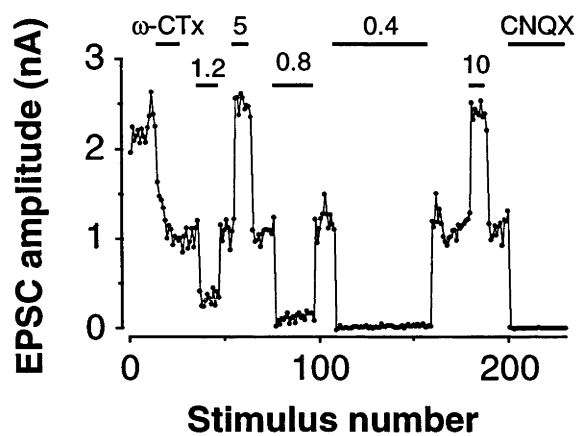
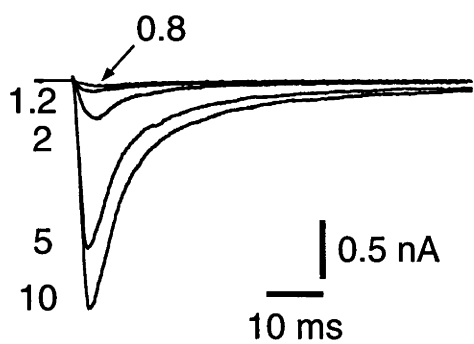
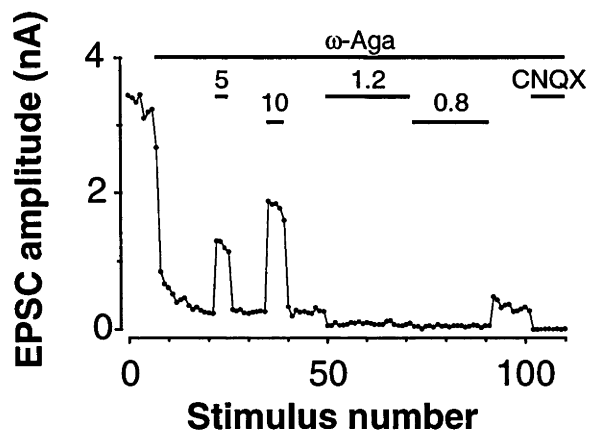
Figure 4.3 Dose-response relationship for EPSCs recorded in the presence of ω -CTx and ω -Aga.

A, AMPA EPSCs recorded at several different $[\text{Ca}^{2+}]_o$ in the presence of ω -CTx. Each trace is the average of 5-20 EPSCs.

B, Amplitude of individual EPSCs (same cell as A) plotted against stimulus number. Each $[\text{Ca}^{2+}]_o$ is bracketed by an epoch at 2mM $[\text{Ca}^{2+}]_o$ to ensure recording stability.

C, AMPA EPSCs recorded at several different $[\text{Ca}^{2+}]_o$ in the presence of ω -Aga. Each trace is the average of 5-20 EPSCs.

D, Amplitude of individual EPSCs (same cell as in C) plotted against stimulus number.

A**B****C****D**

There was no detectable difference between the degree of cooperativity in the presence of ω -Aga, ($N_P = 2.2 \pm 0.4$, $n=4$) or ω -CTx ($N_P = 2.4 \pm 0.2$, $n=7$) (unpaired t -test, $p > 0.05$; Fig. 4.4A, B, C). These estimates are based on a power function fit restricted to the $[Ca^{2+}]_o$ range from 0.8 to 2mM. Similarly, no difference in cooperativity could be detected when the Hill equation was fit over the entire $[Ca^{2+}]_o$ range. In the presence of ω -Aga, N_H was 2.5 ± 0.4 ($n=4$) and in ω -CTx, N_H was 2.6 ± 0.2 ($n=7$).

Non-uniform distribution of Ca^{2+} channel subtypes

If both N-type and P/Q-type Ca^{2+} channels are present in the same ratio on all presynaptic terminals (uniform distribution) and are functionally equivalent, then selective block of one subtype will produce a uniform shift in EC_{50} at all terminals. The dose-response curve will shift to the right with little change in its shape or steepness. In contrast, if the distribution of Ca^{2+} channel subtypes across synaptic terminals is non-uniform (Reuter, 1995; Reid *et al.*, 1997) (see Chapter 3) then selective block will only shift the EC_{50} at the subset of terminals that possess both Ca^{2+} channel subtypes. Other terminals will either be completely blocked, or will have no shift in their EC_{50} . The resulting mixture of terminals with different EC_{50} s will broaden the dose-response relationship and reduce its overall steepness. Thus, a reduction in steepness of the dose-response curve in the presence of a selective Ca^{2+} channel blocker would imply a non-uniform distribution of Ca^{2+} channel subtypes. In contrast, a non-selective Ca^{2+} channel blocker should not alter the overall steepness of the dose-response curve. The selective Ca^{2+} channel blocker, ω -CTx, reduced the Hill constant N_H to 2.6 ± 0.2 ($n=7$) and ω -Aga reduced N_H to 2.5 ± 0.4 ($n=4$) (*cf.* 3.3 in control). Similarly, a reduction in the power function was observed: N_P (ω -CTx) = 2.4 ± 0.2 ($n=7$) and N_P (ω -Aga) = 2.2 ± 0.4 ($n=4$) (*cf.* 3.1 in control). All reductions were significant (unpaired t -test, $p < 0.05$). In contrast, the non-selective blocker, Cd^{2+} (4 μ M), increased N_H to 3.6 ± 0.3 ($n=5$) but this increase was not significant ($p > 0.05$). Also, Cd^{2+} (4 μ M) did not significantly change N_P (3.0 ± 0.1 , $n=5$).

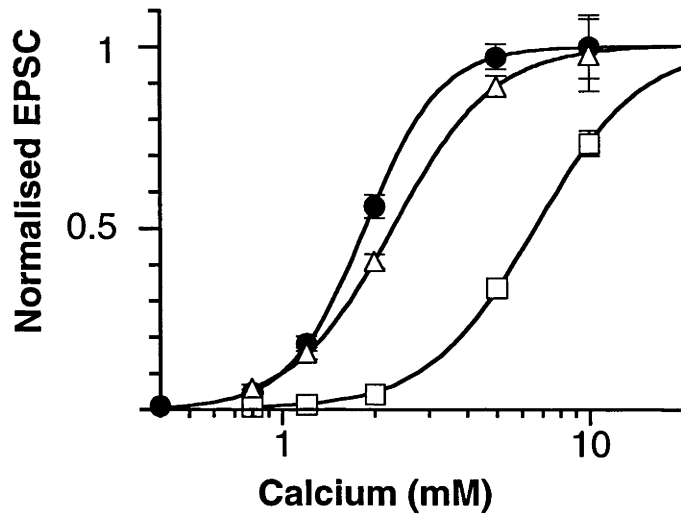
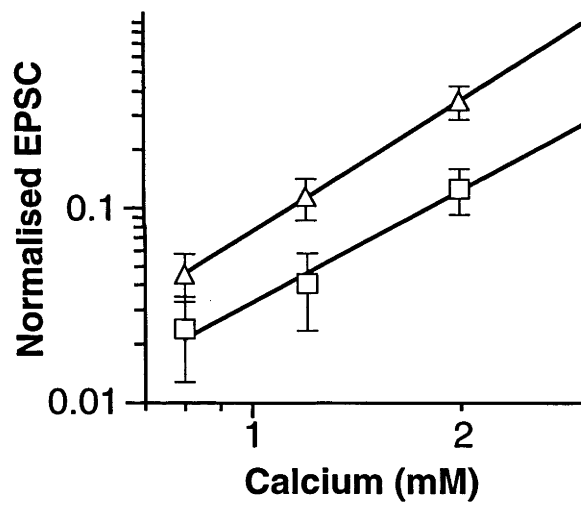
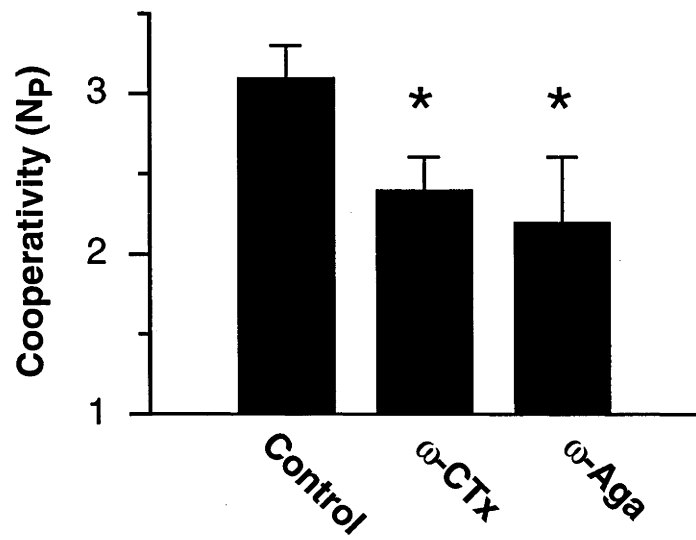
Figure 4. 4

Figure 4.4 ω -CTx and ω -Aga broaden the Ca^{2+} dose-response curve. Selective Ca^{2+} channel blockers shifts the Ca^{2+} dose-response curve to the right and broaden it.

A, Linear-log plot of the normalised EPSC amplitude vs $[\text{Ca}^{2+}]_o$ for three individual cells in normal bath solution (*filled circles*), and in the presence of ω -CTx (*open triangles*) and ω -Aga (*open squares*). Each point is the ensemble average amplitude \pm 1 SD. The solid lines are Hill equation fits to the data.

B, Log-log plot of normalised EPSC amplitude vs $[\text{Ca}^{2+}]_o$ for two individual cells recorded in the presence of ω -CTx (*open triangles*) or ω -Aga (*open circles*). Each point is the ensemble average amplitude \pm 1 SD. The solid lines are power function fits over the $[\text{Ca}^{2+}]_o$ range from 0.8 to 2mM.

C, The broadening of the dose-response curve by selective toxins reduces the cooperativity (N_P). Average N_P is shown in control (n=9), and in the presence of either ω -CTx (n=7) or ω -Aga (n=4). The significant reduction in N_P in the presence of selective toxin is consistent with a non-uniform distribution of Ca^{2+} channel subtypes across presynaptic terminals. Error bars indicate SEM. Stars indicate statistical significance ($p < 0.05$).

A**B****C**

A non-uniform distribution of Ca^{2+} channel subtypes also predicts a smaller shift in EC_{50} for the selective toxin block than the non-selective block of Cd^{2+} . This is because in the presence of the selective toxins only a proportion of terminals will shift to the right on the dose-response curve, while the non-selective blocker will shift all terminals. Both ω -CTx and Cd^{2+} reduced the EPSC amplitude by $\sim 45\%$ at 2mM Ca^{2+} , however, ω -CTx shifted the curve significantly less than Cd^{2+} ($\text{EC}_{50} \text{ Cd}^{2+} = 3.5\text{mM}$ cf. $\text{EC}_{50} \omega\text{-CTx} = 2.8\text{mM}$, $p < 0.05$) consistent with a non-uniform distribution of Ca^{2+} channel subtypes.

Experimental sources of non-linearity

A number of sources of non-linearity may shape the Ca^{2+} dose-response curve at high $[\text{Ca}^{2+}]_o$ (see below and Discussion). One potential source of non-linearity is reduced driving force due to inadequate voltage clamp of larger synaptic currents. To test for this possibility, CNQX ($0.5\mu\text{M}$) was applied at a low and a high $[\text{Ca}^{2+}]_o$ (1.2 and 10mM , Fig. 4.5A). CNQX reduced EPSC amplitude by $80 \pm 6\%$ in low $[\text{Ca}^{2+}]_o$ and by $75 \pm 5\%$ in high $[\text{Ca}^{2+}]_o$ ($n=5$, Fig. 4.5B). This difference was not significant ($p > 0.05$). CNQX reduces the EPSC amplitude making it less sensitive to poor voltage clamp. The two $[\text{Ca}^{2+}]_o$ represent the highest and a lower limit of the Ca^{2+} dose-response curves. There is no significant difference in the scaling by CNQX at these two extremes suggesting that the whole dose-response curve scales linearly. Thus, clamp error is generally small under these recording conditions.

The modified Dodge-Rahamimoff equation

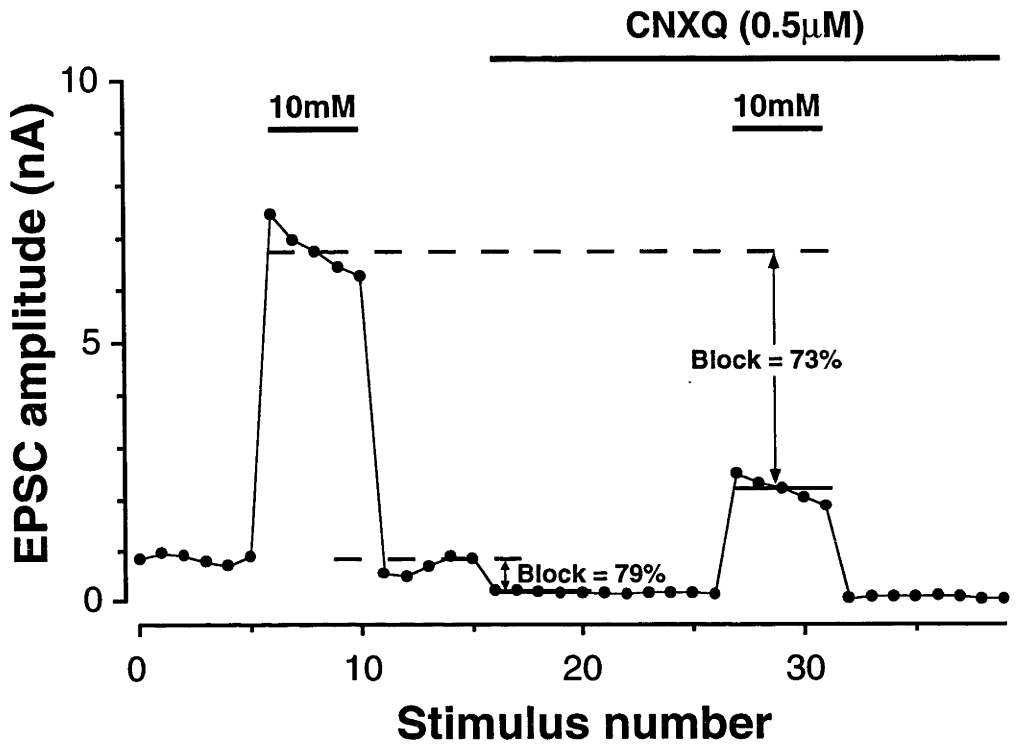
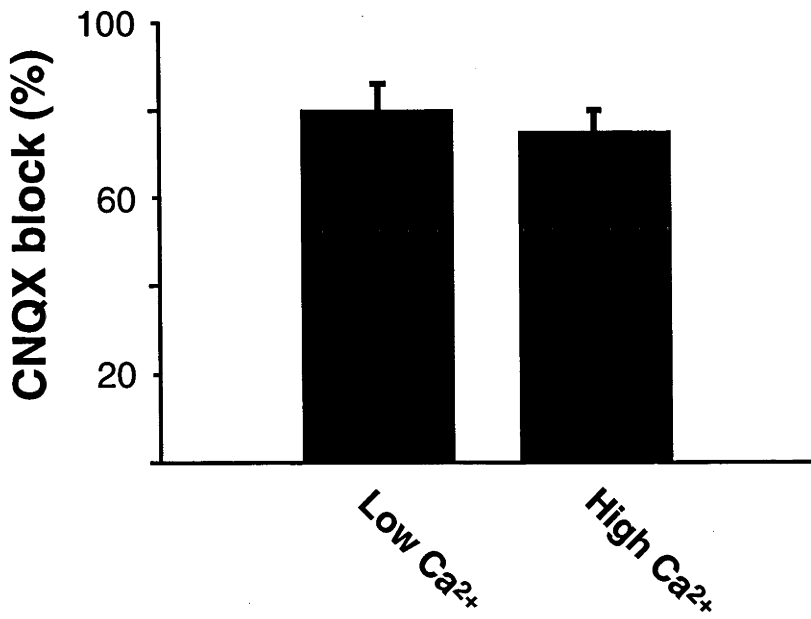
An underlying assumption used to derive the standard Dodge-Rahamimoff equation was that $[\text{Ca}^{2+}]_{it}$ varies linearly with $[\text{Ca}^{2+}]_o$, but this relationship was recently found to be sublinear at central synapses for $[\text{Ca}^{2+}]_o > 1\text{mM}$ (Mintz *et al.*, 1995; Borst and Sakmann, 1996). This sublinearity implies that experimental dose-response curves will reach saturation more rapidly than predicted by the standard Dodge-Rahamimoff equation. Rapid saturation was seen consistently in the present study and was responsible for the poor quality of the fit with this equation (Fig. 4.1C). Note that the

Figure 4. 5

Figure 4. 5 Inadequate voltage clamp is not a major source of non-linearity of the $[Ca^{2+}]_o$ dose-response relationship. If clamp error is a significant problem then larger AMPA EPSCs should be less sensitive to an antagonist.

A, AMPA EPSC amplitude vs stimulus number at 1.2mM and 10mM $[Ca^{2+}]_o$ in the absence and presence of the competitive AMPA receptor antagonist CNQX (0.5 μ M). The block of the EPSC by CNQX in high (10mM) and low (1.2mM) $[Ca^{2+}]_o$ is similar indicating that clamp error is generally small under our recording conditions.

B, Average CNQX block at high and low $[Ca^{2+}]_o$ (n=5). Error bars indicate SEM.

A**B**

discrepancies between the fit and the data appear larger at low $[Ca^{2+}]_o$ due to the log-log coordinates. Similar behaviour has been reported previously (Wheeler *et al.*, 1996). To address this problem, a sublinear relationship between $[Ca^{2+}]_{it}$ and $[Ca^{2+}]_o$ was incorporated into a modified Dodge-Rahamimoff equation. The extracellular calcium concentration term was replaced by an empirical expression for the effective intra terminal concentration in the modified equation,

$$[Ca^{2+}]_{it} = [Ca^{2+}]_o / (1 + ([Ca^{2+}]_o / K_s)^{N_s})^{1/N_s}$$

where:

K_s is the $[Ca^{2+}]_o$ where flux into the terminal is reduced by $(1/2)^{1/N_s}$;

N_s is the degree of cooperativity for Ca^{2+} inhibition of Ca^{2+} flux.

This expression was chosen for two reasons: (i) the relationship between $[Ca^{2+}]_{it}$ and $[Ca^{2+}]_o$ is linear at low extracellular concentrations but is sublinear at higher concentrations; and (ii) when $N_s = 1$, the expression reduces to the form predicted by the Michaelis-Menten expression for Ca^{2+} flux through a channel pore with a single rate-limiting Ca^{2+} binding site (Hille, 1992; Church and Stanley, 1996).

The modified Dodge-Rahamimoff equation could not be used to estimate cooperativity. The cooperativity parameters, N_D and N_s , can interact leading to a non-unique solution. For this reason, both parameters should be fixed when fitting this equation to dose-response data. The modified equation was fit to individual dose-response curves and it produced a good fit in 8 out of 9 cases ($p > 0.05$, Fig. 4.6A). The parameters K_1 and K_2 were fixed at previously reported values for excitatory hippocampal synapses (2.7 and 4.8mM respectively) (Donaldson and Stricker, 1996), N_D was fixed at 4 (Dodge and Rahamimoff, 1967; Borst and Sakmann, 1996), and N_s was fixed at 2. Only the scaling factor, S , and the calcium block affinity, K_s , were free parameters, and the optimum value of K_s was $2.1 \pm 0.2mM$ ($n=9$). In the present study, when the release cooperativity parameter, N_D , was reduced to 3 the quality of the fit was also reduced and an adequate fit was obtained in only 3 out of 9 cells ($p > 0.05$). The fit was also sensitive to the setting of N_s . If this parameter was fixed

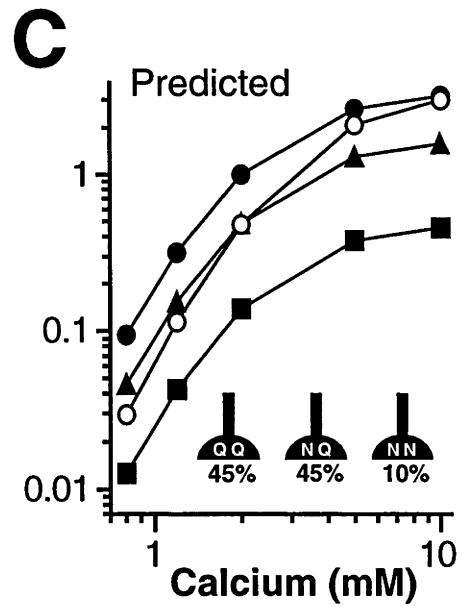
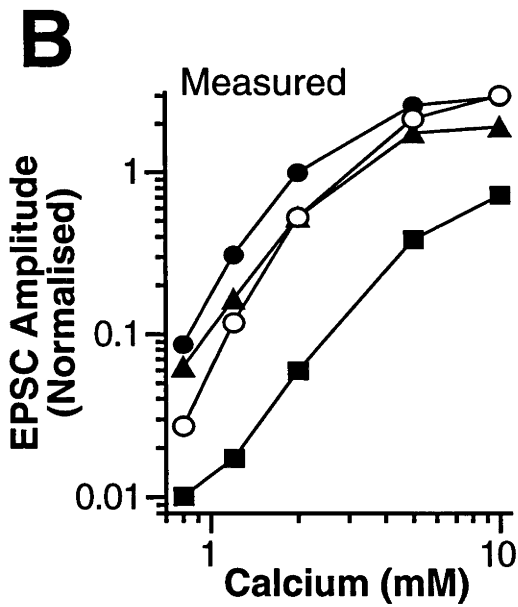
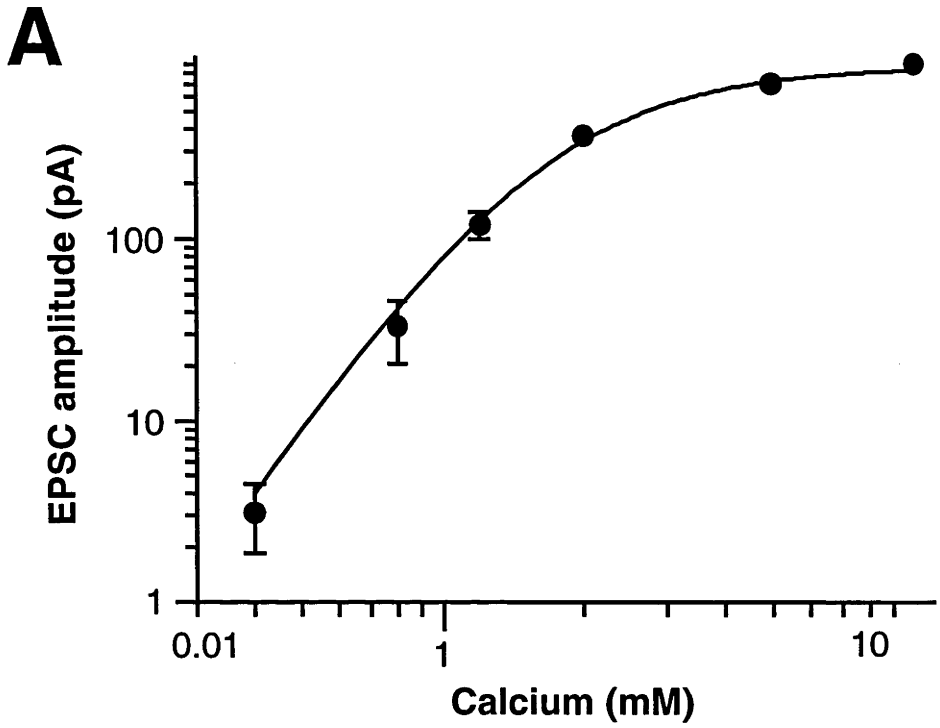
Figure 4. 6

Figure 4. 6 .A synaptic model predicts the Ca^{2+} dose-response curve observed in the presence of ω -CTx, ω -Aga and Cd^{2+} . The modified Dodge-Rahamimoff equation which incorporates a sublinear relationship between $[\text{Ca}^{2+}]_{\text{it}}$ and $[\text{Ca}^{2+}]_{\text{o}}$ provides an accurate description of the Ca^{2+} dose-response curve.

A, Log-log plot of EPSC amplitude vs $[\text{Ca}^{2+}]_{\text{o}}$ is shown for an individual cell. The solid line is the optimally fitted modified Dodge-Rahamimoff equation which represents a good fit ($p < 0.05$).

B, Log-log plot of average normalised EPSC amplitude vs $[\text{Ca}^{2+}]_{\text{o}}$ under four different experimental conditions; control (*filled circles*, $n=9$), ω -Aga ($0.5\mu\text{M}$, *filled square*, $n=5$), ω -CTx ($1\mu\text{M}$, *filled triangle*, $n=5$) and Cd^{2+} ($2\mu\text{M}$, *open circles*, $n=7$). EPSC amplitudes from individual cells were normalised to the amplitude recorded at 2mM $[\text{Ca}^{2+}]_{\text{o}}$ in the absence of blockers.

C, A model based on the modified Dodge-Rahamimoff equation (see Inset and Results) accurately predicted the observed dose-response curves in B. Theoretical dose-response curves are shown in control and in the presence of Ca^{2+} channel blockers. *Inset*, Schematic overview of the model. Presynaptic terminals were divided into three classes; one with only P/Q-type Ca^{2+} channels (QQ), one with only N-type Ca^{2+} channels (NN) and one with both channel subtypes (NQ).



at 1, thereby giving a Michaelis-Menten formulation for Ca^{2+} flux (Church and Stanley, 1996), the modified Dodge-Rahamimoff equation no longer fit any of the dose-response curves ($n=9$, $p < 0.05$). Similarly, in an imaging study, Mintz *et al.* (1995) describe the sublinear relationship between $[\text{Ca}^{2+}]_{\text{it}}$ and $[\text{Ca}^{2+}]_{\text{o}}$ with a bimolecular binding process that has a dissociation constant of 3mM.

A model synapse

A model synapse was constructed to investigate the role of different Ca^{2+} channel subtypes and their distribution across synaptic terminals in synaptic function. The model predicts EPSC amplitude as a function of $[\text{Ca}^{2+}]_{\text{o}}$ in the presence of Ca^{2+} channel blockers. Three classes of terminal were included in the model: one class with only P/Q-type channels (QQ), one class with only N-type channels (NN) and one class with both channel subtypes (NQ) (Fig. 4.6C, see Chapter 3). The postsynaptic response of the three classes was summed to produce the model synaptic response. It was assumed that at an individual terminal Ca^{2+} entering through different channels combined to act on the same vesicle release site or sites (see Discussion). At NQ terminals, N-type channels were assumed to contribute one half of the effective intraterminal Ca^{2+} , and P/Q-type channels the other half. The two channel subtypes were assumed to have similar activation and Ca^{2+} flux properties.

The modified Dodge-Rahamimoff equation was incorporated into a model synapse. Each class of terminal generated a dose-response curve based on a modified Dodge-Rahamimoff equation with parameter values derived from the fits to experimental data recorded in the absence of Ca^{2+} channel blockers. The effects of Cd^{2+} were modelled by reducing Ca^{2+} influx uniformly at each class of terminal. ω -CTx blocked influx at NN terminals, and reduced influx by half at NQ terminals, while ω -Aga blocked influx at QQ terminals, and reduced it by half at NQ terminals. The proportion of model terminals in the three classes were set at 45% QQ, 45% NQ and 10% NN, based on results from a previous study (see Chapter 3). Dose-response curves were generated by the model synapse in the presence and absence of Ca^{2+} channel blockers. The

model predicted all the main features of the data, and the experimental dose-response curves (Fig. 4.6B) are very similar to the model curves (Fig. 4.6C). In constructing Fig. 4.6B and 4.6C, all experimental and theoretical EPSC amplitudes were normalised to the response in 2mM Ca^{2+} with no blockers. The cooperativity parameter, N_P , was calculated from power function fits to the theoretical dose-response data using the same $[\text{Ca}^{2+}]_o$ range and the same number of data points that were used when fitting the experimental data. The theoretical value of N_P was 3.0 in the absence of blockers, 3.0 in Cd^{2+} , and 2.6 in $\omega\text{-CTx}$ or $\omega\text{-Aga}$. These theoretical values all fell within the 95% confidence intervals for experimental estimates of N_P .

The estimated cooperativity, N_P , obtained by fitting a power function to the theoretical dose-response curves was < 4 , even though these curves were constructed from a model with a cooperativity, N_D , of 4. This suggests that power function fits systematically underestimate cooperativity under these experimental conditions. This is because the experimental data could not be extended to sufficiently low $[\text{Ca}^{2+}]_o$. When the power function fit was applied to the extrapolated theoretical dose-response curves over a concentration range from 0.005 to 0.1mM all values of N_P converged to 4, as expected.

Discussion

Dose-response analysis in the presence of Ca^{2+} channel non-linearity

In traditional dose-response studies it is assumed that the effective Ca^{2+} concentration attained at release sites in presynaptic terminals during synaptic activation varies linearly with $[\text{Ca}^{2+}]_o$. On the time-scale of synaptic transmission, the effective intraterminal Ca^{2+} concentration is approximately proportional to the Ca^{2+} flux into the terminal during the presynaptic action potential, and to the duration of the action potential (Augustine, 1990; Wheeler *et al.*, 1996). Studies of Ca^{2+} channel properties suggest that Ca^{2+} flux through a channel varies linearly with $[\text{Ca}^{2+}]_o$ at low concentrations, but is sublinear at higher concentrations due to transient Ca^{2+} dependent block of the channel pore (Church and Stanley, 1996). Another potential

source of non-linearity is the membrane potential shielding effect produced by divalent cations which becomes significant at concentrations above ~2mM (Hille, 1992). This may reduce the presynaptic action potential amplitude and duration, thereby reducing net Ca^{2+} influx and contributing to sublinearity. A further possible source is a non-linear relationship between ion activity and $[\text{Ca}^{2+}]_o$. This is due to the incomplete dissociation of salts at higher concentrations (Hille, 1992). The Ca^{2+} activity was estimated to change less than 6% over the $[\text{Ca}^{2+}]_o$ range in our solutions (Grahame, 1947).

The predicted non-linearity has been directly confirmed using Ca^{2+} imaging techniques (Mintz *et al.*, 1995) and by patch-clamping a large presynaptic terminal (Borst and Sakmann, 1996). The relationship between peak Ca^{2+} concentration in the terminal during synaptic activation and $[\text{Ca}^{2+}]_o$ was approximately linear for $[\text{Ca}^{2+}]_o \leq 1\text{mM}$, but was significantly sublinear at higher concentrations. This finding indicates that power function fits to the dose-response curve should be restricted to the concentration range below about 1mM, or corrected for the observed sublinearity at higher concentrations. In the present study, the dose-response curves recorded in the presence of Ca^{2+} channel blockers were not corrected and were fit from 0.8 to 2mM. Cooperativity may be systematically underestimated under these conditions. However, this does not preclude a useful comparison between the degree of cooperativity in ω -CTx and in ω -Aga, because both values were estimated over the same $[\text{Ca}^{2+}]_o$ range and any systematic error should be similar.

The modified Dodge-Rahamimoff equation

The sublinear relationship between $[\text{Ca}^{2+}]_{it}$ and $[\text{Ca}^{2+}]_o$ was incorporated into the modified Dodge-Rahamimoff equation. This greatly improved the fit to the dose-response data compared with the standard Dodge-Rahamimoff equation. The improvement was due to the faster saturation of the modified Dodge-Rahamimoff curve at higher $[\text{Ca}^{2+}]_o$. The fit had only 2 free parameters (the same as the standard equation), so the improvement was not due to an increase in the degrees of freedom.

When the release cooperativity parameter, N_D , was reduced to 3 the quality of the fit was also reduced. This result is compatible with a Ca^{2+} cooperativity of at least 4 for transmitter release. The fit was also sensitive to the setting of N_S . If this parameter was fixed at 1, thereby giving a Michaelis-Menten formulation for Ca^{2+} flux (Church and Stanley, 1996), the modified Dodge-Rahamimoff equation no longer fit any of the dose-response curves. A similar finding was made by Mintz *et al.* (1995), who describe the sublinear relationship between $[\text{Ca}^{2+}]_{it}$ and $[\text{Ca}^{2+}]_o$ with a bimolecular binding process. Thus, the sublinearity in the relationship between $[\text{Ca}^{2+}]_{it}$ and $[\text{Ca}^{2+}]_o$ is not simply due to Ca^{2+} binding at a single site in the channel (Church and Stanley, 1996). It is possible that there are multiple binding sites for divalent cations in N- and P/Q-type channels (Hille, 1992), or that an independent process, such as membrane potential shielding by Ca^{2+} , contributes to the sublinearity. Voltage clamp error is another possible source of sublinearity as is concentration dependence of Ca^{2+} activity. In summary, the cooperativity for transmitter release, N_D , must be at least 4, and the cooperativity for Ca^{2+} flux inhibition, N_S , must be at least 2 to obtain a good fit between the modified Dodge-Rahamimoff equation and the dose-response curve observed in the absence of blockers.

No difference between cooperativities for N- and P/Q-type channels

The model shows that cooperativity may be systematically underestimated by the power function fit in the experimental $[\text{Ca}^{2+}]_o$ range. Despite this, the comparison of the N_P values under different experimental conditions may still be valid, if the systematic error is similar. This possibility was confirmed by analysing the model dose-response curves. The values obtained for N_P were nearly identical for release mediated by N-type or P/Q-type channels (both 2.6). These results were consistent with the model settings where both channel subtypes were assumed to have a cooperativity of 4. To investigate the sensitivity of the power function fit to differences in cooperativity the model was altered such that Ca^{2+} entering a terminal through N-type and P/Q-type channels induced transmitter release with cooperativities of 2.5 and 4 respectively (Mintz *et al.*, 1995). A power function fit was performed

over the same range used for the experimental data and the results for N_p were 1.6 in the presence of ω -Aga and 2.6 in the presence of ω -CTx. Thus, the different cooperativities could easily be detected from the dose-response curves. This result implies that systematic errors do not preclude useful comparison between cooperativity estimates for N-type and P/Q-type channels under these experimental conditions.

Some Ca^{2+} imaging studies suggest that the N- and P/Q-type Ca^{2+} channels support release with different cooperativities. The most significant advantage of imaging techniques is that they provide a direct measure of Ca^{2+} concentration in the synaptic terminal. This parameter is not measured or accurately controlled in dose-response studies. Two recent studies measured presynaptic Ca^{2+} concentration using the Ca^{2+} sensitive dye, furaptra, while simultaneously recording postsynaptic responses (Wu and Saggau, 1994b; Mintz *et al.*, 1995). Mintz *et al.* (1995) find that release is more steeply dependent on $[Ca^{2+}]_{it}$ for P/Q- than for N-type Ca^{2+} channels at synapses in the cerebellum. Cooperativity was estimated at 4 for P/Q-type Ca^{2+} channels, and 2.5 for N-type channels. They estimated cooperativity from a power function fit to only two data points, one before and one after selective block of a Ca^{2+} channel subtype. The power function fit is only valid at low $[Ca^{2+}]_{it}$ and a fit in the higher $[Ca^{2+}]_{it}$ range would be expected to underestimate N_p . ω -CTx produced a ~25% drop in the fluorescence signal while ω -Aga reduced the fluorescence signal by ~50%. ω -Aga therefore spans a larger $[Ca^{2+}]_{it}$ range than ω -CTx. The lower measured cooperativity for N-type Ca^{2+} channels may, therefore, reflect the relatively high $[Ca^{2+}]_{it}$ range over which cooperativity was estimated. Wu and Saggau (1994) find no significant difference in the cooperativity for N- and P/Q-type channels at excitatory hippocampal neurons. In their experiments the $[Ca^{2+}]_{it}$ range is more extensively explored by observing the $[Ca^{2+}]_{it}$ at various time points of the slow toxin block and at various concentrations of toxins. Also, the $[Ca^{2+}]_{it}$ range over which cooperativity is measured is larger than that used by Mintz *et al.* (1995). ω -CTx produced a ~40%

drop in the fluorescence signal (*cf.* ~25%), while ω -Aga reduced the fluorescence signal by ~60% (*cf.* ~50%) at hippocampal synapses.

The presence of a residual Ca^{2+} fluorescence signal further complicates interpretation of these results. When both the N-type and the P/Q-type Ca^{2+} channels were blocked the peak amplitude of the fluorescence transient was only reduced by ~75%. The remaining 25% was presumably due to Ca^{2+} entry through non-N, non-P/Q type channels. The Ca^{2+} cooperativity estimates assume that these toxin-resistant channels are co-localised on excitatory presynaptic terminals with N-type and P/Q type channels, but there is no evidence to support this assumption. Also, it is not clear to what extent the toxin-resistant channels are involved in excitatory synaptic transmission (Wheeler *et al.*, 1996). The finding of the present study; that cooperativity was similar for release mediated by N- or P/Q- type Ca^{2+} channels is consistent with previous results in the hippocampus (Wu and Saggau, 1994b) but contrasts with results obtained in the cerebellum (Mintz *et al.*, 1995). This may reflect limitations in the experimental method used, although a difference in the functional organisation of Ca^{2+} channel subtypes at synapses in different regions of the brain cannot be ruled out.

The non-uniform distribution of Ca^{2+} channel subtypes

Three changes of the Ca^{2+} dose-response curve in the presence of ω -CTx and ω -Aga are consistent with the non-uniform distribution of Ca^{2+} channel subtypes across presynaptic terminals as described in Chapter 3: (i) both toxins broaden the dose-response relationship; (ii) the shift in the dose-response relations in the presence of ω -CTx is less than that for the non-selective Cd^{2+} despite a similar block; and (iii) the dose-response relationships saturate at a lower amplitude in the presence of the toxins than in control (Fig. 4.6B).

All these observations can be accounted for if the toxins produce a shift to the right in the dose-response EC_{50} at some terminals, completely block other terminals and leave

the remainder unaffected. The resulting mixture of the unchanged dose-response relationship with that of the shifted dose-response relationship predicts a broader dose-response curve (see Results). Similarly, if the dose-response curve of only a proportion terminals are shifted to the right in the presence of the selective toxins, then this shift should be less than that for a non-selective blocker which will shift all terminals.

The Ca^{2+} dose-response curves in the presence of either toxin reaches saturation at an EPSC amplitude lower than that observed in control (Fig. 4.6B). This result indicates that maximal Ca^{2+} influx through P/Q-type channels cannot fully substitute for the Ca^{2+} influx lost on blockade of N-type channels. A similar argument applies when P/Q-type channels are blocked. Consistent with this, an increase in action potential duration (increasing Ca^{2+} influx) or increase in $[\text{Ca}^{2+}]_o$ could not fully reverse the block following the application of either ω -CTx or ω -Aga in hippocampal slice (Wheeler *et al.*, 1996). This result is expected if Ca^{2+} channel subtypes are distributed in a non-uniform manner across different presynaptic. An alternative explanation may be an absolute limit on the rate of Ca^{2+} influx through either channel subtype (Church and Stanley, 1996).

The model synapse incorporating a non-uniform distribution of Ca^{2+} channel subtypes predicts all of these experimental findings. Firstly, it predicts a broader dose-response relationship in the presence of selective Ca^{2+} channel antagonists than in the presence of a non-selective antagonist (Fig. 4.6C). This broadening is reflected in the reduced values for N_p in the presence of ω -CTx and ω -Aga. Secondly, the shift in EC_{50} of the model response in the presence of ω -CTx ($\text{EC}_{50} = 2.8\text{mM}$) is less than that observed in $2\mu\text{M}$ Cd^{2+} ($\text{EC}_{50} = 3.2\text{mM}$), compared with control ($\text{EC}_{50} = 2.3\text{mM}$). Finally, the model dose-response relationships in the presence of the toxins saturate at lower EPSC amplitudes than the control amplitude. Taken together these results are consistent with a non-uniform distribution of Ca^{2+} channel subtypes across excitatory synaptic terminals as described in Chapter 3.

The overlap of Ca²⁺ microdomains

An underlying assumption of the model is that, where terminals contain both Ca²⁺ channel subtypes (N- and P/Q-types), Ca²⁺ influx through the channels combine and contribute jointly to the Ca²⁺ transient responsible for release. The extent to which this overlap of Ca²⁺ influx occurs remains controversial. The opening of presynaptic Ca²⁺ channels by an action potential is known to trigger transmitter release very rapidly (60-200 μs) (Llinas *et al.*, 1981; Sabatini and Regehr, 1996). Imaging of Ca²⁺ within the squid and hair cell presynaptic terminals show that high Ca²⁺ concentrations are achieved rapidly near the transmitter release site (Llinas *et al.*, 1992; Llinas *et al.*, 1995; Tucker and Fettiplace, 1995). Numerous mathematical studies of the Ca²⁺ distribution near an open Ca²⁺ channel suggest that the "Ca²⁺ microdomain" at the mouth of the channel forms rapidly and dissipates quickly upon channel closure, reaching equilibrium within microseconds (Fogelson and Zucker, 1985; Simon and Llinas, 1985; Stern, 1992; Winslow *et al.*, 1994; Issa and Hudspeth, 1996; Sinha *et al.*, 1997). This evidence favours the close apposition of Ca²⁺ channels to the release mechanism and argues against an overlap of Ca²⁺ microdomains.

Stanley (1993) provides further evidence that non-overlapping Ca²⁺ domains are sufficient to elicit transmitter release. By patch clamping the release face of the presynaptic terminals of neurons from the chick ciliary ganglion, he isolated the occurrence of a secretory event after the opening of a single Ca²⁺ channel. It was concluded from these experiments that the opening of an individual channel is sufficient to trigger release. Similar findings have been demonstrated at the frog neuromuscular junction (Yoshikami *et al.*, 1989) and at the squid giant synapse (Augustine, 1990). Ca²⁺ buffers such as EGTA and 1,2-bis(2-aminophenoxy)ethane-N,N,N',N'-tetraacetic acid (BAPTA) are often used to infer details about the spatial localisation of the Ca²⁺ channel and the release mechanism. If the channel is in close apposition to the release mechanism then slow chelators, such as EGTA, will not be effective at reducing release. Consistent with this EGTA did not reduce transmitter

release at the squid giant synapse (Adler *et al.*, 1991). This evidence argues for the involvement of narrow, non-overlapping Ca^{2+} domains in transmitter release, at least at some synapses.

In contrast, two pieces of experimental evidence suggest that an overlap of Ca^{2+} channel microdomains occurs under physiological conditions at central synapses. Firstly, the supra-additive sum (~120-140%) of the block of transmitter release by ω -CTx and ω -Aga argues for the cooperative co-existence of N- and P/Q-type channels on presynaptic terminals (Chapter 1, Part I). If the toxins are selective then the only way that the sum of their individual blocks can be greater than 100% is if the Ca^{2+} influx through each channel contributes jointly to a local Ca^{2+} transient that triggers release (Wheeler *et al.*, 1994; Wu and Saggau, 1994b; Mintz *et al.*, 1995). Results presented in this Chapter and in Chapter 3 are consistent with this finding. Secondly, a reduction of synaptic transmission by the slow Ca^{2+} buffer EGTA (1mM) injected into the presynaptic terminal of the calyx of Held (Borst and Sakmann, 1996) indicates that Ca^{2+} must diffuse a relatively long distance to reach the Ca^{2+} sensor and that an overlap in Ca^{2+} microdomains is likely. A more recent study shows that presynaptic Ca^{2+} channels at the calyx of Held have a high probability of opening (Borst and Sakmann, 1998). This is expected if adjacent Ca^{2+} channels are required to open in order for release to occur.

The results of Stanley (1993) cannot exclude the possibility that the opening of many channels are more effective than the opening of just one Ca^{2+} channel in supporting release. The supra-additivity of the toxin block demonstrates overlapping Ca^{2+} domains but cannot demonstrate the absolute requirement for multiple channel opening to initiate transmitter release. However, it is difficult to reconcile the supra-additivity of the toxins with a non-overlapping domain theory. It therefore seems likely that at some central synapses, including excitatory synapses in hippocampal culture, a degree of overlap occurs between Ca^{2+} microdomains.

Conclusions

Dose-response analysis remains a useful tool for investigating Ca^{2+} cooperativity at central synapses, but it is important to incorporate the sublinear relationship between $[\text{Ca}^{2+}]_{\text{it}}$ and $[\text{Ca}^{2+}]_{\text{o}}$ in the analysis. A modified Dodge-Rahamimoff equation which incorporates a non-linear relationship between $[\text{Ca}^{2+}]_{\text{o}}$ and $[\text{Ca}^{2+}]_{\text{it}}$ and has a cooperativity of 4 accurately describes the Ca^{2+} dose-response curve at excitatory hippocampal synapses. There was no difference in the degree of cooperativity for transmitter release mediated via N-type or P/Q-type Ca^{2+} channels. Selective blockers of N-type or P/Q-type Ca^{2+} channels broadened the dose-response relationship, consistent with a non-uniform distribution of Ca^{2+} channel subtypes across different synaptic terminals. A model of the role of Ca^{2+} in transmitter release was developed. The model uses the modified Dodge-Rahamimoff equation and incorporates a non-uniform distribution of Ca^{2+} channel subtypes across presynaptic terminals. The model describes the Ca^{2+} dose-response curve generated in the presence of both selective and non-selective Ca^{2+} channel blockers. Experimental estimates of Ca^{2+} cooperativity fell in the range 2 - 3, under a variety of recording conditions and using several standard analytical approaches. However, the model results suggest that these values systematically underestimate the true cooperativity. Traditional dose-response analysis cannot be extended to sufficiently low $[\text{Ca}^{2+}]_{\text{o}}$ because of signal-to-noise limitations and therefore systematically underestimates Ca^{2+} cooperativity. Results presented here are consistent with the cooperative involvement of 4 Ca^{2+} ions for each vesicle of transmitter released at a central synapse, and with a non-uniform distribution of Ca^{2+} channel subtypes across synaptic terminals.

Chapter 5

Long Term Potentiation in the Dentate Gyrus

Introduction

Long-term potentiation (LTP) of synaptic transmission is the putative mechanism underlying learning and memory. LTP was first described for the excitatory synaptic contacts made by axons of the perforant path onto dentate granule cells (Bliss and Lomo, 1973). The perforant path is a synaptic pathway between the entorhinal cortex and the dentate gyrus of the hippocampus. The two excitatory input pathways, the medial perforant path (MPP) and the lateral perforant path (LPP), both synapse onto dentate granule cells. Anatomical studies show that the LPP terminates on the distal third, and the MPP on the central third of the dendritic tree (Witter, 1993). Most behavioural studies involving LTP have been completed in the dentate region of the hippocampus (Jeffery, 1997). Determining the physiological mechanism underlying LTP in the dentate region will allow experiments to be designed that could help to link LTP and memory.

LTP induction of the MPP input is blocked by (i) NMDA receptor antagonists; or (ii) by the injection of Ca^{2+} chelating agents into the postsynaptic cell (Colino and Malenka, 1993). This implicates an essential role of Ca^{2+} influx through postsynaptic NMDA receptors in LTP induction. Two lines of evidence support a postsynaptic locus of LTP expression at MPP synapses. Following LTP induction: (i) there is no change in paired-pulse depression (Christie and Abraham, 1994); and (ii) AMPA binding, measured using quantitative autoradiography, increases in parallel with the potentiation of the extracellular field EPSP (Maren *et al.*, 1993). In contrast, several recent studies suggest a presynaptic locus. Following LTP induction: (i) progressive MK-801 block of the NMDA EPSC is faster (Min *et al.*, 1998); (ii) $1/\text{CV}^2$ increases; implying an increase in quantal content (Wang *et al.*, 1996); and (iii) release of

glutamate from the dentate region is potentiated (Bliss *et al.*, 1987; Errington *et al.*, 1987) (see Chapter 1, part II). In summary, the locus of expression of LTP for the MPP synapses onto dentate granule cells remains a contentious question. A similar controversy surrounds this issue at other synapses exhibiting NMDA-dependent LTP (see Chapter 1, Part II)

This chapter describes a novel approach for investigating the site of synaptic modulation. The approach is free of unrealistic assumptions concerning the transmitter release mechanism, and can be applied to multifibre EPSCs. The variance of the evoked synaptic amplitude was plotted against mean synaptic amplitude at several different Cd^{2+} concentrations. The slope of the variance-mean plot estimates the average amplitude of the response following the release of a single vesicle of transmitter (Q_{AV}). The validity of the technique was tested by applying the analysis before and after three different synaptic modulations: (i) a reduction in Q_{AV} by the addition of CNQX, (ii) a reduction in the average probability of transmitter release (P_{T}) by the addition of baclofen, and (iii) an increase in the number of active synaptic terminals (N) by increasing the stimulus strength. The variance-mean technique was used to investigate the question of the site of expression of LTP for the MPP synapses onto dentate granule cells.

Methods

Whole cell voltage clamp recordings were made from dentate granule cells as described in Chapter 2. To induce LTP, cells were voltage-clamped at -20mV while applying three 100Hz stimulus trains of 1s duration, and applied at 60s intervals. EPSC amplitudes were measured by averaging over a 5ms window around the peak after subtracting the average current over the 10ms interval immediately before the stimulus. Mean EPSC amplitude (μ) and variance (σ^2) were calculated from 60 to 150 events recorded during a stable epoch. The variance attributable to recording noise was estimated in the region prior to the test pulse; and was subtracted from the EPSC

variance. All variance-mean plots were fit with a theoretical equation (see below) by minimising χ^2 (see Chapter 3, Methods).

Variance-mean analysis

The variance-mean plot has the form,

$$\sigma^2 = \mu Q_{av} (1 + CV^2 - P_{av})$$

This expression has the same form as a classical equation developed for non-stationary noise analysis of voltage-gated currents (Sigworth, 1980), but is applied here to synaptic amplitude fluctuations. Q_{av} is the weighted average amplitude of the postsynaptic response to a vesicle of transmitter, CV is the coefficient of variation of the response to individual vesicles, and P_{av} is the weighted average vesicle release probability (mathematical derivation is described in Appendix).

$$Q_{av} = \sum Q_i (\mu_i / \mu)$$

$$P_{av} = \sum P_i (\mu_i / \mu) (Q_i / Q_{av})$$

where

P_i = transmitter release probability at the i th terminal

Q_i = average quantal amplitude (response to a single vesicle) at the i th terminal

μ_i = mean synaptic amplitude at the i th terminal

The main assumption needed to derive these equations is that the presynaptic modulation used to construct the variance-mean parabola changes release probability by the same factor at all terminals. This assumption is supported by experimental evidence for the case of modulation by Cd^{2+} . At autaptic hippocampal synapses, Cd^{2+} reduces P_r by the same factor at all terminals, regardless of their initial P_r (Chapter 3). The technique described is an extension of previously reported variance-mean analysis methods (Miyamoto, 1975; Clamann *et al.*, 1989; Frerking and Wilson, 1996). In contrast to these earlier methods, it does not make the unrealistic assumption that release probability or quantal amplitude are uniform at all synaptic terminals. A similar generalisation of the variance-mean approach was reported recently (Silver *et al.*, in press). The approach developed here predicts that the variance-mean plot traces

out a parabola as P_{av} is varied. When P_{av} is low (< 0.3) the plot is approximately linear, rising from the origin with slope, $S_{vm} = Q_{av} (1 + CV^2)$. As P_{av} increases to > 0.3 the parabola "rolls-off" reaching a maximum when $P_{av} = (1 + CV^2) / 2$. Thus, the variance-mean parabola can be analysed to extract Q_{av} and P_{av} .

Results

EPSCs were recorded from dentate granule cells following stimulation of the MPP in rat hippocampal slices. The stimulating electrode was positioned in the central third of the dentate gyrus molecular layer. This preferentially stimulated the MPP, as confirmed by the presence of paired-pulse depression at these synapses (inter stimulus interval 30-60ms, $n=4$, Fig. 5.1A). The EPSC amplitude fluctuated from stimulus-to-stimulus due to random variations in the number of transmitter vesicles that were released (Fig. 5.2A). In contrast, the response to a voltage pulse preceding the stimulus did not fluctuate, and was monitored to ensure stable recording conditions (Fig. 5.2A). Both the mean (μ) and the variance (σ^2) of the EPSC amplitude were reduced following the addition of $2\mu\text{M}$ or $6\mu\text{M}$ Cd^{2+} to the extracellular solution (Fig. 5.2B). The relationship between σ^2 and μ was approximately linear (Fig. 5.2C). The variance-mean plot contains information about pre- and postsynaptic function and was used to investigate the locus of LTP expression.

Computer simulation testing of the variance-mean technique

The variance-mean technique was tested by applying it to simulated data (completed by Dr J. Clements). A model of a compound synaptic input was used to generate fluctuating EPSC amplitudes. The model input consisted of 480 terminals with highly non-uniform properties. The terminals were divided into 8 groups as shown in Table 5.1. Each terminal had a CV of 0.4. Gaussian noise with a standard deviation of 3pA was added to the simulated amplitudes. A 50% synaptic potentiation was modelled via three different mechanisms, each acting in a non-uniform manner: a 100% presynaptic increase in P_f at half the terminals; a 100% postsynaptic increase in q at half the terminals; or a 100% increase in N for half the groups. Application of Cd^{2+}

Table 5.1 A simulation of a compound synaptic input was used to generate randomly fluctuating EPSCs. The model input consisted of 480 terminals with highly non-uniform properties. The terminals were divided into 8 groups.

	1	2	3	4	5	6	7	8
Terminals in Group (N)	80	40	80	40	80	40	80	40
Vesicle Release Probability (P)	0.04	0.2	0.04	0.2	0.04	0.2	0.04	0.2
Average Response to a Vesicle (Q)	3	3	6	6	3	3	6	6

Figure 5. 1

Figure 5. 1 Paired pulse depression confirms preferential stimulation of the medial perforant path (MPP).

A, A paired pulse, with an interstimulus interval of 30ms, results in a depression of the second evoked AMPA EPSC recorded from a dentate granule cell. The trace is the average of 5 EPSCs

A

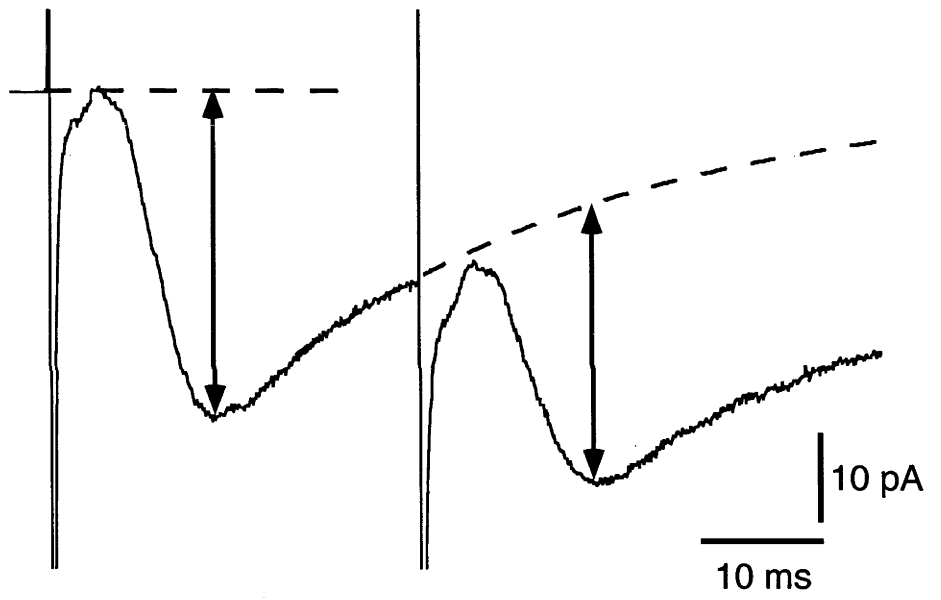


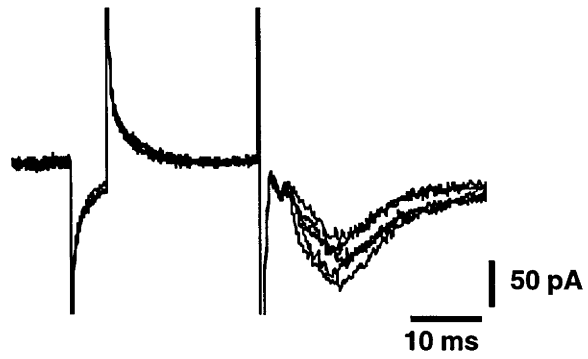
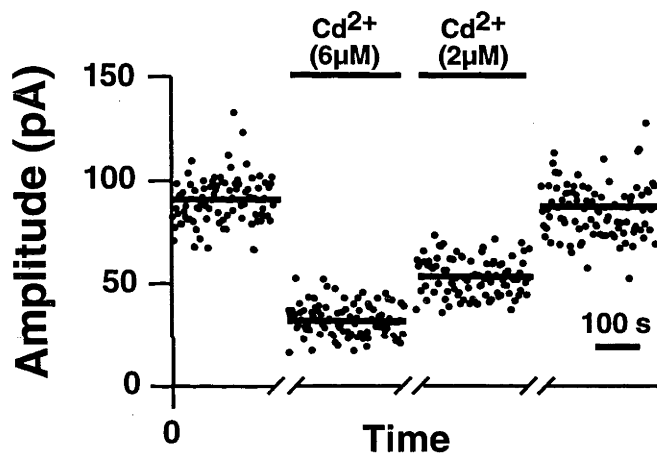
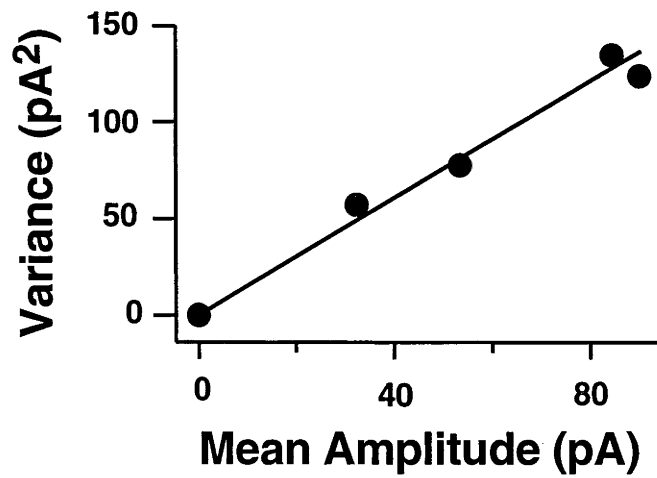
Figure 5. 2

Figure 5. 2 Construction and analysis of a variance-mean plot.

A, Five consecutive EPSCs recorded from a granule cell in the dentate gyrus, exhibits trial-to-trial amplitude fluctuations that contain information about synaptic function. Each EPSC was preceded by a small voltage step to measure R_S , and to ensure that recording conditions remained stable.

B, EPSC amplitude plotted against time. Epochs during which EPSC amplitude remained stable are shown for each Cd^{2+} concentration (0, 2 or $6\mu M$). A bar shows the mean amplitude during each epoch. Addition of Cd^{2+} reduced both the mean and the variance of the EPSC amplitude.

C, The variance of the EPSC amplitude is plotted against the mean for each stable epoch (variance-mean plot). The slope of this plot estimates the average amplitude of the response following the release of a single vesicle, Q_{av} .

A**B****C**

was modelled via a 60% reduction in P_r at all terminals. 50 EPSCs were simulated before and during Cd^{2+} "application" and a variance-mean plot was constructed. A typical data set is shown in Fig. 5.3A and the average variance-mean plots before and after modulation are shown in Fig. 5.3B. Because P_{av} was low in these simulations, the slope of a variance-mean plot (S_{vm}) was used to estimate $Q_{av} = S_v / (1 + CV^2)$.

The results for Q_{av} are summarised in Fig. 5.3C. There was a clear distinction between the postsynaptic modulation which altered Q_{av} , and the other modulations which did not. The results also revealed a small (< 10%) systematic underestimation of Q_{av} that is expected from the linear approximation used to calculate this parameter. Thus, the variance-mean technique provides a robust estimate of Q_{av} from as few as 100 EPSC amplitude measurements. The estimate is insensitive to recording noise, intrinsic variability of the response to a vesicle and non-uniformities in the properties of terminals, including their response to a modulation. Therefore, the technique can be applied confidently to multi-fibre (compound) synaptic inputs.

Variance-mean analysis measures mean quantal amplitude

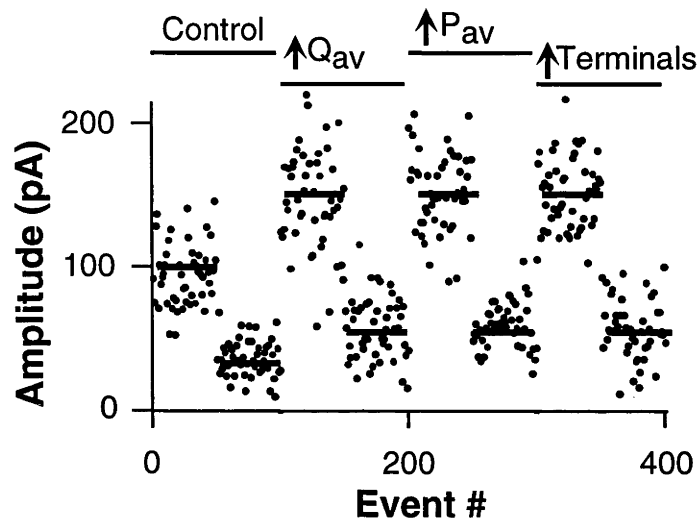
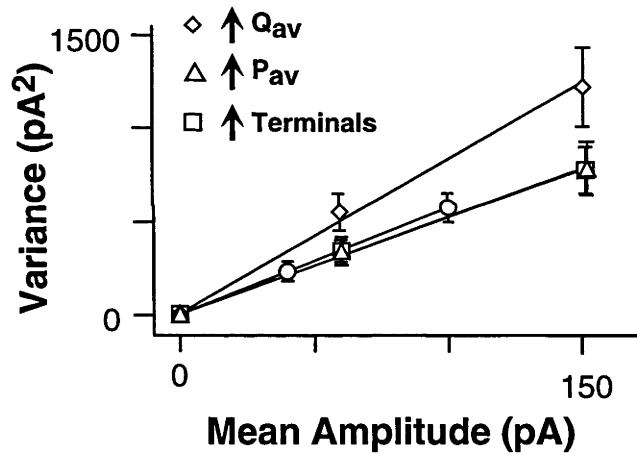
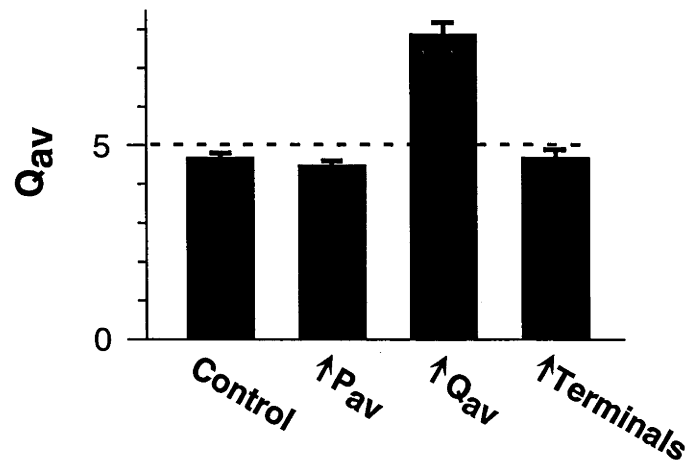
Variance-mean plots for compound EPSCs recorded in the dentate were all approximately linear and exhibited no detectable roll-off (Fig. 5.2C). This implies that average release probability is low (< 0.3) for MPP synapses onto granule cells at physiological Ca^{2+} concentrations, consistent with results at other hippocampal synapses (Hessler *et al.*, 1993; Rosenmund *et al.*, 1993; Dobrunz and Stevens, 1997; Murthy *et al.*, 1997). Therefore, the slope of the variance-mean plot can be used to estimate Q_{av} . The value of CV has been estimated at 0.46 for MPP synapses on dentate granule neurons by measuring asynchronous miniature EPSCs (Bekkers, 1995), therefore, $Q_{av} = S_{vm} / 1.2$ in this preparation. It was estimated that $Q_{av} = 2.3 \pm 0.3\text{pA}$ (n=10) at -70mV. Whole-cell recordings systematically underestimate EPSC peak amplitude and rise-time due to capacitive filtering of high frequencies by the cell membrane. The cut-off frequency decreases as the series resistance (R_s) increases (Stricker *et al.*, 1996a). Consistent with this, Q_{av} was negatively correlated with both

Figure 5.3

Figure 5. 3 The variance-mean plot can identify the locus of synaptic modulation when applied to simulated data.

A, Simulated EPSC amplitude plotted against event number. A model of a compound synaptic contact was used to simulate EPSC amplitudes under control conditions and following each of three types of modulation: postsynaptic modulation that increased Q_{av} ; presynaptic modulation that increased P_{av} and modulation that increased the number of active terminals. Under each condition, an epoch of 50 events was generated before and 50 events after the simulated application of Cd^{2+} .

B, The average variance-mean plot under control conditions (*circles*), and following each type of modulation: postsynaptic (*diamonds*); presynaptic (*squares*), and increased number of terminals (*triangles*). Error bars indicate SEM (n=20). Only postsynaptic modulation produced a detectible change in the slope of the variance-mean plot.

A**B****C**

R_s ($r = -0.55$, $n = 10$, Fig. 5.4A), and with EPSC rise-time ($r = -0.58$, $n = 10$, Fig. 5.4B), but not with EPSC amplitude ($r = 0.13$, $n = 10$, Fig. 5.4C). It should be noted that these correlations were only marginally significant. However, the general trend is in keeping with the expected effects of electrode resistance on measured currents. Filtering of the synaptic signal by the membrane capacitance and series resistance does not invalidate the variance-mean plot as a tool for investigating synaptic plasticity, because EPSC amplitudes will be underestimated by the same factor before and after modulation.

Variance-mean technique reliably identifies site of synaptic modulation

The simulations presented above, show that the variance-mean technique can be used to investigate the locus of a synaptic modulation. The reliability of the technique was tested by applying it to synaptic responses recorded in dentate granule neurons before and after applying each of three different synaptic modulators: (i) CNQX ($0.4\mu\text{M}$), a competitive antagonist at postsynaptic AMPA receptors; (ii) baclofen ($4\mu\text{M}$), a presynaptic modulator acting via GABA_B receptors; and (iii) an increase in the stimulus intensity to activate additional presynaptic terminals. At non-saturating concentrations of CNQX a fraction of postsynaptic AMPA receptors will be blocked reducing the inward current generated in response to one vesicle of transmitter. As expected, CNQX reduced the slope of the variance-mean plot (and hence the estimated Q_{av}) to the same extent that it reduced EPSC amplitude ($37 \pm 2\%$ vs $33 \pm 2\%$, $n = 5$, Fig. 5.5A, D). In contrast, presynaptic manipulations that change P_r or the number of active synapses (N) should not alter Q_{av} . Baclofen acts as a GABA_B agonist initiating a G-protein cascade. Activated G-protein subunits are thought to inhibit Ca^{2+} influx through Ca^{2+} channels thereby reducing P_r (Mintz and Bean, 1993; Hille, 1994) (see Chapter 3, Discussion). There was no significant change in the slope of the variance-mean plot (Q_{av}) after the addition of baclofen despite a reduction in EPSC amplitude ($106 \pm 8\%$ vs $41 \pm 6\%$, $n = 5$, Fig. 5.5B, D). An increase in stimulus strength results in the recruitment of additional axons increasing the number of active terminals contributing to release. There was no significant change in Q_{av} despite an increase in

Figure 5. 4

Figure 5. 4 Whole-cell recordings systematically underestimate EPSC peak amplitude and rise-time.

A, The R_s of the control EPSC is plotted against Q_{av} (n=10).

B, The 20-80% rise-time of the control EPSC is plotted against Q_{av} (n=10). These parameters were negatively correlated due to capacitative filtering by the dendritic and somatic membrane, and the uncompensated series resistance.

C, The Q_{av} of the control EPSC is plotted against AMPA EPSC amplitude (n=10). No correlation is observed.

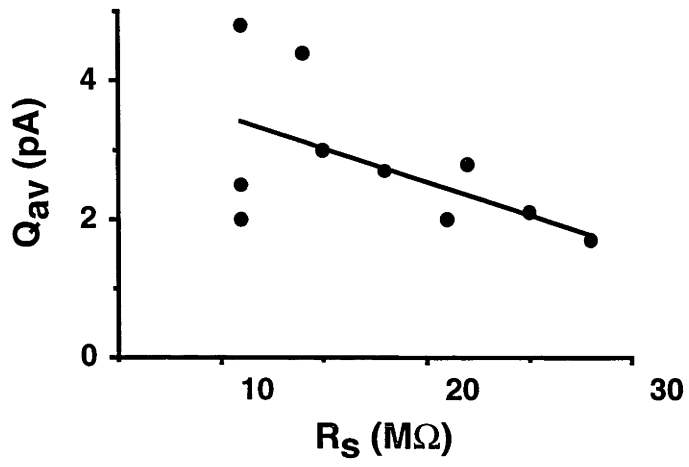
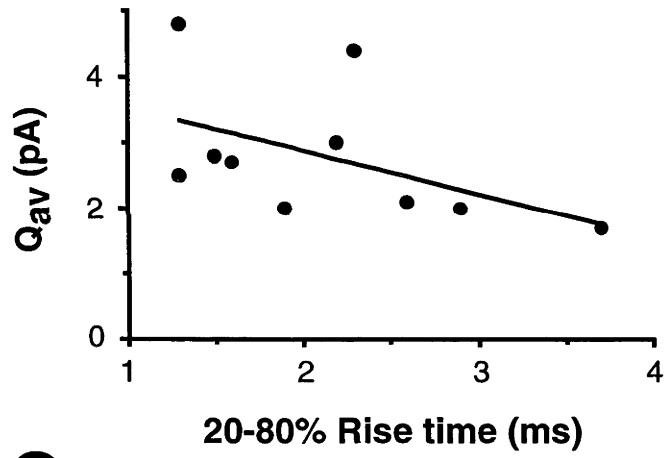
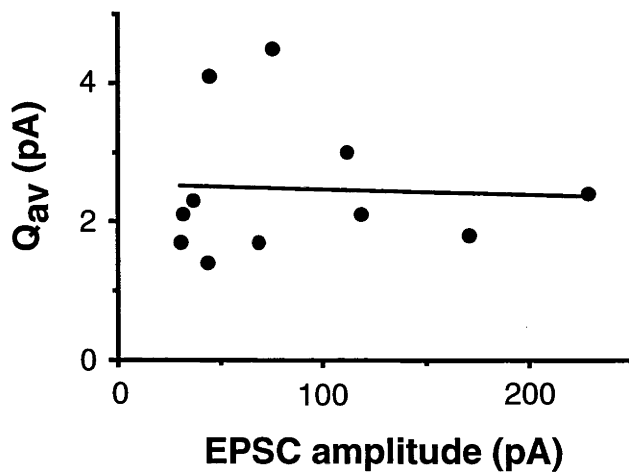
A**B****C**

Figure 5. 5

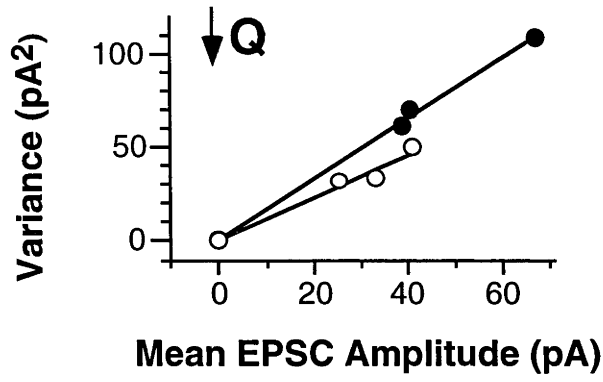
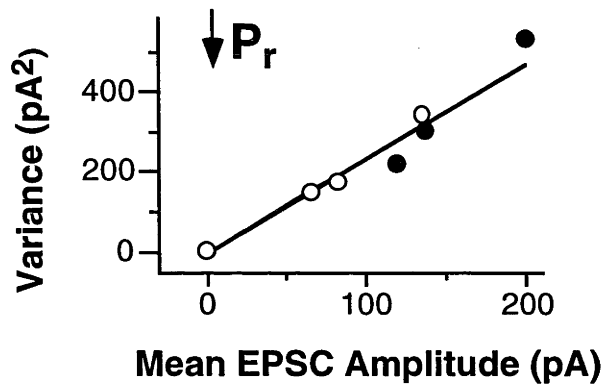
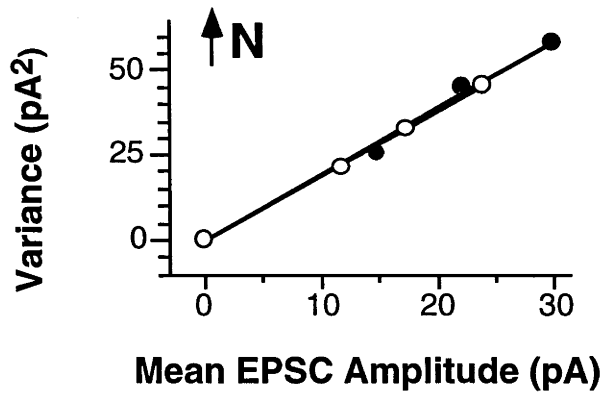
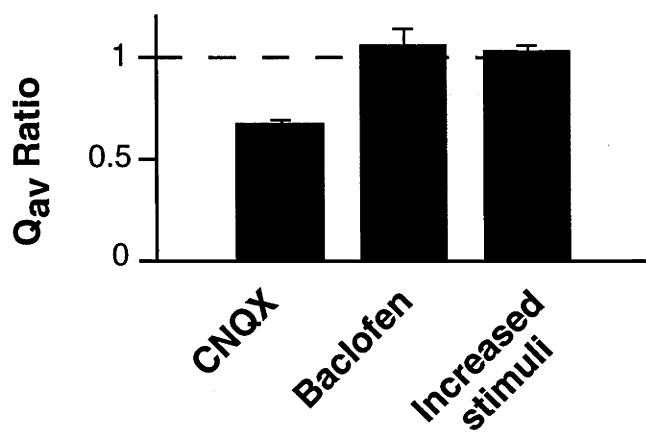
Figure 5. 5 The variance-mean plot can identify the locus of synaptic modulation when applied to EPSCs recorded from dentate granule cells. The variance of the EPSC amplitude is plotted against the mean for each stable epoch at three different Cd^{2+} concentrations, before (*closed circles*) and after (*open circles*) synaptic modulations.

A, Variance-mean plot before (*closed circles*) and after (*open circles*) the application of CNQX ($0.4\mu\text{M}$), a competitive antagonist at postsynaptic AMPA receptors. CNQX reduced the slope of the plot and hence Q_{av} , consistent with a postsynaptic modulation.

B, Variance-mean plot before (*closed circles*) and after (*open circles*) the application of baclofen ($4\mu\text{M}$) which reduces the probability of vesicle release from the presynaptic terminal. There was no change in Q_{av} , consistent with a presynaptic modulation.

C, Variance-mean plot before (*closed circles*) and after (*open circles*) an increase in the strength of the stimulus to the presynaptic axons. There was no change in Q_{av} , consistent with a presynaptic modulation.

D, Average change in Q_{av} after the application of CNQX ($n=5$), baclofen ($n=5$) and an increase in stimulus strength ($n=5$). Error bars indicate SEM. Only CNQX produced a significant change in Q_{av} .

A**B****C****D**

EPSC amplitude after increasing the stimulus strength ($101 \pm 4\%$ vs $160 \pm 12\%$, $n = 5$, Fig. 5.5 C, D). Thus, the technique can distinguish between a postsynaptic modulation which alters Q_{av} , and presynaptic modulations which do not.

A postsynaptic mechanism for LTP

Variance-mean plots were constructed and Q_{av} was measured before and after the induction of LTP. If LTP results from a presynaptic increase in vesicle release probability, or from the unmasking of silent synaptic terminals (ie increase in N), then little or no change in Q_{av} is expected. In contrast, if LTP results from an enhancement of the postsynaptic response, then Q_{av} will increase in parallel with the evoked synaptic amplitude. The induction protocol produced potentiation lasting > 20 minutes in 5/12 cells. LTP increased EPSC amplitude by $50 \pm 0.4\%$ ($n=5$, Fig. 5.6), and in the same cells increased Q_{av} by $47 \pm 0.6\%$ (Fig. 5.6). There was no significant difference between the increase in EPSC amplitude and the increase in Q_{av} ($p=0.6$, paired t-test, $n=5$). Thus, in every cell, LTP of the MPP input to dentate granule cells can be explained by an increase in the postsynaptic response to a vesicle of transmitter. All experimental results are summarised in Fig. 5.7 which plots the change in Q_{av} , against the change in μ following various synaptic modulations. In theory a presynaptic modulation should fall on the horizontal dashed line, and a postsynaptic modulation on the diagonal line. When the variance-mean analysis is restricted to the low P_{av} range, it is a mathematical generalisation of the $1/CV^2$ technique (see discussion). When $1/CV^2$ was calculated from a subset of data recorded in the absence of Cd^{2+} , it did not change following LTP ($p=0.5$, paired t-test, $n=5$). Taken together, these results demonstrate the reliability with which the variance-mean technique can identify the site of synaptic modulation, and strongly supports a postsynaptic site for LTP expression at MPP synapses onto dentate granule cells.

Figure 5. 6

Figure 5. 6 The variance-mean plot identifies a postsynaptic locus for expression of LTP.

A, EPSC amplitude plotted against time. Epochs during which EPSC amplitude remained stable are shown for each Cd^{2+} concentration before and after the induction of LTP. A bar shows the mean amplitude during each epoch.

B, Five consecutive EPSCs measured in 2mM Ca^{2+} before and after the induction of LTP.

C, Variance-mean plot before (*closed circles*) and after (*open circles*) the induction of LTP. The slope of the plot and hence Q_{av} increased following LTP. This increase was very similar to the increase in mean EPSC amplitude following LTP.

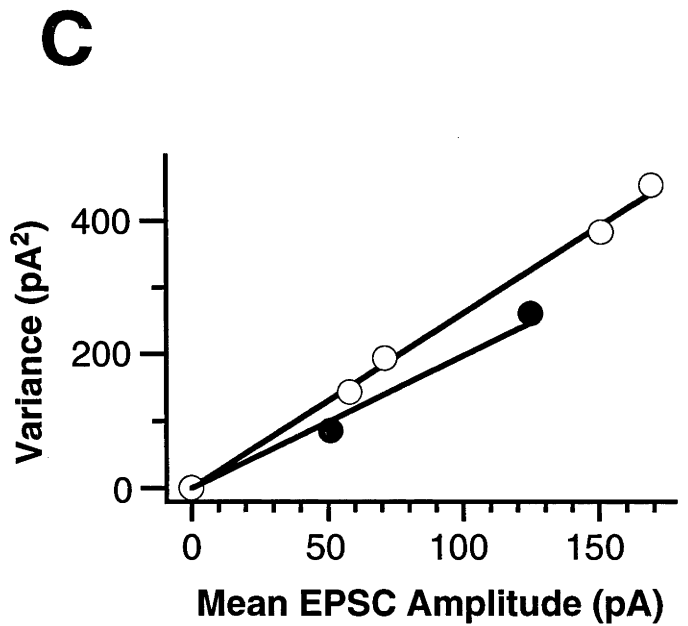
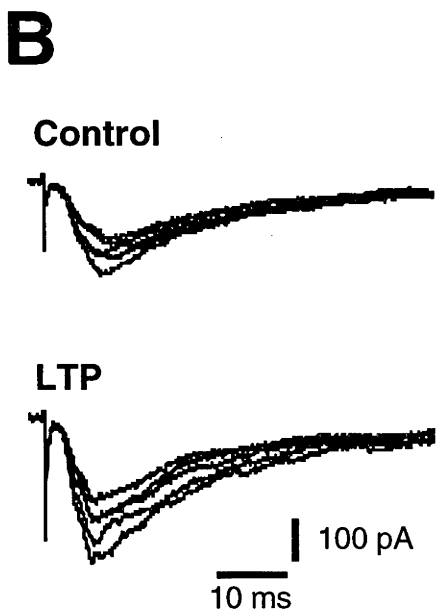
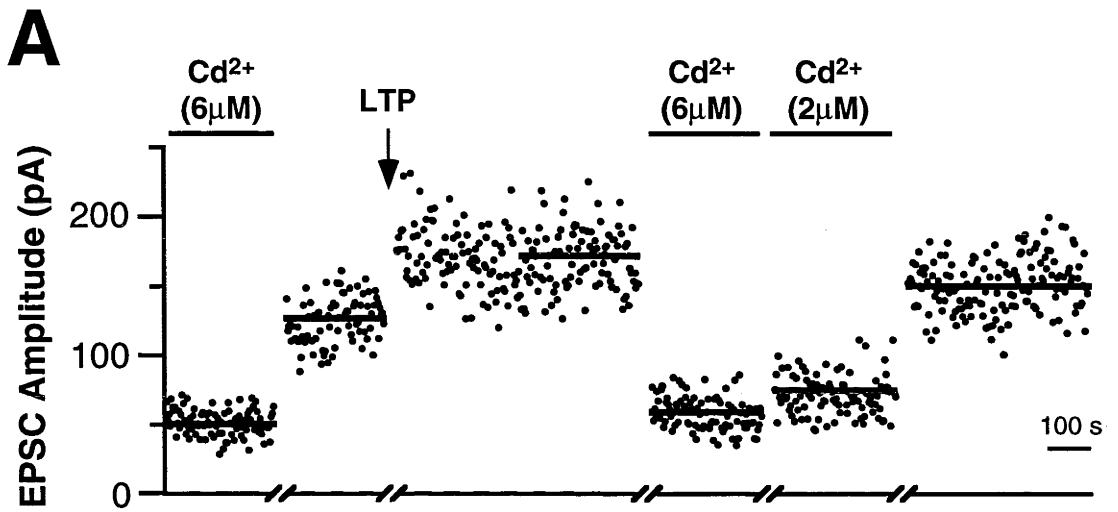
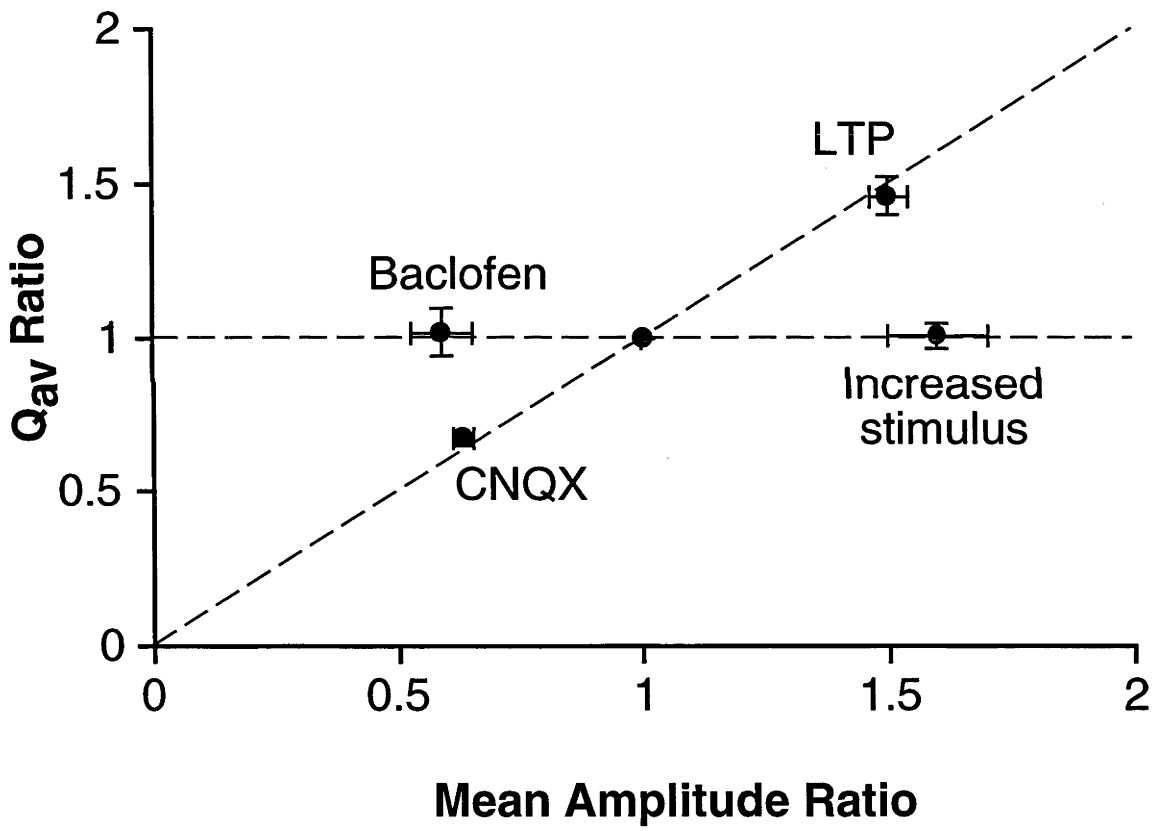


Figure 5.7

Figure 5. 7 Summary of the changes in Q_{av} vs changes in EPSC amplitude after various synaptic modulations.

A, The ratio of Q_{av} after to Q_{av} before modulation is plotted against the ratio of EPSC amplitude after to EPSC amplitude before modulation. The amplitude ratio was measured with no added Cd^{2+} . Baclofen and increased stimulus (two different presynaptic modulations) did not alter Q_{av} (horizontal dashed line). CNQX (a postsynaptic modulation) and LTP altered Q_{av} to the same extent that they altered the EPSC amplitude (diagonal dashed line).

A



Discussion

Other evidence concerning the site of LTP expression in the dentate

LTP induction in the dentate increases AMPA binding measured using quantitative autoradiography. This may reflect an increase in average receptor affinity or an increase in receptor number. The increased binding is highly correlated with the potentiation of the extracellular field EPSP supporting a postsynaptic mechanism for LTP (Maren *et al.*, 1993). No change in paired pulse depression is seen following LTP induction at MPP synapses onto dentate granule cells, implying no change in P_r (Christie and Abraham, 1994). In contrast, an increase in glutamate release from the dentate gyrus following LTP induction suggests a presynaptic mechanism (Bliss *et al.*, 1987; Errington *et al.*, 1987). LTP in the dentate is also associated with an enhancement of synaptosomal glutamate release (Canevari *et al.*, 1994). A weakness of glutamate release studies is that they are not pathway specific. An increase in glutamate release may be accounted for by an increase in P_r at LPP synapses. Consistent with this, a reduction in PPF after LTP induction has been noted for the LPP, suggesting an increase in P_r (Christie and Abraham, 1994).

A presynaptic mechanism was suggested by a recent study that used MK-801 (Min *et al.*, 1998). The rate of progressive block of the NMDA receptor component of the EPSC in the presence of MK-801 was faster following LTP induction, implying an increase in P_r . In contrast, no increase in the rate of the progressive block was noted for the LPP. This is not consistent with the presynaptic locus of LTP expression suggested for LPP LTP based on PPF experiments (Christie and Abraham, 1994). The irreversible nature of the MK-801 block means that it is necessary to compare control progressive block rate with post LTP progressive block rate from different cells. There is a large variation in the rate of progressive block in slice experiments making subtle changes following LTP induction difficult to interpret. Also, if LTP induction alters the open probability, or kinetic parameters of the NMDA receptor (Lu *et al.*, 1998), then the comparison of the rate of progressive block would no longer be valid. For example, the increased rate of progressive block may simply be due to an increase

in NMDA receptor open probability. Also, the enhancement of the AMPA receptor component of the EPSC was observed to be much greater than that of the NMDA component. Traditionally, this has been considered as evidence for a postsynaptic locus of LTP expression (Kauer *et al.*, 1988; Perkel and Nicoll, 1993). Min *et al.* (1998) reconcile the apparent contradiction of their results by postulating that extrasynaptic glutamate spill-over occurs at these synapses (see Chapter 1, Part II). A smaller increase in the NMDA receptor mediated compared with AMPA mediated component of the EPSC can be explained if the majority of the NMDA receptor mediated signal is generated by spill-over of glutamate from synapses which do not undergo LTP.

An increase in $1/CV^2$ has been reported following LTP induction of MPP synapses onto dentate granule cells, implying an increase in quantal content (Wang *et al.*, 1996). In contrast, results presented in this chapter showed no change in $1/CV^2$. This difference is difficult to reconcile. The validity of the $1/CV^2$ method is dependent on low P_r but both experiments were done at similar $[Ca^{2+}]_o$. Methodological differences may partially account for the discrepancy. For example, a minimal stimulation protocol was used by Wang *et al.* (1996), whereas large multifibre EPSCs were analysed in experiments presented here. Alternatively, it is possible that the differences in the LTP induction protocols used may generate different forms of LTP. Methodological considerations may also account for the differences in the average amplitude increase following LTP induction which was 50% in the present study vs 240% reported by Wang *et al.* (1996). In summary, a postsynaptic locus of LTP expression is consistent with finding from many studies on LTP in the dentate region, but is difficult to reconcile with others.

Variance-mean technique vs $1/CV^2$ technique

In the present study, variance-mean analysis was restricted to the linear, low P_{av} range. This meant that only an upper limit could be placed on P_{av} (< 0.3). Additional information could have been extracted by increasing release probability (for example

by increasing extracellular Ca^{2+}) and analysing the parabolic roll-off of the variance-mean plot. Preliminary experiments revealed that the MPP synaptic response ran down during a period of elevated Ca^{2+} , invalidating the analysis.

When variance-mean analysis is restricted to the low P_{av} range, it reduces to the $1/\text{CV}^2$ technique used in some previous LTP studies, (Bekkers and Stevens, 1990; Malinow and Tsien, 1990; Manabe *et al.*, 1993; Wang *et al.*, 1996) but it has several advantages. The graphical demonstration that σ^2 varies linearly with μ directly confirms that P_{av} is low, which is simply assumed in most $1/\text{CV}^2$ studies. Thus, the approach avoids many of the technical difficulties associated with the traditional technique (Faber and Korn, 1991). The variance-mean technique also provides built-in protection against extraneous sources of excess variability such as run-down of the response or active dendritic properties. For example, active dendritic conductances should become more apparent as P_r is increased. If they were to contribute excess variability, then the variance-mean plot would deviate upwards from the straight line. A similar argument holds for synaptic run-down. No systematic upward deviation of the variance-mean relationship was observed in the present study.

Variance-mean technique vs other methods

Previous investigations of the locus of LTP expression have used a change in the amplitude distribution of mEPSCs to indicate a postsynaptic site (Manabe *et al.*, 1992), or a change in their frequency of occurrence to indicate a presynaptic site (Malgaroli and Tsien, 1992). The average amplitude of spontaneous miniature EPSCs (mEPSCs) can, in principle, provide an independent estimate of q across all terminals on a cell, but only if all mEPSCs have amplitudes greater than twice the standard deviation of the recording noise (σ_n) so that they can be reliably detected (Clements and Bekkers, 1997). In the recordings presented, average σ_n was 1.7pA and Q_{av} was 2.3pA, so it is expected that some mEPSCs will go undetected. A direct measure of q has been made in the dentate preparation measuring asynchronous EPSCs (aEPSCs) following proximal stimulation in the presence of extracellular strontium (Bekkers,

1995). A mean amplitude of 3 - 6 pA (at -70mV) was observed, which is greater than that measured here using the variance-mean technique (2.3pA). The discrepancy in the results could be explained if a proportion of smaller aEPSCs were missed. The variance-mean method, which does not depend upon the direct resolution of individual "quantal" events, measures the mean amplitude of all events, both large and small. A further explanation may be related to the fact that the aEPSCs in Bekkers (1995) originated from a more proximal site on the dendritic tree than the MPP axons stimulated in these experiments, and may be less attenuated on average by dendritic filtering.

Another common approach uses a change in the percentage of stimuli that do not evoke a postsynaptic response (failure rate) to indicate a presynaptic site of expression (Malinow and Tsien, 1990; Kullmann and Nicoll, 1992; Stevens and Wang, 1994). An increase in Q_{av} would also make single vesicle evoked events easier to detect, decrease the apparent failure rate and incorrectly assign a presynaptic locus. Quantal analysis based on the detection of peaks in evoked amplitude histograms can also provide an estimate of Q_{av} , but it requires that $Q_{av} \geq 2 \sigma_n$ (Redman, 1990), a condition that is not met in our preparation. Mini detection, peak detection and failure detection all assume that the postsynaptic response to a single vesicle can be detected reliably. The variance-mean technique is free of this constraint. It can identify a postsynaptic site of synaptic modulation under conditions where most traditional techniques may fail.

Presynaptic mechanisms which could increase Q_{av}

The variance-mean technique predicts that for a purely presynaptic modulation, the Q_{av} ratio before and following the modulation will not alter. If both pre- and postsynaptic changes are involved in potentiation, the Q_{av} ratio vs EPSC amplitude ratio would expect to fall between the horizontal (presynaptic) and diagonal (postsynaptic) line (Fig. 5.7). A parallel increase in Q_{av} and average synaptic amplitude precludes this for our data. Simulation data suggests that all conceivable

presynaptic modulations will produce an increase in Q_{av} which is less than the increase in the average synaptic amplitude (J. D. Clements, personal communication). However, if synaptic strength increased via both pre- and postsynaptic mechanisms in other systems then the variance-mean technique may not be able to predict the relative contribution of each to the potentiation. This is especially true if the modulations are nonuniform across different terminals.

There are at least two presynaptic mechanisms that could increase both EPSC amplitude and Q_{av} . One possibility is an increase in the frequency with which multiple vesicles are released simultaneously at an individual terminal (Tong and Jahr, 1994; Silver *et al.*, 1996). If postsynaptic AMPA receptors are not saturated by the release of one vesicle then simultaneous release of two vesicles would be expected to increase the postsynaptic response (Silver *et al.*, 1996). An increase in P_r has been shown to increase the likelihood of multiple vesicular release at central synapses (Tong and Jahr, 1994; Silver *et al.*, 1996). However, it has been shown that the NMDA receptor and AMPA receptor components of the EPSC increase linearly with increasing P_r (Perkel and Nicoll, 1993; Tong and Jahr, 1994). This argues for the saturation of both NMDA and AMPA receptors at hippocampal synapses. An alternative interpretation is that both AMPA receptors and NMDA receptors are far from saturated. Multi-vesicular release would then result in the linear addition of the postsynaptic response, essentially increasing N .

A second possibility is that presynaptic modulation acts selectively at a sub-population of terminals with below average release probability, but with above average postsynaptic amplitude. This is inconsistent with recent findings suggesting that large presynaptic terminals have above average release probability (Murthy *et al.*, 1997), more docked vesicles and larger postsynaptic size (Harris and Sultan, 1995). To obtain a parallel increase in Q_{av} and EPSC amplitude, just the right amount of selective modulation would be required at the large amplitude terminals, and this amount would be different at different synapses. A uniform or non-selective

postsynaptic modulation offers the simplest, most plausible explanation of our LTP results.

Signal transduction mechanisms

A postsynaptic locus of expression at MPP synapses onto dentate granule cells is likely to involve alterations in the number and/or properties of ion channels that mediate synaptic transmission. Either an increase in the number of AMPA receptors per synaptic terminal, or a change in their kinetics could account for an increase in synaptic efficacy. Many studies have suggested a change in AMPA receptor mediated currents following LTP. The induction of LTP has been shown to increase the AMPA component of the synaptic response (Kauer *et al.*, 1988; Muller *et al.*, 1988; Perkel and Nicoll, 1993; Wang *et al.*, 1996; Min *et al.*, 1998). Also, an increase in sensitivity of AMPA receptors was noted after LTP (Davies *et al.*, 1989) and an increase in AMPA receptor binding was illustrated using quantitative autoradiography (Maren *et al.*, 1993). NMDA-dependent LTP relies on the postsynaptic influx of Ca^{2+} and several different Ca^{2+} sensitive enzymes have been proposed to play a role in LTP. Ca^{2+} /calmodulin-dependent protein kinase II (CaM kinase II), protein kinase C, tyrosine kinases, phospholipase A_2 , Ca^{2+} dependent proteases, guanylyl cyclase and cyclic GMP-dependent protein kinases have all been implicated in the induction of LTP (Fukunaga *et al.*, 1996). Among these enzymes, CaM kinase II is of particular interest.

CaM Kinase II and LTP

Many studies have implicated an essential role of CaM kinase II in the induction of LTP. The autophosphorylation of CaM kinase II, triggered by Ca^{2+} , converts the enzyme from the Ca^{2+} -dependent to the Ca^{2+} -independent form which is constitutively active (Miller *et al.*, 1988). LTP induction triggers a long-lasting increase in the autophosphorylated form of CaM kinase II (Barria *et al.*, 1997). Barria *et al.* (1997) also illustrated a long lasting phosphorylation of AMPA receptors after

LTP induction. Synthetic peptides designed to block the action of CaM kinase II injected into the postsynaptic cell, or bath applied KN-62, a blocker of CaM kinase II, were shown to inhibit LTP (Malenka *et al.*, 1989; Malinow *et al.*, 1989; Ito *et al.*, 1991; Otmakhov *et al.*, 1997). Knockout of the gene encoding the α subunit of CaM kinase II resulted in a decreased expression of LTP in hippocampal slices and a reduction in spatial learning ability of the mice (Silva *et al.*, 1992a; Silva *et al.*, 1992b).

The introduction of autothiophosphorylated CaM kinase II (constitutively active form) into cultured hippocampal cells resulted in a three fold increase in whole cell AMPA receptor mediated current (McGlade McCulloh *et al.*, 1993). Similarly, when a constitutively active form of CaM kinase II was transfected into the CA1 hippocampal region, slice experiments showed a four fold increase in AMPA EPSC size compared with control slices (Pettit *et al.*, 1994). Slices which expressed the constitutively active form of CaM kinase II were unable to express LTP suggesting a saturation of the enhancement mechanism. The phosphorylation of AMPA receptors expressed in HEK cells resulted in an increase in whole cell current generated by exogenously applied glutamate (Barria *et al.*, 1997). In summary, these studies suggest that the phosphorylation of AMPA receptors by the constitutively active form of CaM Kinase II underlies a postsynaptic mechanism for LTP. Whether the phosphorylation increases the probability of opening or increases the single channel conductance of the AMPA receptors remains unknown. A recent study suggests that an increase in the single channel conductance of AMPA receptors occurs following LTP induction at the CA3-CA1 synapse (Benke *et al.*, 1998). The involvement of other kinases in the mechanisms of LTP cannot be ruled out. For example, protein kinase A (PKA) has been shown to alter the kinetic properties of the AMPA receptor (Greengard *et al.*, 1991).

Conclusion

The variance-mean technique was shown to be a reliable and robust tool for identifying the site of synaptic modulation. It has practical advantages over traditional quantal analysis methods such as the $1/CV^2$ and peak detection. This new approach strongly supports a postsynaptic site for LTP expression at MPP synapses onto dentate granule cells. Based on current literature and the finding presented in this chapter the following model of early phase LTP at MPP synapses is proposed: (i) the LTP induction stimulus opens NMDA receptors allowing the influx of postsynaptic Ca^{2+} ; (ii) a local Ca^{2+} transient interacts with CaM kinase II converting the enzyme into its constitutively active form; (iii) CaM kinase II phosphorylates AMPA receptors resulting in an unmasking of latent receptors or an increase in current passing through individual AMPA channels.

Appendix

The mathematical derivation of the variance mean equation used in this chapter was done by Dr John D. Clements.

Derivation

Consider a synaptic input consisting of a single terminal.

Let,

P = transmitter release probability

Q = average amplitude of the synaptic response following release

CV = coefficient of variation of the synaptic response

Now,

μ = average synaptic amplitude

$$= P Q$$

σ^2 = synaptic variance

$$= P (Q - \mu)^2 + (1 - P) (0 - \mu)^2 + P Q^2 CV^2$$

$$= \mu Q (1 + CV^2 - P)$$

$$= \mu Q (1 + CV^2) - \mu^2$$

This equation describes a parabola with initial slope $Q (1 + CV^2)$, and a maximum when

$$P = (1 + CV^2) / 2.$$

Consider a synaptic input consisting of many terminals, each with different properties. Both mean and variance add linearly, so the ensemble variance-mean plot will again be a parabola.

Let,

P_i = transmitter release probability at the i th terminal

Q_i = average amplitude of the synaptic response at the i th terminal

CV_i = coefficient of variation at the i th terminal

μ_i = mean synaptic amplitude at the i th terminal

$$= P_i Q_i$$

Now,

$$\mu = \sum \mu_i$$

$$\sigma^2 = \sum \mu_i Q_i (1 + CV_i^2 - P_i)$$

Define,

Q_{av} = weighted average amplitude of the synaptic response at a terminal

$$= \sum Q_i (\mu_i / \mu)$$

P_{av} = weighted average transmitter release probability at a terminal

$$= \sum P_i (\mu_i / \mu) (Q_i / Q_{av})$$

CV_{av}^2 = weighted average coefficient of variation of the synaptic response at a terminal

$$= \sum CV_i^2 (\mu_i / \mu) (Q_i / Q_{av})$$

For Q_{av} , the weighting factor for a given terminal is the relative contribution of that terminal to the total postsynaptic current amplitude. For CV_{av}^2 and P_{av} , the weighting factor for a given terminal is the relative contribution of that terminal to the postsynaptic current amplitude multiplied by the amplitude of the synaptic response at that terminal relative to the weighted mean amplitude of the response.

Now, substitute P_{av} , CV_{av}^2 and Q_{av} into the equation for σ^2 ,

$$\sigma^2 = \mu Q_{av} (1 + CV_{av}^2 - P_{av})$$

So, under low release conditions ($P_{av} \rightarrow 0$), the σ^2 vs μ plot will be approximately linear with slope $Q_{av} (1 + CV_{av}^2)$.

Consider a presynaptic modulation where the values of P_i are all scaled by the same fraction, M , and the values of Q_i and CV_i remain constant. Let,

P_i' = release probability at the i th terminal after modulation

$$= M P_i$$

So,

$$P_{av}' = M P_{av}$$

$$\mu' = M \mu$$

and,

$$\sigma^{2'} = \mu' Q_{av} (1 + CV_{av}^2 - P_{av}')$$

$$= \mu' Q_{av} (1 + CV_{av}^2) - \mu'^2 Q_{av} P_{av} / \mu$$

If M is adjusted to several different values and $\sigma^{2'}$ is plotted against μ' , the graph will have the form of a parabola ($A \mu'^2 + B \mu'$), where

$$B = Q_{av} (1 + CV_{av}^2)$$

$$A = - Q_{av} P_{av} / \mu$$

Define,

$$C = (1 + CV_{av}^2)$$

So,

$$Q_{av} = B / C$$

$$P_{av} = -\mu C (A / B)$$

These estimates of average quantal amplitude and release probability require very few assumptions about the release process. The main assumption is that the presynaptic modulation used to construct the variance-mean parabola acts to change release probability by the same factor at all terminals. This assumption is supported by experimental evidence for the case of modulation by Cd^{2+} (see Chapter 3, Fig. 3.2A). Cd^{2+} reduced the P_r equally at both the high P_r and low P_r class. Another implicit assumption is that release of a vesicle at one synaptic terminal does not influence the release probability or the amplitude of the postsynaptic response at any other terminal participating in the synaptic input.

Chapter 6

General Discussion:

This thesis addresses three questions relating to synaptic function at excitatory hippocampal neurons: (i) How are Ca²⁺ channel subtypes distributed across different presynaptic terminals? (ii) Is there a difference in the Ca²⁺ sensitivity of the release mechanism associated with different Ca²⁺ channel subtypes? (iii) What is the site of LTP expression at synapses of the medial perforant pathway onto dentate granule cells? Conclusions drawn from the findings presented here have important ramifications for both short- and long-term synaptic plasticity.

In the study described in Chapter 3, the pattern of co-localisation of Ca²⁺ channel subtypes on presynaptic terminals was investigated at excitatory hippocampal synapses. N-type or P/Q-type Ca²⁺ channels were selectively blocked by ω -CTx or ω -Aga respectively, and the changes in P_r were measured using a technique based on the drug MK-801. The toxins completely blocked release at some terminals, reduced P_r at others, and failed to affect the remainder. It was concluded from these results that the mixture of N-type and P/Q-type channels must vary markedly between terminals on the same afferent. A simple model was developed which described all the data and allowed quantitative limits to be placed on the relative distributions of N- and P/Q-type Ca²⁺ channels. The model predicts that on average, about 10% of terminals have only N-type channels, about 45% of terminals have only P/Q-type channels and the remaining 45% have a mixture of subtypes.

The concept of a non-uniform distribution of Ca²⁺ channel subtypes across different presynaptic terminals is new to the scientific literature. The functional implication of this finding remains unknown. It is well established that different Ca²⁺ channel subtypes are differentially modulated by G-protein linked neuromodulators. A non-uniform distribution of Ca²⁺ channel subtypes could therefore permit selective

alteration of transmitter release at groups of terminals on a single afferent. A protective role may also be postulated. In the presence of toxins or other insults, a subset of terminals with a fortuitous combination of channels may continue to function normally. Thus, a non-uniform distribution of Ca^{2+} channel subtypes across different presynaptic terminals may make synaptic transmission more robust while creating rich possibilities for neuromodulation.

A further issue raised by this finding is the mechanism by which presynaptic terminals determine what mix of Ca^{2+} channel subtypes will support release. One possibility is that all terminals are non-selective and Ca^{2+} channel subtypes are inserted randomly. If only a few Ca^{2+} channels are functional at a given terminal then a simple binomial distribution of channels would automatically produce the non-uniform distribution. Alternatively, Ca^{2+} channel subtypes could be targeted to specific terminals, either by directed transport along the axon or by selective insertion at the terminal. If Ca^{2+} channels are targeted, what cues determine which Ca^{2+} channel subtype is to be used at a given terminal? The developmental change in Ca^{2+} channel subtype composition supporting transmitter release may provide a clue (Scholz and Miller, 1995). Early in development the N-type channel predominates while later in development the P/Q-type Ca^{2+} channel becomes more dominant in supporting release at excitatory hippocampal neurons. The non-uniform distribution of subtypes may therefore simply be a function of synaptic maturity, with N-type channels predominant at immature synapses and the P/Q-type channels dominating at mature synapses. If this was so, immature synapses would be affected to a greater extent by neuromodulators. This is because N-type channels tend to be more heavily modulated than the P/Q-types (see Chapter 3, Discussion). The non-uniform distribution may also have a structural basis, with the Ca^{2+} channel subtype expression dependent on where synapses form on the dendritic tree.

The study presented in Chapter 4 examines the Ca^{2+} sensitivity of the transmitter release mechanism. A steeply non-linear relationship between $[\text{Ca}^{2+}]_o$ and the EPSC

amplitude was observed at excitatory hippocampal neurons implicating the cooperative involvement of multiple Ca^{2+} ions in triggering release. The Dodge-Rahamimoff equation was unable to describe the dose-response relationship between $[\text{Ca}^{2+}]_o$ and transmitter release. However, the Ca^{2+} dose-response curve was described by a modified Dodge-Rahamimoff equation that incorporated a sublinear relationship between $[\text{Ca}^{2+}]_o$ and $[\text{Ca}^{2+}]_{it}$. The selective Ca^{2+} channel blockers, ω -CTx and ω -Aga, and traditional dose-response analysis were used to investigate the cooperativity associated with N- and P/Q-type Ca^{2+} channel subtypes. No difference was found between the degree of cooperativity for transmitter release mediated via N-type or P/Q-type Ca^{2+} channels. The selective Ca^{2+} channel blockers broadened the dose-response relationship, consistent with a non-uniform distribution of Ca^{2+} channel subtypes across synaptic terminals. A model of calcium's role in synaptic transmission was developed. The model was based on the modified Dodge-Rahamimoff equation, included a Ca^{2+} cooperativity of 4, and a non-uniform distribution of Ca^{2+} channel subtypes. These experiments were compatible with the results described in Chapter 3.

The model developed in Chapter 4 predicts that there is only one type of release machine, incorporating a Ca^{2+} sensor that exhibits a cooperativity of 4. The model suggests that in this study, the measured cooperativity underestimated the true cooperativity. Numerous other studies have estimated the degree of Ca^{2+} cooperativity to be between 2 and 4 at different central synapses. Signal-to-noise limitations may explain why some studies measure the degree of cooperativity at less than 4. If the true cooperativity can be established at 4, this criterion could be used for identifying the Ca^{2+} sensor(s) of the release machine.

Experiments in Chapter 5 test the utility of the variance-mean technique, a novel approach for investigating the site of synaptic modulation. The technique was shown to be a reliable and robust tool for identifying the site of synaptic modulation. It has advantages over traditional quantal analysis methods such as the $1/\text{CV}^2$ and peak detection methods. First, it confirms the assumption, usually made implicitly in $1/\text{CV}^2$

analysis, that P_r is low. Second, it does not require that the postsynaptic response to a single vesicle can be detected reliably. The locus of LTP expression of the MPP synapses onto dentate granule cells was investigated using the variance-mean technique. This new approach strongly supports a postsynaptic site for LTP expression at these synapses.

Future studies

Further studies on the co-localisation of presynaptic Ca^{2+} channels

Several experimental approaches could be used to confirm the non-uniform distribution of Ca^{2+} channels across different presynaptic terminals. It may be possible to directly visualise the inter-terminal variability in the Ca^{2+} channel subtypes. Such visualisation could be achieved by using an immunohistochemical approach. A double labelling technique is envisaged, using commercially available antibodies directed against synapsin I (as a synaptic terminal marker) and Ca^{2+} channel subtype specific antibodies ($\alpha 1B$, N-type or $\alpha 1A$, P/Q-type Ca^{2+} channel). If the primary antibodies are generated in different animal systems then secondary antibodies with different wavelength fluorescent tags could be used to identify the synaptic terminal and the expression of the Ca^{2+} channel subtype simultaneously. A comparison of the Ca^{2+} channel subtype expression between synaptic terminals could then be made using a confocal microscope. It is likely that the heterogeneity in the distribution will be graded. A "semi-quantitative" densitometry measurement may be required to illustrate the non-uniformity.

It is possible to optically estimate P_r in culture using the synaptic specific dye FM1-43 (Liu and Tsien, 1995; Reuter, 1995; Murthy *et al.*, 1997). An extension of experiments completed by Reuter (1995) is envisaged. FM1-43 is selectively taken up by synaptic vesicles, allowing the visualisation of individual synaptic terminals under epifluorescence. Depletion of the dye occurs when a cell is stimulated and releases vesicles of neurotransmitter. The rate of depletion can be used as a measure of P_r at the individual terminal. This technique could be used to extend the analysis of P_r to

interneurons, for which the MK-801 technique cannot be used. This technique could also be used to explore any developmental changes in the proportion of terminal classes.

The hippocampal slice preparation has two major advantages over the culture preparation: (i) the structural organisation of the tissue is preserved and (ii) neurons have developed within an intact brain and have been subject to all the developmental influences associated with normal brain growth. An extension of experiments described in Chapter 3 could determine if a non-uniform distribution of Ca^{2+} channel subtypes across different presynaptic terminals occurs in the slice preparation. An alternative approach would be to use two photon laser scanning microscopy, which allows the direct study of a single, visually identified synaptic terminal in the slice preparation. The all or none nature of the Ca^{2+} transients in dendritic spines implies that transmitter is required to be released from a presynaptic terminal for a transient to be observed (Emptage *et al.*, 1997). The visualisation of postsynaptic calcium transients using two photon laser scanning microscopy can therefore be used as an indicator of the success or failure of transmission at a particular synapse. The mean failure rate reflects P_r at an individual synapse. P_r at an individual terminal would be measured using this imaging technique before and after the addition of the selective blockers. Comparison between different synapses would then build up a picture of the degree of Ca^{2+} channel subtype heterogeneity in the slice preparation.

Further studies on Ca^{2+} cooperativity

The identification of the Ca^{2+} "sensor(s)" that triggers release remains a major challenge. A better understanding of the meaning of Ca^{2+} cooperativity should be possible if the sensor(s) was identified. The calyx of Held is a large synaptic terminal and allows the simultaneous recording from both presynaptic terminals and the postsynaptic cell. This preparation provides an exciting opportunity for investigating the molecular mechanisms underlying the control of transmitter release at a central synapse. Substances can be directly injected into the presynaptic terminal and the

effects on transmitter release can be monitored simultaneously. Flash photolysis of caged Ca^{2+} (eg. DM-Nitrophen) to raise $[\text{Ca}^{2+}]_{\text{it}}$ at this synapse could be used to investigate the Ca^{2+} cooperativity of transmitter release. Flash photolysis provides a means by which $[\text{Ca}^{2+}]_{\text{it}}$ can be uniformly increased. The co-injection of a Ca^{2+} indicator could be used to measure $[\text{Ca}^{2+}]_{\text{it}}$ in the presynaptic terminal while simultaneously recording the size of the postsynaptic EPSC. The uniform increase in $[\text{Ca}^{2+}]_{\text{it}}$ is free of many of the complications associated with the influx of Ca^{2+} through Ca^{2+} channels.

Future applications of the variance-mean technique

The variance-mean technique has proved to be a powerful tool in identifying the locus of LTP expression in the dentate. A natural continuation of this study would be to look at LTP and LTD in other regions of the brain. It could be applied to mossy fibre LTP (thought to have a presynaptic locus of expression) and the CA3-CA1 synapse where most LTP studies have concentrated. The technique could also be used to address the issue of pre- or postsynaptic locus of expression of short term plasticity such as paired pulse depression or paired pulse facilitation. Numerous neuroactive drugs have neuromodulatory actions with an unknown mechanism and site of expression. A number of these drugs could act on receptors that are found on both the pre- and postsynaptic membranes. The technique could be used to determine the site of action of such drugs.

References:

- Adler EM, Augustine GJ, Duffy SN, Charlton MP (1991) Alien intracellular calcium chelators attenuate neurotransmitter release at the squid giant synapse. *J Neurosci* 11: 1496-1507.
- Andersen P, Sundberg SH, Sveen O, Wigstrom H (1977) Specific long-lasting potentiation of synaptic transmission in hippocampal slices. *Nature* 266: 736-737.
- Ascher P, Nowak L (1988) The role of divalent cations in the N-methyl-D-aspartate responses of mouse central neurones in culture. *J Physiol (Lond)* 399: 247-266.
- Augustine GJ (1990) Regulation of transmitter release at the squid giant synapse by presynaptic delayed rectifier potassium current. *J Physiol (Lond)* 431: 343-364.
- Augustine GJ, Charlton MP (1986) Calcium dependence of presynaptic calcium current and post-synaptic response at the squid giant synapse. *J Physiol Lond* 381: 619-640.
- Barria A, Muller D, Derkach V, Griffith LC, Soderling TR (1997) Regulatory phosphorylation of AMPA-type glutamate receptors by CaM-KII during long-term potentiation. *Science* 276: 2042-2045.
- Bashir ZI, Alford S, Davies SN, Randall AD, Collingridge GL (1991) Long-term potentiation of NMDA receptor-mediated synaptic transmission in the hippocampus. *Nature* 349: 156-158.
- Baskys A, Carlen PL, Wojtowicz JM (1991) Long-term potentiation of synaptic responses in the rat dentate gyrus is due to increased quantal content. *Neurosci Lett* 127: 169-172.
- Bean BP (1989) Neurotransmitter inhibition of neuronal calcium currents by changes in channel voltage dependence. *Nature* 340: 153-156.

- Bekkers JM (1995) Synchronous and asynchronous EPSCs evoked in hippocampal slices: A test of the quantal model of neurotransmission. *Soc Neurosci Abstr* 21: 1091.
- Bekkers JM, Richerson GB, Stevens CF (1990) Origin of variability in quantal size in cultured hippocampal neurons and hippocampal slices. *Proc Natl Acad Sci U S A* 87: 5359-5362.
- Bekkers JM, Stevens CF (1989) NMDA and non-NMDA receptors are co-localized at individual excitatory synapses in cultured rat hippocampus. *Nature* 341: 230-233.
- Bekkers JM, Stevens CF (1990) Presynaptic mechanism for long-term potentiation in the hippocampus. *Nature* 346: 724-729.
- Bekkers JM, Stevens CF (1991) Excitatory and inhibitory autaptic currents in isolated hippocampal neurons maintained in cell culture. *Proc Natl Acad Sci U S A* 88: 7834-7838.
- Benke TA, Lüthi A, Issac JTR, Collingridge GL (1998) Modulation of AMPA receptor unitary conductance by synaptic activity. *Nature* 393: 790-793.
- Birnbaumer L, Campbell KP, Catterall WA, Harpold MM, Hofmann F, Horne WA, Mori Y, Schwartz A, Snutch TP, Tanabe T, Tsien RW (1994) The naming of voltage-gated calcium channels. *Neuron* 13: 505-506.
- Blanton MG, Lo Turco JJ, Kriegstein AR (1989) Whole cell recording from neurons in slices of reptilian and mammalian cerebral cortex. *J Neurosci Methods* 30: 203-210.
- Bliss TV, Collingridge GL (1993) A synaptic model of memory: long-term potentiation in the hippocampus. *Nature* 361: 31-39.
- Bliss TV, Errington ML, Laroche S, Lynch MA (1987) Increase in K⁺-stimulated, Ca²⁺-dependent release of [3H]glutamate from rat dentate gyrus three days after induction of long-term potentiation. *Neurosci Lett* 83: 107-112.

- Bliss TV, Lomo T (1973) Long-lasting potentiation of synaptic transmission in the dentate area of the anaesthetized rabbit following stimulation of the perforant path. *J Physiol (Lond)* 232: 331-356.
- Bolshakov VY, Siegelbaum SA (1995) Regulation of hippocampal transmitter release during development and long-term potentiation. *Science* 269: 1730-1734.
- Borst JG, Sakmann B (1998) Calcium current during a single action potential in a large presynaptic terminal of the rat brainstem. *J Physiol (Lond)* 506: 143-157.
- Borst JGG, Sakmann B (1996) Calcium influx and transmitter release in fast CNS synapse. *Nature* 383: 431- 434.
- Canevari L, Richter Levin G, Bliss TV (1994) LTP in the dentate gyrus is associated with a persistent NMDA receptor-dependent enhancement of synaptosomal glutamate release. *Brain Res* 667: 115-117.
- Catterall WA (1991) Functional subunit structure of voltage-gated calcium channels. *Science* 253: 1499-1500.
- Catterall WA (1995) Structure and function of voltage-gated ion channels. *Annu Rev Biochem* 64: 493-531.
- Christie BR, Abraham WC (1994) Differential regulation of paired-pulse plasticity following LTP in the dentate gyrus. *Neuroreport* 5: 385-388.
- Church PJ, Stanley EF (1996) Single L-type calcium channel conductance with physiological levels of calcium in chick ciliary ganglion neurons. *J Physiol Lond* 496: 59-68.
- Clamann HP, Mathis J, Luscher HR (1989) Variance analysis of excitatory postsynaptic potentials in cat spinal motoneurons during posttetanic potentiation. *J Neurophysiol* 61: 403-416.
- Clements J (1991) Quantal synaptic transmission? *Nature* 353: 396.

- Clements JD, Bekkers JM (1997) Detection of spontaneous synaptic events with an optimally scaled template. *Biophys J* 73: 220-229.
- Colino A, Malenka RC (1993) Mechanisms underlying induction of long-term potentiation in rat medial and lateral perforant paths in vitro. *J Neurophysiol* 69: 1150-1159.
- Cormier RJ, Kelly PT (1996) Glutamate-induced long-term potentiation enhances spontaneous EPSC amplitude but not frequency. *J Neurophysiol* 75: 1909-1918.
- Cowan AI, Stricker C, Reece LJ, Redman SJ (1998) Long-term plasticity at excitatory synapses on aspiny interneurons in area CA1 lacks synaptic specificity. *J Neurophysiol* 79: 13-20.
- Currie KP, Fox AP (1997) Comparison of N- and P/Q-type voltage-gated calcium channel current inhibition. *J Neurosci* 17: 4570-4579.
- Davies SN, Lester RA, Reymann KG, Collingridge GL (1989) Temporally distinct pre- and post-synaptic mechanisms maintain long-term potentiation. *Nature* 338: 500-503.
- Del Castillo J, Katz B (1954) Quantal components of the end plate potential. *J Physiol (Lond)* 124: 560-573.
- Dobrunz LE, Stevens CF (1997) Heterogeneity of release probability, facilitation, and depletion at central synapses. *Neuron* 18: 995-1008.
- Dodge FA, Jr., Rahamimoff R (1967) Co-operative action a calcium ions in transmitter release at the neuromuscular junction. *J Physiol Lond* 193: 419-432.
- Donaldson C, Stricker C (1996) Assaying the release probability at CA1 pyramidal cell synapses. *Proc Aust Neurosci Soc* 7: 85.
- Dubel SJ, Starr TV, Hell J, Ahljianian MK, Enyeart JJ, Catterall WA, Snutch TP (1992) Molecular cloning of the alpha-1 subunit of an omega-conotoxin-sensitive calcium channel. *Proc Natl Acad Sci U S A* 89: 5058-5062.

- Dunlap K, Luebke JI, Turner TJ (1995) Exocytotic Ca^{2+} channels in mammalian central neurons. *Trends Neurosci* 18: 89-98.
- Edwards FA, Konnerth A, Sakmann B, Takahashi T (1989) A thin slice preparation for patch clamp recordings from neurones of the mammalian central nervous system. *Pflugers Arch* 414: 600-612.
- Ellinor PT, Zhang JF, Randall AD, Zhou M, Schwarz TL, Tsien RW, Horne WA (1993) Functional expression of a rapidly inactivating neuronal calcium channel. *Nature* 363: 455-458.
- Elmslie KS, Zhou W, Jones SW (1990) LHRH and GTP-gamma-S modify calcium current activation in bullfrog sympathetic neurons. *Neuron* 5: 75-80.
- Emptage N, Bliss T, V. P. , Fine A (1997) Confocal imaging of synaptic calcium transients in dendritic spines of organotypic hippocampal culture. *Soc Neurosci Abstr* 23: 370.
- Errington ML, Lynch MA, Bliss TV (1987) Long-term potentiation in the dentate gyrus: induction and increased glutamate release are blocked by D(-) aminophosphonovalerate. *Neuroscience* 20: 279-284.
- Faber DS, Korn H (1991) Applicability of the coefficient of variation method for analyzing synaptic plasticity. *Biophys J* 60: 1288-1294.
- Fogelson AL, Zucker RS (1985) Presynaptic calcium diffusion from various arrays of single channels. Implications for transmitter release and synaptic facilitation. *Biophys J* 48: 1003-1017.
- Foster TC, McNaughton BL (1991) Long-term enhancement of CA1 synaptic transmission is due to increased quantal size, not quantal content. *Hippocampus* 1: 79-91.
- Fox AP, Nowycky MC, Tsien RW (1987) Kinetic and pharmacological properties distinguishing three types of calcium currents in chick sensory neurones. *J Physiol (Lond)* 394: 149-172.

- Frerking M, Wilson M (1996) Effects of variance in mini amplitude on stimulus-evoked release: a comparison of two models. *Biophys J* 70: 2078-2091.
- Fujita Y, Mynlieff M, Dirksen RT, Kim MS, Niidome T, Nakai J, Friedrich T, Iwabe N, Miyata T, Furuichi T, Furutama D, Mikoshiba K, Mori Y, Beam KG (1993) Primary structure and functional expression of the omega-conotoxin-sensitive N-type calcium channel from rabbit brain. *Neuron* 10: 585-598.
- Fukunaga K, Muller D, Miyamoto E (1995) Increased phosphorylation of Ca^{2+} /calmodulin-dependent protein kinase II and its endogenous substrates in the induction of long-term potentiation. *J Biol Chem* 270: 6119-6124.
- Fukunaga K, Muller D, Miyamoto E (1996) CaM kinase II in long-term potentiation. *Neurochem Int* 28: 343-358.
- Furshpan EJ, Landis SC, Matsumoto SG, Potter DD (1986) Synaptic functions in rat sympathetic neurons in microcultures. I. Secretion of norepinephrine and acetylcholine. *J Neurosci* 6: 1061-1079.
- Glaum SR, Miller RJ (1995) Presynaptic metabotropic glutamate receptors modulate omega-conotoxin-GVIA-insensitive calcium channels in the rat medulla. *Neuropharmacology* 34: 953-964.
- Grahame DC (1947) The electrical double layer and the theory of electrocapillarity. *Chem Rev* 41: 441-501.
- Greengard P, Jen J, Nairn AC, Stevens CF (1991) Enhancement of the glutamate response by cAMP-dependent protein kinase in hippocampal neurons. *Science* 253: 1135-1138.
- Greengard P, Valtorta F, Czernik AJ, Benfenati F (1993) Synaptic vesicle phosphoproteins and regulation of synaptic function. *Science* 259: 780-785.
- Gurnett CA, De Waard M, Campbell KP (1996) Dual function of the voltage-dependent Ca^{2+} channel alpha 2 delta subunit in current stimulation and subunit interaction. *Neuron* 16: 431-440.

- Haage D, Karlsson U, Johansson S (1998) Heterogeneous presynaptic Ca^{2+} channel types triggering GABA release onto medial preoptic neurons from rat. *J Physiol (Lond)* 507: 77-91.
- Harris KM, Sultan P (1995) Variation in the number, location and size of synaptic vesicles provide an anatomical basis for the nonuniform probability of release at hippocampal CA1 synapses. *Neuropharmacology* 34: 1387-1395.
- Hebb DO (1949) *The organization of behavior*. New York: John Wiley & Sons.
- Heidelberger R, Heinemann C, Neher E, Matthews G (1994) Calcium dependence of the rate of exocytosis in a synaptic terminal. *Nature* 371: 513-515.
- Herlitze S, Garcia DE, Mackie K, Hille B, Scheuer T, Catterall WA (1996) Modulation of Ca^{2+} channels by G-protein beta gamma subunits. *Nature* 380: 258-262.
- Hess P, Lansman JB, Tsien RW (1986) Calcium channel selectivity for divalent and monovalent cations. Voltage and concentration dependence of single channel current in ventricular heart cells. *J Gen Physiol* 88: 293-319.
- Hessler NA, Shirke AM, Malinow R (1993) The probability of transmitter release at a mammalian central synapse. *Nature* 366: 569-572.
- Hille B (1992) *Ionic channels of excitable membranes*. Sunderland, MA: Sinauer Associates Inc.
- Hille B (1994) Modulation of ion-channel function by G-protein-coupled receptors. *Trends Neurosci* 17: 531-536.
- Hjelmstad GO, Nicoll RA, Malenka RC (1997) Synaptic refractory period provides a measure of probability of release in the hippocampus. *Neuron* 19: 1309-1318.
- Huang CC, Wang SJ, Gean PW (1998) Selective enhancement of P-type calcium currents by isoproterenol in the rat amygdala. *J Neurosci* 18: 2276-2282.

- Huang EP, Stevens CF (1997) Estimating the distribution of synaptic reliabilities. *J Neurophysiol* 78: 2870-2880.
- Huang YY, Colino A, Selig DK, Malenka RC (1992) The influence of prior synaptic activity on the induction of long-term potentiation. *Science* 255: 730-733.
- Huettner JE, Bean BP (1988) Block of N-methyl-D-aspartate-activated current by the anticonvulsant MK-801: selective binding to open channels. *Proc Natl Acad Sci U S A* 85: 1307-1311.
- Ikeda SR (1996) Voltage-dependent modulation of N-type calcium channels by G-protein beta gamma subunits. *Nature* 380: 255-258.
- Isaac JT, Hjelmstad GO, Nicoll RA, Malenka RC (1996) Long-term potentiation at single fiber inputs to hippocampal CA1 pyramidal cells. *Proc Natl Acad Sci U S A* 93: 8710-8715.
- Isaac JT, Nicoll RA, Malenka RC (1995) Evidence for silent synapses: implications for the expression of LTP. *Neuron* 15: 427-434.
- Issa NP, Hudspeth AJ (1996) The entry and clearance of Ca^{2+} at individual presynaptic active zones of hair cells from the bullfrog's sacculus. *Proc Natl Acad Sci U S A* 93: 9527-9532.
- Ito I, Hidaka H, Sugiyama H (1991) Effects of KN-62, a specific inhibitor of calcium/calmodulin-dependent protein kinase II, on long-term potentiation in the rat hippocampus. *Neurosci Lett* 121: 119-121.
- Jay SD, Sharp AH, Kahl SD, Vedvick TS, Harpold MM, Campbell KP (1991) Structural characterization of the dihydropyridine-sensitive calcium channel alpha 2-subunit and the associated delta peptides. *J Biol Chem* 266: 3287-3293.
- Jeffery KJ (1997) LTP and spatial learning--where to next? *Hippocampus* 7: 95-110.

- Jonas P, Major G, Sakmann B (1993) Quantal components of unitary EPSCs at the mossy fibre synapse on CA3 pyramidal cells of rat hippocampus. *J Physiol (Lond)* 472: 615-663.
- Katz B, Miledi R (1968) The role of calcium in neuromuscular facilitation. *J Physiol Lond* 195: 481-492.
- Kauer JA, Malenka RC, Nicoll RA (1988) A persistent postsynaptic modification mediates long-term potentiation in the hippocampus. *Neuron* 1: 911-917.
- Kuhnt U, Voronin LL (1994) Interaction between paired-pulse facilitation and long-term potentiation in area CA1 of guinea-pig hippocampal slices: application of quantal analysis. *Neuroscience* 62: 391-397.
- Kullmann DM (1994) Amplitude fluctuations of dual-component EPSCs in hippocampal pyramidal cells: implications for long-term potentiation. *Neuron* 12: 1111-1120.
- Kullmann DM, Asztely F (1998) Extrasynaptic glutamate spillover in the hippocampus: evidence and implications. *Trends Neurosci* 21: 8-14.
- Kullmann DM, Erdemli G, Asztely F (1996) LTP of AMPA and NMDA receptor-mediated signals: evidence for presynaptic expression and extrasynaptic glutamate spill-over. *Neuron* 17: 461-474.
- Kullmann DM, Nicoll RA (1992) Long-term potentiation is associated with increases in quantal content and quantal amplitude. *Nature* 357: 240-244.
- Kullmann DM, Siegelbaum SA (1995) The site of expression of NMDA receptor-dependent LTP: new fuel for an old fire. *Neuron* 15: 997-1002.
- Lando L, Zucker RS (1994) Ca^{2+} cooperativity in neurosecretion measured using photolabile Ca^{2+} chelators. *J Neurophysiol* 72: 825-830.
- Larkman A, Hannay T, Stratford K, Jack J (1992) Presynaptic release probability influences the locus of long-term potentiation. *Nature* 360: 70-73.

- Levy WB, Steward O (1979) Synapses as associative memory elements in the hippocampal formation. *Brain Res* 175: 233-245.
- Liao D, Hessler NA, Malinow R (1995) Activation of postsynaptically silent synapses during pairing-induced LTP in CA1 region of hippocampal slice. *Nature* 375: 400-404.
- Liao D, Jones A, Malinow R (1992) Direct measurement of quantal changes underlying long-term potentiation in CA1 hippocampus. *Neuron* 9: 1089-1097.
- Liu G, Tsien RW (1995) Properties of synaptic transmission at single hippocampal synaptic boutons. *Nature* 375: 404-408.
- Llinas R, Steinberg IZ, Walton K (1981) Relationship between presynaptic calcium current and postsynaptic potential in squid giant synapse. *Biophys J* 33: 323-351.
- Llinas R, Sugimori M, Silver RB (1992) Microdomains of high calcium concentration in a presynaptic terminal. *Science* 256: 677-679.
- Llinas R, Sugimori M, Silver RB (1995) The concept of calcium concentration microdomains in synaptic transmission. *Neuropharmacology* 34: 1443-1451.
- Lu YM, Roder JC, Davidow J, Salter MW (1998) Src activation in the induction of long-term potentiation in CA1 hippocampal neurons. *Science* 279: 1363-1367.
- Luebke JI, Dunlap K, Turner TJ (1993) Multiple calcium channel types control glutamatergic synaptic transmission in the hippocampus. *Neuron* 11: 895-902.
- Lynch G, Larson J, Kelso S, Barrionuevo G, Schottler F (1983) Intracellular injections of EGTA block induction of hippocampal long-term potentiation. *Nature* 305: 719-721.
- Lynch GS, Dunwiddie T, Gribkoff V (1977) Heterosynaptic depression: a postsynaptic correlate of long-term potentiation. *Nature* 266: 737-739.

- Malenka RC (1991) Postsynaptic factors control the duration of synaptic enhancement in area CA1 of the hippocampus. *Neuron* 6: 53-60.
- Malenka RC, Kauer JA, Perkel DJ, Mauk MD, Kelly PT, Nicoll RA, Waxham MN (1989) An essential role for postsynaptic calmodulin and protein kinase activity in long-term potentiation. *Nature* 340: 554-557.
- Malenka RC, Kauer JA, Zucker RS, Nicoll RA (1988) Postsynaptic calcium is sufficient for potentiation of hippocampal synaptic transmission. *Science* 242: 81-84.
- Malgaroli A, Ting AE, Wendland B, Bergamaschi A, Villa A, Tsien RW, Scheller RH (1995) Presynaptic component of long-term potentiation visualized at individual hippocampal synapses. *Science* 268: 1624-1628.
- Malgaroli A, Tsien RW (1992) Glutamate-induced long-term potentiation of the frequency of miniature synaptic currents in cultured hippocampal neurons. *Nature* 357: 134-139.
- Malinow R (1991) Transmission between pairs of hippocampal slice neurons: quantal levels, oscillations, and LTP. *Science* 252: 722-724.
- Malinow R, Schulman H, Tsien RW (1989) Inhibition of postsynaptic PKC or CaMKII blocks induction but not expression of LTP. *Science* 245: 862-866.
- Malinow R, Tsien RW (1990) Presynaptic enhancement shown by whole-cell recordings of long-term potentiation in hippocampal slices. *Nature* 346: 177-180.
- Manabe T, Nicoll RA (1994) Long-term potentiation: evidence against an increase in transmitter release probability in the CA1 region of the hippocampus. *Science* 265: 1888-1892.
- Manabe T, Renner P, Nicoll RA (1992) Postsynaptic contribution to long-term potentiation revealed by the analysis of miniature synaptic currents. *Nature* 355: 50-55.

- Manabe T, Wyllie DJ, Perkel DJ, Nicoll RA (1993) Modulation of synaptic transmission and long-term potentiation: effects on paired pulse facilitation and EPSC variance in the CA1 region of the hippocampus. *J Neurophysiol* 70: 1451-1459.
- Maren S, Tocco G, Standley S, Baudry M, Thompson RF (1993) Postsynaptic factors in the expression of long-term potentiation (LTP): increased glutamate receptor binding following LTP induction in vivo. *Proc Natl Acad Sci U S A* 90: 9654-9658.
- Martin AR (1977) Junctional transmission. II. Presynaptic mechanisms. In: *Handbook of Physiology. Section 1: The Nervous System.* (Kandel ER, ed), pp 329-355. Bethesda, MD: American Physiological Society.
- Martin-Moutot N, Charvin N, Leveque C, Sato K, Nishiki T, Kozaki S, Takahashi M, Seagar M (1996) Interaction of SNARE complexes with P/Q-type calcium channels in rat cerebellar synaptosomes. *J Biol Chem* 271: 6567-6570
- Mayer ML, Vyklicky L, Jr., Westbrook GL (1989) Modulation of excitatory amino acid receptors by group IIB metal cations in cultured mouse hippocampal neurones. *J Physiol Lond* 415: 329-350.
- McGlade McCulloh E, Yamamoto H, Tan SE, Brickey DA, Soderling TR (1993) Phosphorylation and regulation of glutamate receptors by calcium/calmodulin-dependent protein kinase II. *Nature* 362: 640-642.
- McLachlan EM (1978) *The statistics of transmitter release at chemical synapses.* Baltimore, Maryland: University park.
- McNaughton BL (1980) Evidence for two physiologically distinct perforant pathways to the fascia dentata. *Brain Res* 199: 1-19.
- McNaughton BL (1982) Long-term synaptic enhancement and short-term potentiation in rat fascia dentata act through different mechanisms. *J Physiol (Lond)* 324: 249-262.

- McNaughton BL, Douglas RM, Goddard GV (1978) Synaptic enhancement in fascia dentata: cooperativity among coactive afferents. *Brain Res* 157: 277-293.
- Medina JH, Izquierdo I (1995) Retrograde messengers, long-term potentiation and memory. *Brain Res Brain Res Rev* 21: 185-194.
- Mikami A, Imoto K, Tanabe T, Niidome T, Mori Y, Takeshima H, Narumiya S, Numa S (1989) Primary structure and functional expression of the cardiac dihydropyridine-sensitive calcium channel. *Nature* 340: 230-233.
- Miller SG, Patton BL, Kennedy MB (1988) Sequences of autophosphorylation sites in neuronal type II CaM kinase that control Ca²⁺-independent activity. *Neuron* 1: 593-604.
- Min MY, Asztely F, Kokaia M, Kullmann DM (1998) Long-term potentiation and dual-component quantal signaling in the dentate gyrus. *Proc Natl Acad Sci U S A* 95: 4702-4707.
- Mintz IM, Adams ME, Bean BP (1992a) P-type calcium channels in rat central and peripheral neurons. *Neuron* 9: 85-95.
- Mintz IM, Bean BP (1993) GABAB receptor inhibition of P-type Ca²⁺ channels in central neurons. *Neuron* 10: 889-898.
- Mintz IM, Sabatini BL, Regehr WG (1995) Calcium control of transmitter release at a cerebellar synapse. *Neuron* 15: 675-688.
- Mintz IM, Venema VJ, Swiderek KM, Lee TD, Bean BP, Adams ME (1992b) P-type calcium channels blocked by the spider toxin omega-Aga-IVA. *Nature* 355: 827-829.
- Miyamoto MD (1975) Binomial analysis of quantal transmitter release at glycerol treated frog neuromuscular junctions. *J Physiol (Lond)* 250: 121-142.

- Moreno H, Rudy B, Llinas R (1997) beta subunits influence the biophysical and pharmacological differences between P- and Q-type calcium currents expressed in a mammalian cell line. *Proc Natl Acad Sci U S A* 94: 14042-14047.
- Mori Y, Friedrich T, Kim MS, Mikami A, Nakai J, Ruth P, Bosse E, Hofmann F, Flockerzi V, Furuichi T, Mikoshiba K, Imoto K, Tanabe T, Numa S (1991) Primary structure and functional expression from complementary DNA of a brain calcium channel. *Nature* 350: 398-402.
- Muller D, Joly M, Lynch G (1988) Contributions of quisqualate and NMDA receptors to the induction and expression of LTP. *Science* 242: 1694-1697.
- Muller D, Lynch G (1989) Evidence that changes in presynaptic calcium currents are not responsible for long-term potentiation in hippocampus. *Brain Res* 479: 290-299.
- Murthy VN, Sejnowski TJ, Stevens CF (1997) Heterogeneous release properties of visualized individual hippocampal synapses. *Neuron* 18: 599-612.
- Neher E (1998) Vesicle pools and Ca²⁺ microdomains: new tools for understanding their roles in neurotransmitter release. *Neuron* 20: 389-399.
- Nguyen PV, Abel T, Kandel ER (1994) Requirement of a critical period of transcription for induction of a late phase of LTP. *Science* 265: 1104-1107.
- Nicoll RA, Malenka RC (1995) Contrasting properties of two forms of long-term potentiation in the hippocampus. *Nature* 377: 115-118.
- Nowycky MC, Fox AP, Tsien RW (1985) Three types of neuronal calcium channel with different calcium agonist sensitivity. *Nature* 316: 440-443.
- Olivera BM, Gray WR, Zeikus R, McIntosh JM, Varga J, Rivier J, de Santos V, Cruz LJ (1985) Peptide neurotoxins from fish-hunting cone snails. *Science* 230: 1338-1343.

- Otmakhov N, Griffith LC, Lisman JE (1997) Postsynaptic inhibitors of calcium/calmodulin-dependent protein kinase type II block induction but not maintenance of pairing-induced long-term potentiation. *J Neurosci* 17: 5357-5365.
- Patneau DK, Mayer ML (1990) Structure-activity relationships for amino acid transmitter candidates acting at N-methyl-D-aspartate and quisqualate receptors. *J Neurosci* 10: 2385-2399.
- Penington NJ, Kelly JS, Fox AP (1991) A study of the mechanism of Ca²⁺ current inhibition produced by serotonin in rat dorsal raphe neurons. *J Neurosci* 11: 3594-3609.
- Perez-Reyes E, Cribbs LL, Daud A, Lacerda AE, Barclay J, Williamson MP, Fox M, Rees M, Lee JH (1998) Molecular characterization of a neuronal low-voltage-activated T-type calcium channel. *Nature* 391: 896-900.
- Perkel DJ, Nicoll RA (1993) Evidence for all-or-none regulation of neurotransmitter release: implications for long-term potentiation. *J Physiol Lond* 471: 481-500.
- Perkel DJ, Petrozzino JJ, Nicoll RA, Connor JA (1993) The role of Ca²⁺ entry via synaptically activated NMDA receptors in the induction of long-term potentiation. *Neuron* 11: 817-823.
- Pettit DL, Perlman S, Malinow R (1994) Potentiated transmission and prevention of further LTP by increased CaMKII activity in postsynaptic hippocampal slice neurons. *Science* 266: 1881-1885.
- Pfriefer FW, Veselovsky NS, Gottmann K, Lux HD (1992) Pharmacological characterization of calcium currents and synaptic transmission between thalamic neurons in vitro. *J Neurosci* 12: 4347-4357.
- Poncer JC, McKinney RA, Gahwiler BH, Thompson SM (1997) Either N- or P-type calcium channels mediate GABA release at distinct hippocampal inhibitory synapses. *Neuron* 18: 463-472.

- Qian J, Saggau P (1997) Presynaptic inhibition of synaptic transmission in the rat hippocampus by activation of muscarinic receptors: involvement of presynaptic calcium influx. *Br J Pharmacol* 122: 511-519.
- Randall A, Tsien RW (1995) Pharmacological dissection of multiple types of Ca^{2+} channel currents in rat cerebellar granule neurons. *J Neurosci* 15: 2995-3012.
- Randall AD, Tsien RW (1997) Contrasting biophysical and pharmacological properties of T-type and R-type calcium channels. *Neuropharmacology* 36: 879-893.
- Redman S (1990) Quantal analysis of synaptic potentials in neurons of the central nervous system. *Physiol Rev* 70: 165-198.
- Regehr WG, Mintz IM (1994) Participation of multiple calcium channel types in transmission at single climbing fiber to Purkinje cell synapses. *Neuron* 12: 605-613.
- Reid CA, Clements JD, Bekkers JB (1997) Nonuniform distribution of Ca^{2+} channel subtypes on presynaptic terminals of excitatory synapses in hippocampal cultures. *J Neurosci* 15: 2738-2745.
- Reuter H (1995) Measurements of exocytosis from single presynaptic nerve terminals reveal heterogeneous inhibition by Ca^{2+} -channel blockers. *Neuron* 14: 773-779.
- Rosenmund C, Clements JD, Westbrook GL (1993) Nonuniform probability of glutamate release at a hippocampal synapse. *Science* 262: 754-757.
- Sabatini BL, Regehr WG (1995) Detecting changes in calcium influx which contribute to synaptic modulation in mammalian brain slice. *Neuropharmacology* 34: 1453-1467.
- Sabatini BL, Regehr WG (1996) Timing of neurotransmission at fast synapses in the mammalian brain. *Nature* 384: 170-172.

- Sather WA, Tanabe T, Zhang JF, Mori Y, Adams ME, Tsien RW (1993) Distinctive biophysical and pharmacological properties of class A (BI) calcium channel alpha 1 subunits. *Neuron* 11: 291-303.
- Scholz KP, Miller RJ (1995) Developmental changes in presynaptic calcium channels coupled to glutamate release in cultured rat hippocampal neurons. *J Neurosci* 15: 4612-4617.
- Scholz KP, Miller RJ (1996) Presynaptic inhibition at excitatory hippocampal synapses: development and role of presynaptic Ca²⁺ channels. *J Neurophysiol* 76: 39-46.
- Schulz PE, Cook EP, Johnston D (1995) Using paired-pulse facilitation to probe the mechanisms for long-term potentiation (LTP). *J Physiol Paris* 89: 3-9.
- Schulz PE, Fitzgibbons JC (1997) Differing mechanisms of expression for short- and long-term potentiation. *J Neurophysiol* 78: 321-334.
- Sheng ZH, Rettig J, Cook T, Catterall WA (1996) Calcium-dependent interaction of N-type calcium channels with the synaptic core complex. *Nature* 379: 451-454.
- Sigworth FJ (1980) The variance of sodium current fluctuations at the node of Ranvier. *J Physiol (Lond)* 307: 97-129.
- Silva AJ, Paylor R, Wehner JM, Tonegawa S (1992a) Impaired spatial learning in alpha-calcium-calmodulin kinase II mutant mice. *Science* 257: 206-211.
- Silva AJ, Stevens CF, Tonegawa S, Wang Y (1992b) Deficient hippocampal long-term potentiation in alpha-calcium-calmodulin kinase II mutant mice. *Science* 257: 201-206.
- Silver RA, Cull-Candy SG, Takahashi T (1996) Non-NMDA glutamate receptor occupancy and open probability at a rat cerebellar synapse with single and multiple release sites. *J Physiol (Lond)* 494: 231-250.

- Silver RA, Momiyama A, Cull-Candy SG (in press) Locus of frequency-dependent depression at climbing fibre-Purkinje cell synapses identified with multiple-probability fluctuation analysis. *J Physiol*
- Simon SM, Llinas RR (1985) Compartmentalization of the submembrane calcium activity during calcium influx and its significance in transmitter release. *Biophys J* 48: 485-498.
- Sinha SR, Wu LG, Saggau P (1997) Presynaptic calcium dynamics and transmitter release evoked by single action potentials at mammalian central synapses. *Biophys J* 72: 637-651.
- Snutch TP, Tomlinson WJ, Leonard JP, Gilbert MM (1991) Distinct calcium channels are generated by alternative splicing and are differentially expressed in the mammalian CNS. *Neuron* 7: 45-57.
- Son H, Carpenter DO (1996) Interactions among paired-pulse facilitation and post-tetanic and long-term potentiation in the mossy fiber-CA3 pathway in rat hippocampus. *Synapse* 23: 302-311.
- Stanley EF (1986) Decline in calcium cooperativity as the basis of facilitation at the squid giant synapse. *J Neurosci* 6: 782-789.
- Stanley EF (1993) Single calcium channels and acetylcholine release at a presynaptic nerve terminal. *Neuron* 11: 1007-1011.
- Stea A, Dubel SJ, Pragnell M, Leonard JP, Campbell KP, Snutch TP (1993) A beta-subunit normalizes the electrophysiological properties of a cloned N-type Ca^{2+} channel alpha 1-subunit. *Neuropharmacology* 32: 1103-1116.
- Stea A, Tomlinson WJ, Soong TW, Bourinet E, Dubel SJ, Vincent SR, Snutch TP (1994) Localization and functional properties of a rat brain alpha 1A calcium channel reflect similarities to neuronal Q- and P-type channels. *Proc Natl Acad Sci U S A* 91: 10576-10580.
- Stern MD (1992) Buffering of calcium in the vicinity of a channel pore. *Cell Calcium* 13: 183-192.

- Stevens CF, Wang Y (1994) Changes in reliability of synaptic function as a mechanism for plasticity. *Nature* 371: 704-707.
- Stricker C, Field AC, Redman SJ (1996a) Changes in quantal parameters of EPSCs in rat CA1 neurones in vitro after the induction of long-term potentiation. *J Physiol (Lond)* 490: 443-454.
- Stricker C, Field AC, Redman SJ (1996b) Statistical analysis of amplitude fluctuations in EPSCs evoked in rat CA1 pyramidal neurones in vitro. *J Physiol (Lond)* 490: 419-441.
- Swandulla D, Hans M, Zipser K, Augustine GJ (1991) Role of residual calcium in synaptic depression and posttetanic potentiation: fast and slow calcium signaling in nerve terminals. *Neuron* 7: 915-926.
- Takahashi T, Forsythe ID, Tsujimoto T, Barnes Davies M, Onodera K (1996) Presynaptic calcium current modulation by a metabotropic glutamate receptor. *Science* 274: 594-597.
- Tong G, Jahr CE (1994) Multivesicular release from excitatory synapses of cultured hippocampal neurons. *Neuron* 12: 51-59.
- Tsien RW, Lipscombe D, Madison D, Bley K, Fox A (1995) Reflections on Ca(2+)-channel diversity, 1988-1994. *Trends Neurosci* 18: 52-54.
- Tsien RW, Lipscombe D, Madison DV, Bley KR, Fox AP (1988) Multiple types of neuronal calcium channels and their selective modulation. *Trends Neurosci* 11: 431-438.
- Tucker T, Fettiplace R (1995) Confocal imaging of calcium microdomains and calcium extrusion in turtle hair cells. *Neuron* 15: 1323-1335.
- Van der Loos H, Glaser EM (1972) Autapses in neocortex cerebri: synapses between a pyramidal cell's axon and its own dendrites. *Brain Res* 48: 355-360.

- Vazquez E, Sanchez-Prieto J (1997) Presynaptic modulation of glutamate release targets different calcium channels in rat cerebrocortical nerve terminals. *Eur J Neurosci* 9: 2009-2018.
- Voronin LL (1983) Long-term potentiation in the hippocampus. *Neuroscience* 10: 1051-1069.
- Wagner JA, Snowman AM, Biswas A, Olivera BM, Snyder SH (1988) Omega-conotoxin GVIA binding to a high-affinity receptor in brain: characterization, calcium sensitivity, and solubilization. *J Neurosci* 8: 3354-3359.
- Wang JH, Kelly PT (1996) Regulation of synaptic facilitation by postsynaptic Ca^{2+} /CaM pathways in hippocampal CA1 neurons. *J Neurophysiol* 76: 276-286.
- Wang JH, Kelly PT (1997) Attenuation of paired-pulse facilitation associated with synaptic potentiation mediated by postsynaptic mechanisms. *J Neurophysiol* 78: 2707-2716.
- Wang S, Wojtowicz JM, Atwood HL (1996) Synaptic recruitment during long-term potentiation at synapses of the medial perforant pathway in the dentate gyrus of the rat brain. *Synapse* 22: 78-86.
- Weiss JN (1997) The Hill equation revisited: uses and misuses. *Faseb J* 11: 835-841.
- Weisskopf MG, Nicoll RA (1995) Presynaptic changes during mossy fibre LTP revealed by NMDA receptor-mediated synaptic responses. *Nature* 376: 256-259.
- Wheeler DB, Randall A, Tsien RW (1994) Roles of N-type and Q-type Ca^{2+} channels in supporting hippocampal synaptic transmission. *Science* 264: 107-111.
- Wheeler DB, Randall A, Tsien RW (1996) Change in action potential duration alter reliance of excitatory synaptic transmission on multiple types of Ca^{2+} channels in rat hippocampus. *J Neurosci* 16: 2226-2237.

- Williams ME, Brust PF, Feldman DH, Patthi S, Simerson S, Maroufi A, McCue AF, Velicelebi G, Ellis SB, Harpold MM (1992a) Structure and functional expression of an omega-conotoxin-sensitive human N-type calcium channel. *Science* 257: 389-395.
- Williams ME, Feldman DH, McCue AF, Brenner R, Velicelebi G, Ellis SB, Harpold MM (1992b) Structure and functional expression of alpha 1, alpha 2, and beta subunits of a novel human neuronal calcium channel subtype. *Neuron* 8: 71-84.
- Winslow JL, Duffy SN, Charlton MP (1994) Homosynaptic facilitation of transmitter release in crayfish is not affected by mobile calcium chelators: implications for the residual ionized calcium hypothesis from electrophysiological and computational analyses. *J Neurophysiol* 72: 1769-1793.
- Witter MP (1993) Organization of the entorhinal-hippocampal system: a review of current anatomical data. *Hippocampus* 3 Spec No: 33-44.
- Wu LG, Borst JG, Sakmann B (1998) R-type Ca^{2+} currents evoke transmitter release at a rat central synapse. *Proc Natl Acad Sci USA* 95: 4720-4725.
- Wu LG, Saggau P (1994a) Adenosine inhibits evoked synaptic transmission primarily by reducing presynaptic calcium influx in area CA1 of hippocampus. *Neuron* 12: 1139-1148.
- Wu LG, Saggau P (1994b) Pharmacological identification of two types of presynaptic voltage-dependent calcium channels at CA3-CA1 synapses of the hippocampus. *J Neurosci* 14: 5613-5622.
- Wu LG, Saggau P (1995a) Block of multiple presynaptic calcium channel types by omega-conotoxin-MVIIIC at hippocampal CA3 to CA1 synapses. *J Neurophysiol* 73: 1965-1972.
- Wu LG, Saggau P (1995b) GABAB receptor-mediated presynaptic inhibition in guinea-pig hippocampus is caused by reduction of presynaptic Ca^{2+} influx. *J Physiol Lond* 485: 649-657.

- Xie X, Berger TW, Barrionuevo G (1992) Isolated NMDA receptor-mediated synaptic responses express both LTP and LTD. *J Neurophysiol* 67: 1009-1013.
- Yoshikami D, Bagabaldo Z, Olivera BM (1989) The inhibitory effects of omega-conotoxins on Ca channels and synapses. *Ann N Y Acad Sci* 560: 230-248.
- Zalutsky RA, Nicoll RA (1990) Comparison of two forms of long-term potentiation in single hippocampal neurons. *Science* 248: 1619-1624.
- Zhang JF, Randall AD, Ellinor PT, Horne WA, Sather WA, Tanabe T, Schwarz TL, Tsien RW (1993) Distinctive pharmacology and kinetics of cloned neuronal Ca^{2+} channels and their possible counterparts in mammalian CNS neurons. *Neuropharmacology* 32: 1075-1088.
- Zucker RS (1989) Short-term synaptic plasticity. *Annu Rev Neurosci* 12: 13-31.